The what, when & how of seedling growth regulation.

Jodi Lorraine Stewart Lilley

A dissertation

submitted in partial fulfillment of the

requirements for the degree of

Doctor of Philosophy

University of Washington

2013

Reading Committee:

Jennifer Nemhauser, Chair

Takato Imaizumi

Benjamin Kerr

Program Authorized to Offer Degree:

Biology

University of Washington

Abstract

The what, when & how of seedling growth regulation.

Jodi Lorraine Stewart Lilley

Chair of the Supervisory Committee:
Associate Professor Jennifer Nemhauser
Biology

Photomorphogenesis has two stages. First, seedlings detect light and open their embryonic leaves (cotyledons). Second, seedlings optimize their light environment by regulated elongation of the embryonic stem (hypocotyl). Several hormones, including auxin, brassinosteroids and gibberellins, orchestrate the growth of the seedlings stem. In this dissertation research, time-lapse imaging was coupled with molecular biology to investigate the dynamics of hormone effects across photomorphogenesis. These studies revealed distinct growth dynamics during each stage, in addition to changes in growth hormone sensitivity across these stages. For example, the interaction between the brassinosteroid and gibberellin pathways is quite different in early versus late promotion of seedling growth. In late stages of seedling development, the hormone auxin and the *PHYTOCHROME INTERACTING FACTOR (PIF)* family of transcription factors mediate an endogenous carbon-sensing mechanism regulating 'light-foraging' hypocotyl growth. Dynamic analysis of growth, protein abundance and gene expression support a 'regulatory relay' model of the seedling growth network where the importance of each hub changes over time.

Acknowledgements

I want to thank the Biology department for providing alternative funding sources to support me through the Sargent Award and the WRF Hall Fellowship. These funds really enriched my graduate school experience. This department has extremely helpful staff members that make the logistics of graduate school and research possible for all of us. Among these staff I would like to especially acknowledge Doug Ewing, Judy Farrow, Robert Goff, Alex Hansen, Dave Hurley, and Ben Wiggins.

The faculty I have interacted with during my time in the Biology department have been a constant source of encouragement, curiosity and inspiration. I would like to thank Toby Bradshaw, Bob Cleland, Janneke Hille Ris Lambers, Ray Huey, Linda Martin-Morris and Liz Van Volkenburgh for all of their support along the way. Bob always made time to sit down and have a chat with me about papers, milestones and life decisions. Janneke always caught me in the hallway with some motivational observation that helped keep me going. One that I think about often is sometimes giving 70% to something is the best you can do. One time I asked Ray how I was supposed to deal with all the worry of the global climate catastrophe and all the species dying and he profoundly said "Buy a good bottle of Scotch." Liz always had something unique and interesting to say, which always brought me joy. I'd like to thank Dave Parichy, Billie Swalla and Keiko Torii for all of their insightful feedback and brilliant contributions to my understanding of molecular biology.

My supervisory committee has been a pure joy to work with. What I fondly refer to as my 'Jedi Council' includes Jennifer Nemhauser ('Yoda'), Takato Imaizumi ('Mace Windu') and Ben Kerr ('Obi-Wan Kerr-nobi'). My GSR for most of grad school was Christine Queitsch and Soo-Hyung Kim graciously stepped in for my final exam. I was lucky enough to see Takato nearly every week in our joint lab meetings and I always appreciated his sound advice, invaluable observations and candid sense of humor. Half way through my first conversation with Ben, which was about whether or not plants could feel pain, I found out he was not a graduate student like I assumed but a professor in the department. This speaks volumes to his unassumingly humble nature and his willingness and delight for mental adventures. Christine always had some really clever and unexpected suggestion during my committee meetings which was wonderful. I am so thankful for all their guidance.

I have met a number of characters during grad school that I will never forget. The amount of revelry that has been shared with the following was awesome but never enough:

Jessica & Adam, Dou & Katherine, Jen & Justin, Cristy, Emily, and Steve.

You are all amazing freaks in this Freak Kingdom.

The members of the Nemhauser lab whether they like it or not are all now members of my family. These people have been there through good times and bad times. We have laughed, cried and foosed together and I cannot repay the debt I owe them all for their understanding and encouragement. Members I have over-lapped with include:

Andrej Arsovski, Anahit Galstyan, Chris Gee, Jessica Gusman, Yingying Li, Danny Liang, Britney Moss, Edith Pierre-Jerome, Autumn Walker, Julia Weisbrod, Vincent Wei Liu, Morgan Matz, Cristy Walcher, Zachary McCauley, Andy Chen, Rachel Denney, Edison Calaunan, Selma Alkafeef, Cameron Gomez, Kavitha Kuppusamy and Jesse Session. I would like to give a special thank you to Chris, Danny and Vincent for putting in all the hours necessary to make my research possible. Also for pretending to listen as my propaganda babbled on and on…

Thanks also to Matt Offenbacher for just being an amazing person to be around.

Endless appreciation goes to Jennifer Nemhauser. There are not enough words to say how lucky and honored I feel to have been a part of your lab. I was looking for a master to teach me how to do science. I got that and so much more. I feel like I can do anything with the tools you have given me (and hopefully continue to share). Thank you for being my vampire slayer.

The Master doesn't talk, she acts.
When her work is done,
the people say,
"Amazing: we did it, all by ourselves!"
--Tao Te Ching

The biology department has given me the best gift in the world, my husband. Travis Lilley and I met in the greenhouse while I was interviewing to be a grad student in the department. It was not long into my first year that we starting dating and became instantly inseparable. We have already been through so much and I am excited to see where life takes us. Travis had the hard job of

propping me up when there was not a single other force in the world that could do that. I thank him with all my heart.

"Nothing in biology makes sense except in the light of evolution."
--Theodosius Dobzhansky

Nothing in my life ever made any sense except in the light of Travis.

I also thank all my friends and family, which have been there in the past, present and future, who make my life so rich.

Dedication

This thesis is dedicated to all the people who loved and lost Simon Chan. Simon was a bright light in the world and I am so grateful to have known him. Wherever you are Simon, I send you my gratitude for setting me on this path with heart.

Chapter 1

Do trees grow on money? Auxin as the currency of the cellular economy

Stewart JL, Nemhauser JL (2010) Do trees grow on money? Auxin as the currency of the cellular economy. Cold Spring Harb Perspect Biol 2(2): a001420.

ABSTRACT

Auxin plays a role in nearly every aspect of a plant's life. Signals from the developmental program, physiological status and encounters with other organisms all converge on the auxin pathway. The molecular mechanisms facilitating these interactions are diverse; yet, common themes emerge. Auxin can be regulated by modulating rates of biosynthesis, conjugation and transport, as well as sensitivity of a cell to the auxin signal. In this chapter, we describe some well-studied examples of auxin's interactions with other pathways.

INTRODUCTION

It has often been said—sometimes in joyful wonderment, sometimes in teeth-grinding frustration—auxin does everything. While the major molecular details of the auxin pathway are largely known, many questions remain about how this one simple signaling molecule is responsible for directing so many diverse responses. The focus of this chapter is to try to illustrate several themes of how auxin acts in concert with other pathways to trigger specific cellular events in time and space.

One potentially useful analogy in trying to understand auxin's complicated roles is to think of it as money. Auxin does not have much intrinsic value—it stores very little energy or raw materials. However, like paper currency, it has great symbolic value, as an easily circulated means of facilitating transactions in the dynamic economy of plant life. As with currency, the amount, form, and location of auxin affects which transactions are possible. Other factors, such as what commodities are available in a given time and place, constrain which transactions auxin can facilitate. For instance, you cannot usually buy a goldfish at a shoe store, and it is quite challenging to purchase an ice cream sundae at 8 am.

Here, we describe some of the ways in which the developmental program, the abiotic environment, the circadian clock, other hormones, and other organisms modify the auxin response. Auxin can be regulated by modulating rates of biosynthesis, conjugation and transport,

as well as sensitivity of a cell to the auxin signal. In addition, the dominant pathway of biosynthesis, the composition and levels of IAA conjugates, the direction of auxin transport, and the downstream consequences of sensing auxin can all be radically altered by the cellular milieu. These context-specific networks help shape the outcome (transactions) of cellular exposure to auxin. Each of the networks impinging on the cellular response to auxin could easily fill a long chapter (or entire book) on their own. For brevity's sake, only a handful of examples will be described highlighting some of the molecular mechanisms by which other signaling networks intersect with the auxin pathway.

THE DEVELOPMENTAL PROGRAM

Auxin has been implicated in a disconcertingly large number of developmental events. Its role in embryonic polarity, organ initiation, and stem cell maintenance have all been extensively reviewed (De Smet and Jurgens 2007; Bowman and Floyd 2008; Vanneste and Friml 2009). In many of these cases, a general model can be discerned. First, auxin accumulates in a subset of cells, triggering a change in cell fate. This is followed by establishment of a graded distribution of auxin, often setting up an axis. Finally, this axis is used, sometimes in combination with other signals, to establish zones of cell identity. In these scenarios, auxin acts both to initiate early events and subsequently to refine the locations of specific programs.

The relationship between auxin and the developmental program can be viewed as bidirectional. A genetically-encoded developmental program pushes auxin into some cells and the auxin changes which genes are expressed in these cells. Part of the cellular response to auxin is to change auxin biosynthesis, conjugation, transport, and response. This then further alters the cellular environment. If auxin is cellular currency, the developmental program could be said to act like the government. By directing money to some programs and by levying or refunding taxes to certain groups or entities, governmental bodies exert a strong influence on where money flows. Within the cell, the suite of transcription factors are analogous to elected officials. Importantly, there is also a strong feedback from the auxin flux on which transcription factors are present. Similarly, how money is spent or saved often determines who gets elected. A few recent examples from the developing *Arabidopsis* fruit illustrate the coordination between auxin and the developmental program.

Auxin maxima are crucial for several steps in the development of the *Arabidopsis* gynoecium (Balanza et al. 2006; Ostergaard 2009). For example, auxin levels must be high for proper development of the apical tissues called the stigma and the style (Fig 1). Current models propose that auxin levels are manipulated through coordinated regulation of SHORT INTERNODE (SHI)/STYLISH (STY) transcription factor family-induced local auxin biosynthesis and the relative efficiency of auxin transport away from sites of synthesis (Sohlberg et al. 2006; Alvarez et al. 2009; Trigueros et al. 2009). The balance of production and transport determines the timing and location of style and stigmatic tissue development. Expression of *STY1* and *STY2* become restricted to the apical end of the gynoecium 1-2 days before stigmatic papillae become visible. An inducible *STY1* causes rapid induction of the gene encoding the auxin biosynthetic enzyme YUCCA4 and a concomitant increase in free auxin levels (Sohlberg et al. 2006). This auxin maximum in the ring of cells near the apex of gynoecium primordia triggers activation of the *NGATHA* (*NGA*) genes (Alvarez et al. 2009; Trigueros et al. 2009). These in turn alter the suite of transcription factors expressed in these cells, promoting apical cell identity. The NGA family also induces the *SHI/STY* genes, providing a positive feedback loop. Thus, the location and timing of the auxin maxima is genetically programmed and is required to trigger the next step in development.

The absence of auxin is also a potent signal, as demonstrated in the development of the valve margin separation layer where *Arabidopsis* fruits open for seed dispersal (Fig. 1). In wild-type plants, there is a marked reduction in auxin response (and likely auxin levels) in these boundary cells (Sorefan et al. 2009). The gene encoding the transcription factor INDEHISCENT (IND) is expressed in a thin stripe of cells at the boundary of the valves (Liljegren et al. 2004). IND is both necessary and sufficient to create these auxin minima and to direct the subsequent development of the boundary separation layer. IND regulates auxin transport away from these cells by directly regulating the expression of *PINOID* and related kinases (Sorefan et al. 2009). These kinases are able to direct the localization of PIN-FORMED (PIN) auxin efflux carriers (Friml et al. 2004; Robert and Offringa 2008). This is perhaps the first described case of a developmental program pushing a signaling molecule away from a subset of cells as a specific developmental trigger.

Recent work in the female gametophyte provides a striking example for the action of auxin gradients as positional cues on cell fate programs (Fig. 1). Several lines of evidence

suggest that location within the synctial gametophyte is a major determinant of egg cell fate (Pagnussat et al. 2009). By examining and manipulating auxin response in the embryo sac, researchers strongly implicated a gradient of auxin—highest at the micropylar end and lowest at the chalazal end—as a morphogenic factor directing cell fate (Pagnussat et al. 2009). In contrast to sporophytic tissue where graded auxin levels have thus far largely been attributed to balanced biosynthesis and transport, the gametophytic gradient appears to be maintained via regulated biosynthesis and conjugation/degradation. How this gradient is interpreted remains to be determined.

ABIOTIC ENVIRONMENT

The modulation of auxin in response to abiotic changes in the environment is heavily documented, including a well-studied role for auxin in tropic responses to gravity (Morita and Tasaka 2004) and light (Holland et al. 2009), a connection between auxin and response to salt stress (Wang et al. 2009), and an interaction between auxin and high temperature (Gray et al., 1998, Koini et al. 2009). Just as the distribution of money by the government is affected by lobbyists and special interest groups, the developmental program is strongly influenced by information from the abiotic environment. Among these various lobbies, light is perhaps the most powerful, and its intimate relationship with auxin regulation is among the most complex. Here we will focus on light's influence over auxin as an example of how auxin integrates environmental information into the developmental program. During light/dark transitions, plants change auxin responsiveness by regulating auxin signaling components. In contrast, when optimizing light access in crowded environments, plants appear to act primarily by altering auxin biosynthesis and transport.

Light is perceived by a number of photoreceptors. Blue light is perceived mainly by cryptochromes and phototropins, while red and far/red light is sensed by phytochromes. All three classes of photoreceptors have been linked with the auxin response (Chen et al. 2004; Li and Yang 2007; Salisbury et al. 2007; Holland et al. 2009). Here, we focus on the phytochromes, as one example. When the family of red/far-red light receptor proteins known as the phytochromes are stimulated by light, the equilibrium of the phytochrome pool shifts towards the active form. Activated phytochromes move into the nucleus and facilitate the degradation of the PHYTOCHROME INTERACTING FACTOR (PIF) and PHYTOCHROME INTERACTING

FACTOR-LIKE (PIL) proteins and help stabilize other transcription factors such as LONG HYPOCOTYL 5 (HY5) (Bae and Choi 2008). The degradation of HY5 in the dark requires the ubiquitin ligase CONSTITUTIVE PHOTOMORPHOGENIC 1 (COP1) and the multi-protein CONSTITUTIVE PHOTOMORPHOGENIC 9 (COP9) signalosome (CSN) (Cluis et al. 2004).

In the light, HY5 accumulates and drives transcription associated with the light program. Plants deficient in HY5 show many hyper-auxin response phenotypes, such as faster growing lateral roots, higher number of lateral root primordia, and altered lateral root emergence. These phenotypes depend on the auxin receptor TRANSPORT INHIBITOR RESPONSE 1 (TIR1). When the *hy5* mutation is combined with a knock-out allele of *HY5 HOMOLOG (HYH),* the de-repression of auxin signaling is more severe (Sibout et al. 2006). Transcriptome analysis of *hy5* mutants reveals a widespread reduction in the expression level of many early auxin response genes, including the auxin transcriptional repressors *Aux/IAA*s. Consistent with this finding, HY5 can directly bind the promoter of *AXR2/IAA7 in vitro*. Over-expression of *AXR2* rescues the *hy5* long hypocotyl phenotype (Cluis et al. 2004). A genome-wide survey of DNA bound by HY5 revealed binding sites in the promoters of nine *Aux/IAA* genes and six *ARF* genes (Lee et al. 2007). Interestingly, phyA can phosphorylate many Aux/IAAs *in vitro* (Colon-Carmona et al. 2000), though the relevance of this phosphorylation is still unknown. Thus, light strongly reduces cellular response to auxin by simultaneously increasing expression of the *Aux/IAAs* and perhaps by stabilizing the encoded proteins (Fig. 2A).

While light blocks auxin transactions in the cell, the absence of light promotes them (Fig 2B). When light levels are low, positive regulators of light signaling such as HY5 and HYH are degraded, leading to lower levels of auxin repressors. Mutations in many CSN subunits result in plants exhibiting a light-grown phenotype when grown in the dark (Schwechheimer et al. 2001). Such mutants also show decreased apical dominance, dwarfism, and decreased root growth inhibition by auxin. Antisense lines with reduced expression of the CSN5 subunit of the CSN have lower expression levels of *Aux/IAA* genes and increased Aux/IAA stability, similar to what is observed in low auxin conditions. The explanation for these effects is that the CSN directly facilitates the formation of SCF^{TIR1} complexes responsible for auxin-induced degradation of the Aux/IAAs. Another negative regulator of auxin transcription, AUXIN RESONSE FACTOR2 (ARF2), is repressed in the dark (Li et al. 2004). Reduced levels of Aux/IAAs and repressor ARFs would together elevate auxin sensitivity in dark-grown plants.

In addition to absolute presence or absence of light, light quality can also change the auxin balance (Fig. 2C). Appropriate response to changing light conditions is an essential part of a plant's daily routine. Light quality can be strongly altered by the proximity and positioning of nearby plants. Transcriptional studies show that auxin-related genes make up the largest group of genes up-regulated by shade (Devlin et al. 2003) and auxin signaling mutants are impaired in their shade-avoidance responses (Vandenbussche et al. 2003). Free IAA accumulates in shaded plants through a process that requires an enzyme that catalyzes an early step in the auxin biosynthetic pathway known as SHADE AVOIDANCE 3 (SAV3) (Tao et al. 2008) or TRYPTOPHAN AMINOTRANSERASE 1 (TAA1) (Stepanova et al. 2008). Plant deficient in SAV3/TAA1 show shorter hypocotyls in shaded conditions (Tao et al. 2008). *SAV3/TAA1* is highly expressed in the leaves in a similar pattern as the auxin-responsive reporter DR5::GUS. In shaded conditions, DR5::GUS activity moves into the hypocotyl. This shift from leaves to stem is blocked by pre-treatment with the polar auxin transport inhibitor naphthylphthalamic acid (NPA). This is consistent with previous evidence for the involvement of polar auxin transport during hypocotyl elongation in response to far-red light (Jensen et al. 1998). It is still unclear how the light signal regulates this change in transport pattern.

Shade avoidance also requires the *PHYTOCHROME RAPIDLY REGULATED (PAR)* genes up-regulated shortly after experiencing shaded conditions. *PAR1* and *PAR2* encode transcription factors that negatively regulate shade avoidance response (Roig-Villanova et al. 2007). PAR1 and PAR2 locate to the nucleus and repress the expression of a subset of auxin responsive genes including *SAUR15* and *SAUR68*. This same ability of negatively regulating auxin-induced transcription during shade-avoidance was seen for the transcription factor *ATHB4,* another *PAR* gene (Sorin et al. 2009). Though the precise role of these negative regulators is unclear, auxin appears to be the target of both positive and negative control.

CIRCADIAN CLOCK

Complementing the guidance from the developmental program and the environment, plants use the circadian system to regulate auxin response. There is emerging evidence that the clock modulates auxin metabolism, transport, and signaling, determining how much auxin is available and how readily auxin can be perceived at different times of the day (Fig. 3). In effect,

the circadian system sets the operating hours during which specific transactions may be conducted.

Decapitation experiments show that circadian controlled rhythmic elongation of the *Arabidopsis* inflorescence stem requires auxin transport from the apex (Jouve et al. 1999). Rhythmic growth can be restored by adding exogenous auxin to the tip of a decapitated stem. If polar auxin transport is blocked with NPA, rhythmic growth stops. Circadian fluctuations of IAA-aspartic acid conjugates in the stem suggest that the clock may control availability of auxin by regulated de-conjugation in combination with polar auxin transport. In a genome-wide study of clock-regulated genes, a large over-representation of auxin-related genes were identified (Covington and Harmer 2007). Genes in this group are involved in auxin biosynthesis, conjugation, transport, and signaling. In addition, more than half of highly auxin-induced genes are regulated by the clock. Neither elevated rates of auxin biosynthesis nor transport is required for these auxin-induced transcriptional oscillations, as treatment with auxin does not affect the phase or amplitude of an auxin-responsive reporter and NPA could cause slight phase delays but no change in amplitude. Timing of maximum induction of transcription by exogenous auxin is perfectly aligned with the time of peak endogenous auxin responses for untreated plants. This gating of auxin perception seems to extend to auxin physiological responses as well. Elongation of the hypocotyl under constant light in response to auxin was only induced when the auxin was applied during subjective night.

Unlike the bidirectional relationship observed with the developmental program, auxin does not play a major role in clock activity. While the SCF complex is involved in both auxin signal transduction and generating circadian rhythms, turn-over of the core clock component TOC1 is not affected by auxin (Harmon et al. 2008). Auxin applied at a range of concentrations is not able to reset the phase of the clock (Covington and Harmer 2007). Very high concentrations can dampen oscillations of clock reporter genes and produce slightly longer periods under constant conditions; however, near normal rhythms persist.

INTERACTIONS WITH OTHER HORMONES

Other hormones intersect with the auxin pathway at many levels. Cytokinin, brassinosteroids, gibberellins, jasmonic acid, ethylene, abscisic acid, and strigolactones all act at least in part through modifying auxin. If auxin is cellular currency, we could stretch our analogy

(perhaps to the breaking point) to say that other hormones are responsible for setting up the various types of shops into which auxin might flow, each stocking its own merchandise. Here, we present a small number of examples from this rapidly growing area of research.

The molecular details of the classical antagonism of cytokinin and auxin action in differentiation are becoming clear. In root meristems, auxin produced locally and transported from the shoot promotes cell division and stem cell identity (Dello Ioio et al. 2008; Chapman and Estelle 2009). Cytokinin acts to promote differentiation. It does this by altering levels of auxin transport and response (Fig. 4) (Dello Ioio et al. 2008; Chapman and Estelle 2009). Cytokinin exerts this effect by up-regulating *SHY2*, a member of the *Aux/IAA* family, repressors of the transcriptional response to auxin. Among the genes negatively regulated by high levels of *SHY2* are the *PIN* auxin transporters and *IPT5*, encoding a cytokinin biosynthetic enzyme. So, as cytokinin levels rise, SHY2 reduces auxin flow into meristematic cells while increasing the levels of auxin required to turn on genes needed for stem cell identity. At the same time, SHY2 likely causes a reduction in the local levels of cytokinin, leading to a negative feedback loop. Such a loop combined with local production of auxin at the root tip may be sufficient to establish the spatial architecture observed in the root—with stem cells at the tip, followed by cells transitioning into the differentiation program further away from the auxin pool.

In many cases, a large number of hormones may be coordinating auxin responses (Fig. 4). In the root apical meristem, auxin levels are also being modulated by jasmonic acid (Sun et al. 2009). In addition to down-regulating levels of auxin transporters, jasmonates increase expression of ASA1. ASA1 is an enzyme in tryptophan biosynthesis, a precursor to auxin. The size of the auxin pool and rate of transport laterally away from the tip directly determine the location and density of lateral root primordia. There is also new evidence that IAA or JA conjugates to tryptophan act as potent anti-auxins (Staswick 2009). How these compounds interfere with auxin response is currently unknown, though preliminary *in vitro* studies suggest that they are not competing with free IAA for TIR1 binding. Ethylene is also acting with auxin in the root. It inhibits root growth in part by modulating auxin levels and transport (Ruzicka et al. 2007; Stepanova et al. 2007; Stepanova et al. 2008; Yoo et al. 2009). In the root tip, ethylene induces expression of several genes important for auxin biosynthesis, including ASA1, enhancing local levels of auxin (Stepanova et al. 2008). Ethylene also up-regulates PIN2 and AUX1 likely facilitating auxin transport into the elongation and differentiation zones (Ruzicka et

al. 2007; Stepanova et al. 2007). The increase in auxin levels is proposed to inhibit cell growth and further sensitize cells to the effects of ethylene. Like light, ethylene stimulates turn-over of the repressor ARF2, likely further promoting auxin response in some cells (Li et al. 2004).

In addition to joining the fray in the root, brassinosteroids act on many aspects of auxin biology throughout the plant (Hardtke et al. 2007) (Fig. 4). In the presence of both hormones, many responses are greatly enhanced; while in the absence of brassinosteroids, auxin transcriptional responses are severely reduced (Nakamura et al. 2003; Bao et al. 2004; Nemhauser et al. 2004; Vert et al. 2008). How brassinosteroids are connected to the auxin pathway is an area of active investigation. It is known that prolonged exposure to brassinosteroids increases the polar transport of auxin (Bao et al. 2004; Li et al. 2005) and that brassinosteroids regulate the expression of many early auxin response genes (Nakamura et al. 2003; Goda et al. 2004; Nemhauser et al. 2004; Vert et al. 2005). These include Aux/IAA and PIN genes, likely leading to changes in the dynamics of auxin transcriptional responses and transport. Like light and ethylene, brassinosteroids appear to act on ARF2, a repressor ARF thought to compete with activator ARFs for cis-regulatory elements (Vert et al. 2008).

In roots, auxin regulates both the expression and intracellular localization of the putative transcription factor BREVIS RADIX (BRX) (Scacchi et al. 2009). *brx* mutants have short roots and impaired auxin responses (Mouchel et al. 2006). Both of these phenotypes can be rescued by application of brassinosteroids or by constitutively elevating expression of auxin-responsive genes through introduction of a loss-of-function mutation in *hy5* (Mouchel et al. 2006; Scacchi et al. 2009). Nuclear-localized BRX is required for cells to maintain normal levels of CONSTITUTIVE PHOTOMORPHOGENIC DWARF (CPD), a brassinosteroid biosynthetic enzyme. The strong loss of auxin responsiveness caused by reduced CPD expression in *brx* mutants further emphasizes the requirement of brassinosteroids for normal auxin responses. Treatment of wild-type roots with the polar auxin transport inhibitor NPA produces roots closely resembling those of *brx* mutants. Moreover, in low auxin conditions, BRX appears to co-localize with PIN1 at the plasma membrane. Together, these findings suggest that brassinosteroids are needed for normal auxin transport and that this transport is required for normal auxin response. Determining how transport feeds back on response and how brassinosteroids fit into this picture remain to be determined.

One potential insight into the brassinosteroid-auxin connection comes from the study of embryonic patterning. In the presence of high auxin levels at the tips of embryonic cotyledons, an ARF transcription factor MONOPTEROS (MP) directly induces expression of the transcription factor DORNROSCHEN (DRN) (Cole et al. 2009). *In vitro* and *in vivo* interaction studies showed that DRN interacts with the transcription factor BIM1 (Chandler et al. 2009), known to enhance brassinosteroid transcriptional responses (Yin et al. 2005). Loss of BIM1 causes similar patterning defects as loss of DRN, suggesting that this interaction is required for DRN function (Chandler et al. 2009). These and yet-to-be-described interactions among transcription factors on promoters of shared target genes are a compelling model to explain the interdependency observed between the two pathways.

PATHOGENS

If auxin acts as a currency driving the cellular economy, it is not surprising that many pathogens use auxin to aid infection and disease. Pathogens manipulate their hosts' auxin pathway at many stages throughout growth and development and in diverse ways (Fig. 5). They can synthesize their own auxin (Ali et al. 2009), increase native auxin biosynthesis (Chen et al. 2007), re-route auxin transport (Grunewald et al. 2009), or alter auxin signal transduction (Padmanabhan et al. 2008). In this way, pathogens act as counterfeiters flooding cells with their auxin knock-offs or as greedy speculators manipulating the currency market for their own enrichment.

An association between increased disease development and auxin accumulation is well supported in diverse plant-pathogen interactions (Wang et al. 2007; Ding et al. 2008). In part, this may reflect auxin's ability to activate expansins that soften and degrade the cell wall (Ding et al. 2008). For example, the bacterial pathogen *Pseudomonas syringae* uses the type III effector AvrRpt2 to increase auxin content in host cells (Chen et al. 2007). Expressing *AvrRpt2* in plants is sufficient to increase levels of free IAA. This effect can be enhanced by inoculating *AvrRpt2*-expressing transgenic plants with either virulent or avirulent *P. syringae* strains. How *AvrRpt2* alters auxin levels is still not known, but the effect of this increase is clear. Whether auxin levels are manipulated by infection with the bacteria or by treatment of wild-type seedlings with exogenous auxin, the bacteria's ability to multiply within host tissues is positively correlated with auxin levels.

Pathogens can also redirect transport in order to increase auxin in particular cells. To exploit a host's resources, parasitic nematodes must establish nematode feeding sites, creating cysts of multiple cells that release nutrients easily and can spread to adjacent cells. Degrading the cell wall using auxin is an important part of this process (Grunewald et al. 2009). Shortly after exposure to the model parasitic nematode *Heterodera schachtii*, expression of the auxin transporters *PIN3* and *PIN4* are induced at the site of nematode attack (Grunewald et al. 2009). PIN3 localization is changed to orient the flow of auxin towards the sites adjacent to the initially parasitized plant cells. Conversely, the expression of *PIN1* and *PIN4* is strongly repressed after nematode infection. The current model suggests that down-regulating PIN1 and PIN4 prevents auxin efflux from the nematode feeding sites while PIN3 and PIN4 are repositioned to push auxin into adjacent cells priming them for feeding site expansion. This hypothesis is supported by the fact that *PIN1* knockouts show a decrease in cyst number, while double mutants such as *pin1pin3* and *pin1pin4* show an increased proportion of small cysts compared to wild-type.

Since high auxin levels aid in pathogen success, it is not surprising that many components of the plant's immune system—both basal and R-gene-mediated—are geared toward controlling auxin during an attack. Plants treated with flg22, the conserved N-terminal peptide from bacterial flagellin, produce the microRNA miR393, thought to target TIR1 (Navarro et al. 2006). Plants over-expressing miR393 show increased Aux/IAA stabilization and decreased transcription of auxin-responsive genes. Down-regulation of auxin response is accompanied by an increased ability to fight off infection by virulent Pto DC3000 as shown in *tir1* mutants or miR393 over-expressing plants. Moreover, infection of resistant rice plants by *Xanthomonas oryzae* pv *oryzae* causes rapid up-regulation *GH3.8*, an auxin conjugating enzyme. Overexpression of *GH3.8* results in plants with less free auxin, higher levels of IAA-amino acid conjugates, and reduced auxin induced transcriptional response. These plants, like many resistant plants carrying R genes, are able to suppress the auxin-induced expression of expansins early after pathogen inoculation.

Systemic acquired resistance allows plants to anticipate future pathogen attacks and is under the control of salicylic acid (Durrant and Dong 2004). Salicylic acid promotes disease resistance in part though repression of the auxin pathway (Wang et al. 2007). Salicylic acid down-regulates auxin transporters and receptors leading to decreased expression of auxin responsive genes. At the same time, salicylic acid up-regulates IAA conjugating enzymes and

increases the stability of Aux/IAA repressors. Consistent with these findings, accumulation of salicylic acid prevents expression of auxin reporters following fungal infection. When salicylic acid is not allowed to accumulate or when salicylic acid-targeted Aux/IAAs are knocked-out, fungal disease development is enhanced.

One major difference between disease resistant and susceptible plants may be their ability to detect and prevent acute spikes of auxin activity at the onset of infection. However, if auxin responses are suppressed for prolonged periods, the reward of limiting pathogen spread may come at the expense of host growth. This may explain the observed trade-offs between plant productivity and disease resistance (Durrant and Dong 2004). Plants may be further constrained in their ability to limit pathogen access to auxin, because auxin plays a critical role in beneficial interactions between plants and microbes, especially during colonization (Contreras-Cornejo et al. 2009; Schafer et al. 2009). Auxin spending is risky business. It may lead to great growth and success, or leave the plant open to exploitation and ruin.

CONCLUDING REMARKS

Biologists know a tremendous amount about auxin—how levels can be manipulated, how its presence (or absence) can trigger specific cellular programs, and, increasingly, how auxin plays a central role in integrating diverse pathways directing plant life. An informal survey of auxin research over the last 20 years reveals some striking trends. Most obvious is that interest in this pathway remains strong. There has been an approximately 8-fold increase in the number of research articles where the term “auxin” appears between 1989 and 2009. In addition, a clear shift in the direction of research can be observed. In 1989, approximately 60% of papers described a core auxin signaling component—genes involved in auxin metabolism, signaling, or transport. Approximately 40% were primarily concerned with connecting auxin with a developmental or physiological program (including other hormones and biotic interactions). By 1999, the relative proportions of papers on core auxin components versus those relating auxin to other pathways had been reversed. This switch appears permanent. More than 70% of papers published in the first half of 2009 are primarily concerned with how auxin interacts with other pathways. Areas of particularly dramatic gains are connections with other hormones (~5% in 1989 vs. ~20% in 2009) and the role of auxin in biotic interactions (~10% in 1989 vs. ~20% in 2009). This reflects the logical progression of a field: initiating exploration close to the starting

point, then using these initial findings to explore more distant areas. From another vantage, this trend likely reflects the development of sufficiently sophisticated tools to tackle more complex problems. Either way, it is clear that the future of auxin research, like studies of the global economy, is only going to get more focused on connections.

ACKNOWLEDGEMENTS

We are indebted to Robert Cleland, Cristina Walcher, Andrew Chen, and Matthew Offenbacher for careful reading of this manuscript and stimulating discussions about the centrality of auxin in plant life. The idea that auxin might act as cellular money was first proposed to JLN by Niko Geldner several years ago. Any fault for its exuberant elaboration here is entirely our own. JLS is supported by the University of Washington Royalty Research Fund and the National Science Foundation Graduate Research Fellowship Program. Funding for work on auxin in our lab is provided by the University of Washington Royalty Research Fund and National Science Foundation IOS-0919021.

LITERATURE CITED

Ali, B., Sabri, A.N., Ljung, K., and Hasnain, S. 2009. Auxin production by plant associated bacteria: impact on endogenous IAA content and growth of Triticum aestivum L. *Lett Appl Microbiol* **48**(5): 542-547.

Alvarez, J.P., Goldshmidt, A., Efroni, I., Bowman, J.L., and Eshed, Y. 2009. The NGATHA Distal Organ Development Genes Are Essential for Style Specification in Arabidopsis. *Plant Cell*. **21**(5):1373-93

Bae, G. and Choi, G. 2008. Decoding of light signals by plant phytochromes and their interacting proteins. *Annu Rev Plant Biol* **59**: 281-311.

Balanza, V., Navarrete, M., Trigueros, M., and Ferrandiz, C. 2006. Patterning the female side of Arabidopsis: the importance of hormones. *J Exp Bot* **57**(13): 3457-3469.

Bao, F., Shen, J., Brady, S.R., Muday, G.K., Asami, T., and Yang, Z. 2004. Brassinosteroids interact with auxin to promote lateral root development in Arabidopsis. *Plant Physiology* **134**(4): 1624-1631.

Bowman, J.L. and Floyd, S.K. 2008. Patterning and polarity in seed plant shoots. *Annual Review of Plant Biology* **59**: 67-88.

Chandler, J.W., Cole, M., Flier, A., and Werr, W. 2009. BIM1, a bHLH protein involved in brassinosteroid signalling, controls Arabidopsis embryonic patterning via interaction with DORNROSCHEN and DORNROSCHEN-LIKE. *Plant Mol Biol* **69**(1-2): 57-68.

Chapman, E.J. and Estelle, M. 2009. Cytokinin and auxin intersection in root meristems. *Genome Biol* **10**(2): 210.

Chen, M., Chory, J., and Fankhauser, C. 2004. Light signal transduction in higher plants. Annu Rev Genet. **38**: 87-117

Chen, Z., Agnew, J.L., Cohen, J.D., He, P., Shan, L., Sheen, J., and Kunkel, B.N. 2007. Pseudomonas syringae type III effector AvrRpt2 alters Arabidopsis thaliana auxin physiology. *Proc Natl Acad Sci U S A* **104**(50): 20131-20136.

Cluis, C.P., Mouchel, C.F., and Hardtke, C.S. 2004. The Arabidopsis transcription factor HY5 integrates light and hormone signaling pathways. *Plant J* **38**(2): 332-347.

Cole, M., Chandler, J., Weijers, D., Jacobs, B., Comelli, P., and Werr, W. 2009. DORNROSCHEN is a direct target of the auxin response factor MONOPTEROS in the Arabidopsis embryo. *Development* **136**(10): 1643-1651.

Colon-Carmona, A., Chen, D.L., Yeh, K.C., and Abel, S. 2000. Aux/IAA proteins are phosphorylated by phytochrome in vitro. *Plant Physiol* **124**(4): 1728-1738.

Contreras-Cornejo, H.A., Macias-Rodriguez, L., Cortes-Penagos, C., and Lopez-Bucio, J. 2009. Trichoderma virens, a plant beneficial fungus, enhances biomass production and promotes lateral root growth through an auxin-dependent mechanism in Arabidopsis. *Plant Physiol* **149**(3): 1579-1592.

Covington, M.F. and Harmer, S.L. 2007. The circadian clock regulates auxin signaling and responses in Arabidopsis. *PLoS Biol* **5**(8): e222.

De Smet, I. and Jurgens, G. 2007. Patterning the axis in plants--auxin in control. *Current Opinion in Genetics & Development* **17**(4): 337-343.

Dello Ioio, R., Nakamura, K., Moubayidin, L., Perilli, S., Taniguchi, M., Morita, M.T., Aoyama, T., Costantino, P., and Sabatini, S. 2008. A genetic framework for the control of cell division and differentiation in the root meristem. *Science* **322**(5906): 1380-1384.

Devlin, P.F., Yanovsky, M.J., and Kay, S.A. 2003. A genomic analysis of the shade avoidance response in Arabidopsis. *Plant Physiol* **133**(4): 1617-1629.

Ding, X., Cao, Y., Huang, L., Zhao, J., Xu, C., Li, X., and Wang, S. 2008. Activation of the indole-3-acetic acid-amido synthetase GH3-8 suppresses expansin expression and promotes salicylate- and jasmonate-independent basal immunity in rice. *Plant Cell* **20**(1): 228-240.

Durrant, W.E. and Dong, X. 2004. Systemic acquired resistance. *Annu Rev Phytopathol* **42**: 185-209.

Friml, J., Yang, X., Michniewicz, M., Weijers, D., Quint, A., Tietz, O., Benjamins, R., Ouwerkerk, P.B., Ljung, K., Sandberg, G., Hooykaas, P.J., Palme, K., and Offringa, R. 2004. A PINOID-dependent binary switch in apical-basal PIN polar targeting directs auxin efflux. *Science* **306**(5697): 862-865.

Goda, H., Sawa, S., Asami, T., Fujioka, S., Shimada, Y., and Yoshida, S. 2004. Comprehensive comparison of auxin-regulated and brassinosteroid-regulated genes in Arabidopsis. *Plant Physiology* **134**(4): 1555-1573.

Gray, W.M., Ostin, A., Sandberg, G., Romano, C.P., and Estelle, M. 1998. High temperature promotes auxin-mediated hypocotyl elongation in Arabidopsis. *Proc Natl Acad Sci U S A* **95**(12): 7197-202.

Grunewald, W., Cannoot, B., Friml, J., and Gheysen, G. 2009. Parasitic nematodes modulate PIN-mediated auxin transport to facilitate infection. *PLoS Pathog* **5**(1): e1000266.

Hardtke, C.S., Dorcey, E., Osmont, K.S., and Sibout, R. 2007. Phytohormone collaboration: zooming in on auxin-brassinosteroid interactions. *Trends in Cell Biology* **17**(10): 485-492.

Harmon, F., Imaizumi, T., and Gray, W.M. 2008. CUL1 regulates TOC1 protein stability in the Arabidopsis circadian clock. *Plant J* **55**(4): 568-579.

Holland, J.J., Roberts, D., and Liscum, E. 2009. Understanding phototropism: from Darwin to today. *J Exp Bot* **60**(7): 1969-1978.

Jensen, P.J., Hangarter, R.P., and Estelle, M. 1998. Auxin transport is required for hypocotyl elongation in light-grown but not dark-grown Arabidopsis. *Plant Physiol* **116**(2): 455-462.

Jouve, L., Gaspar, T., Kevers, C., Greppin, H., and Degli Agosti, R. 1999. Involvement of indole-3-acetic acid in the circadian growth of the first internode of Arabidopsis. *Planta* **209**(1): 136-142.

Koini, M.A., Alvey, L., Allen, T., Tilley, C.A., Harberd, N.P., Whitelam, G.C., and Franklin, K.A. 2009. High temperature-mediated adaptations in plant architecture require the bHLH transcription factor PIF4. *Curr Biol* **19**(5): 408-413.

Lee, J., He, K., Stolc, V., Lee, H., Figueroa, P., Gao, Y., Tongprasit, W., Zhao, H., Lee, I., and Deng, X.W. 2007. Analysis of transcription factor HY5 genomic binding sites revealed its hierarchical role in light regulation of development. *Plant Cell* **19**(3): 731-749.

Li, H., Johnson, P., Stepanova, A., Alonso, J.M., and Ecker, J.R. 2004. Convergence of signaling pathways in the control of differential cell growth in Arabidopsis. *Dev Cell* **7**(2): 193-204.

Li, L., Xu, J., Xu, Z.H., and Xue, H.W. 2005. Brassinosteroids stimulate plant tropisms through modulation of polar auxin transport in Brassica and Arabidopsis. *The Plant Cell* **17**(10): 2738-2753.

Li, Q.H. and Yang, H.Q. 2007. Cryptochrome signaling in plants. *Photochem Photobiol* **83**(1): 94-101.

Liljegren, S.J., Roeder, A.H., Kempin, S.A., Gremski, K., Ostergaard, L., Guimil, S., Reyes, D.K., and Yanofsky, M.F. 2004. Control of fruit patterning in Arabidopsis by INDEHISCENT. *Cell* **116**(6): 843-853.

Morita, M.T. and Tasaka, M. 2004. Gravity sensing and signaling. *Curr Opin Plant Biol* **7**(6): 712-718.

Mouchel, C.F., Osmont, K.S., and Hardtke, C.S. 2006. BRX mediates feedback between brassinosteroid levels and auxin signalling in root growth. *Nature* **443**(7110): 458-461.

Nakamura, A., Higuchi, K., Goda, H., Fujiwara, M.T., Sawa, S., Koshiba, T., Shimada, Y., and Yoshida, S. 2003. Brassinolide induces IAA5, IAA19, and DR5, a synthetic auxin response element in Arabidopsis, implying a cross talk point of brassinosteroid and auxin signaling. *Plant Physiology* **133**(4): 1843-1853.

Navarro, L., Dunoyer, P., Jay, F., Arnold, B., Dharmasiri, N., Estelle, M., Voinnet, O., and Jones, J.D. 2006. A plant miRNA contributes to antibacterial resistance by repressing auxin signaling. *Science* **312**(5772): 436-439.

Nemhauser, J.L., Mockler, T.C., and Chory, J. 2004. Interdependency of brassinosteroid and auxin signaling in Arabidopsis. *PLoS Biology* **2**(9): E258.

Ostergaard, L. 2009. Don't 'leaf' now. The making of a fruit. *Current Opinion in Plant Biology* **12**(1): 36-41.

Padmanabhan, M.S., Kramer, S.R., Wang, X., and Culver, J.N. 2008. Tobacco mosaic virus replicase-auxin/indole acetic acid protein interactions: reprogramming the auxin response pathway to enhance virus infection. *J Virol* **82**(5): 2477-2485.

Pagnussat, G.C., Alandete-Saez, M., Bowman, J.L., and Sundaresan, V. 2009. Auxin-dependent patterning and gamete specification in the Arabidopsis female gametophyte. *Science* **324**(5935): 1684-1689.

Robert, H.S. and Offringa, R. 2008. Regulation of auxin transport polarity by AGC kinases. *Current Opinion in Plant Biology* **11**(5): 495-502.

Roig-Villanova, I., Bou-Torrent, J., Galstyan, A., Carretero-Paulet, L., Portoles, S., Rodriguez-Concepcion, M., and Martinez-Garcia, J.F. 2007. Interaction of shade avoidance and auxin responses: a role for two novel atypical bHLH proteins. *EMBO J* **26**(22): 4756-4767.

Ruzicka, K., Ljung, K., Vanneste, S., Podhorska, R., Beeckman, T., Friml, J., and Benkova, E. 2007. Ethylene regulates root growth through effects on auxin biosynthesis and transport-dependent auxin distribution. *The Plant Cell* **19**(7): 2197-2212.

Salisbury, F.J., Hall, A., Grierson, C.S., and Halliday, K.J. 2007. Phytochrome coordinates Arabidopsis shoot and root development. *Plant J*. **50**(3):429-38.

Scacchi, E., Osmont, K.S., Beuchat, J., Salinas, P., Navarrete-Gomez, M., Trigueros, M., Ferrandiz, C., and Hardtke, C.S. 2009. Dynamic, auxin-responsive plasma membrane-to-nucleus movement of Arabidopsis BRX. *Development* **136**(12): 2059-2067.

Schafer, P., Pfiffi, S., Voll, L.M., Zajic, D., Chandler, P.M., Waller, F., Scholz, U., Pons-Kuhnemann, J., Sonnewald, S., Sonnewald, U., and Kogel, K.H. 2009. Manipulation of plant innate immunity and gibberellin as factor of compatibility in the mutualistic association of barley roots with Piriformospora indica. *Plant J*. **59**(3): 461-474.

Schwechheimer, C., Serino, G., Callis, J., Crosby, W.L., Lyapina, S., Deshaies, R.J., Gray, W.M., Estelle, M., and Deng, X.W. 2001. Interactions of the COP9 signalosome with the E3 ubiquitin ligase SCFTIRI in mediating auxin response. *Science* **292**(5520): 1379-1382.

Sibout, R., Sukumar, P., Hettiarachchi, C., Holm, M., Muday, G.K., and Hardtke, C.S. 2006. Opposite root growth phenotypes of hy5 versus hy5 hyh mutants correlate with increased constitutive auxin signaling. *PLoS Genet* **2**(11): e202.

Sohlberg, J.J., Myrenas, M., Kuusk, S., Lagercrantz, U., Kowalczyk, M., Sandberg, G., and Sundberg, E. 2006. STY1 regulates auxin homeostasis and affects apical-basal patterning of the Arabidopsis gynoecium. *Plant J* **47**(1): 112-123.

Sorefan, K., Girin, T., Liljegren, S.J., Ljung, K., Robles, P., Galvan-Ampudia, C.S., Offringa, R., Friml, J., Yanofsky, M.F., and Ostergaard, L. 2009. A regulated auxin minimum is required for seed dispersal in Arabidopsis. *Nature* **459**(7246): 583-586.

Sorin, C., Salla-Martret, M., Bou-Torrent, J., Roig-Villanova, I., and Martinez-Garcia, J.F. 2009. ATHB4, a regulator of shade avoidance, modulates hormone response in Arabidopsis seedlings. *Plant J* **59**(2): 266-277.

Staswick, P.E. 2009. The tryptophan conjugates of jasmonic and indole-3-acetic acids are endogenous auxin inhibitors. *Plant Physiol* **150**(3): 1310-1321.

Stepanova, A.N., Robertson-Hoyt, J., Yun, J., Benavente, L.M., Xie, D.Y., Dolezal, K., Schlereth, A., Jurgens, G., and Alonso, J.M. 2008. TAA1-mediated auxin biosynthesis is essential for hormone crosstalk and plant development. *Cell* **133**(1): 177-191.

Stepanova, A.N., Yun, J., Likhacheva, A.V., and Alonso, J.M. 2007. Multilevel interactions between ethylene and auxin in Arabidopsis roots. *Plant Cell* **19**(7): 2169-2185.

Sun, J., Xu, Y., Ye, S., Jiang, H., Chen, Q., Liu, F., Zhou, W., Chen, R., Li, X., Tietz, O., Wu, X., Cohen, J.D., Palme, K., and Li, C. 2009. Arabidopsis ASA1 Is Important for Jasmonate-Mediated Regulation of Auxin Biosynthesis and Transport during Lateral Root Formation. *Plant Cell* **21**(5): 1495-1511.

Tao, Y., Ferrer, J.L., Ljung, K., Pojer, F., Hong, F., Long, J.A., Li, L., Moreno, J.E., Bowman, M.E., Ivans, L.J., Cheng, Y., Lim, J., Zhao, Y., Ballare, C.L., Sandberg, G., Noel, J.P., and Chory, J. 2008. Rapid synthesis of auxin via a new tryptophan-dependent pathway is required for shade avoidance in plants. *Cell* **133**(1): 164-176.

Trigueros, M., Navarrete-Gomez, M., Sato, S., Christensen, S.K., Pelaz, S., Weigel, D., Yanofsky, M.F., and Ferrandiz, C. 2009. The NGATHA Genes Direct Style Development in the Arabidopsis Gynoecium. *Plant Cell* **21**(5): 1394-1409.

Vandenbussche, F., Vriezen, W.H., Smalle, J., Laarhoven, L.J., Harren, F.J., and Van Der Straeten, D. 2003. Ethylene and auxin control the Arabidopsis response to decreased light intensity. *Plant Physiol* **133**(2): 517-527.

Vanneste, S. and Friml, J. 2009. Auxin: a trigger for change in plant development. *Cell* **136**(6): 1005-1016.

Vert, G., Nemhauser, J.L., Geldner, N., Hong, F., and Chory, J. 2005. Molecular mechanisms of steroid hormone signaling in plants. *Annual Review of Cell and Developmental Biology* **21**: 177-201.

Vert, G., Walcher, C.L., Chory, J., and Nemhauser, J.L. 2008. Integration of auxin and brassinosteroid pathways by Auxin Response Factor 2. *Proc Natl Acad Sci U S A* **105**(28): 9829-9834.

Wang, D., Pajerowska-Mukhtar, K., Culler, A.H., and Dong, X. 2007. Salicylic acid inhibits pathogen growth in plants through repression of the auxin signaling pathway. *Curr Biol* **17**(20): 1784-1790.

Wang, Y., Li, K., and Li, X. 2009. Auxin redistribution modulates plastic development of root system architecture under salt stress in Arabidopsis thaliana. *J Plant Physiol*.

Yin, Y., Vafeados, D., Tao, Y., Yoshida, S., Asami, T., and Chory, J. 2005. A new class of transcription factors mediates brassinosteroid-regulated gene expression in Arabidopsis. *Cell* **120**(2): 249-259.

Yoo, S.D., Cho, Y., and Sheen, J. 2009. Emerging connections in the ethylene signaling network. *Trends Plant Sci* **14**(5): 270-279.

FIGURE LEGENDS

Figure 1. Many developmental events require modulation of auxin.

In the *Arabidopsis* fruit (gynoecium), auxin maxima, minima, and gradients are used to define the location and timing of crucial developmental milestones. In the apical tissues, a suite of transcription factors acts in a positive feedback loop to produce a local auxin pool. This spatially precise auxin accumulation triggers a change in the transcriptional network, leading to the development of style and stigma. More basal tissues also use auxin during development. Auxin is actively transported out of a thin stripe of cells at the valve margin. The change in localization of auxin transporters needed for creating this auxin minima is caused by developmentally-regulated expression of the transcription factor IND. Finally, in the female gametophyte, cell fate is highly correlated with position within the embryo sac. An auxin gradient—high at the micropylar end (near the egg cell) and low at the chalazal end—is essential for conveying this positional information. Coordinated regulation of biosynthesis and perhaps conjugation establish this pattern. Solid arrows represent strongly supported links, while dashed arrows indicate possible connections.

Figure 2. The auxin pathway is affected by the presence and quality of light.

A. Light stimulation reduces sensitivity to auxin. Activated phytochrome promotes the accumulation of auxin transcriptional repressors. Repression of degradation machinery, including the COP9 signalosome, results in stabilization of transcription factors such as HY5. B. In the dark, active degradation of light transcription factors results in reduced accumulation of auxin transcriptional repressors and high auxin sensitivity. C. In shaded conditions or close proximity to a neighboring plant, increased auxin biosynthesis and transport result in an increased transcriptional response that contributes to the shade avoidance syndrome. Dotted lines indicate decreased levels of proteins or complexes.

Figure 3. Plants use the circadian system to regulate auxin response.

Circadian regulation has been observed at every level of the auxin pathway. In continuous conditions, expression of genes involved in biosynthesis, transport, conjugation, and transcriptional repression peaks during subjective day or dusk. Conversely, receptor gene expression and the auxin transcriptional response peaks during subjective night or dawn. Thus,

transcriptional and growth effects show peak sensitivity to exogenous auxin treatment during subjective night.

Figure 4. Other hormones impact auxin levels and response.
Jasmonates, cytokinin, ethylene, and brassinosteroids all modulate cellular auxin levels through changes in biosynthesis and transport. Cytokinin, ethylene and brassinosteroids also alter how sensitive a cell is to the auxin available by manipulating levels of repressors of auxin transcription. Brassinosteroids likely interact with transcriptional activators as well, though the precise mechanism is still unknown.

Figure 5. The auxin pathway is a target of pathogen attack.
High auxin levels are correlated with increased disease development. Pathogens increase their chances of success through increased auxin biosynthesis and altered auxin transport. Plant hosts defend against this strategy by conjugating free auxin, inhibiting receptor production, and promoting accumulation of auxin transcriptional repressors. In counter-offensive strategies, pathogens target the host's ability to control auxin response.

Figure 1

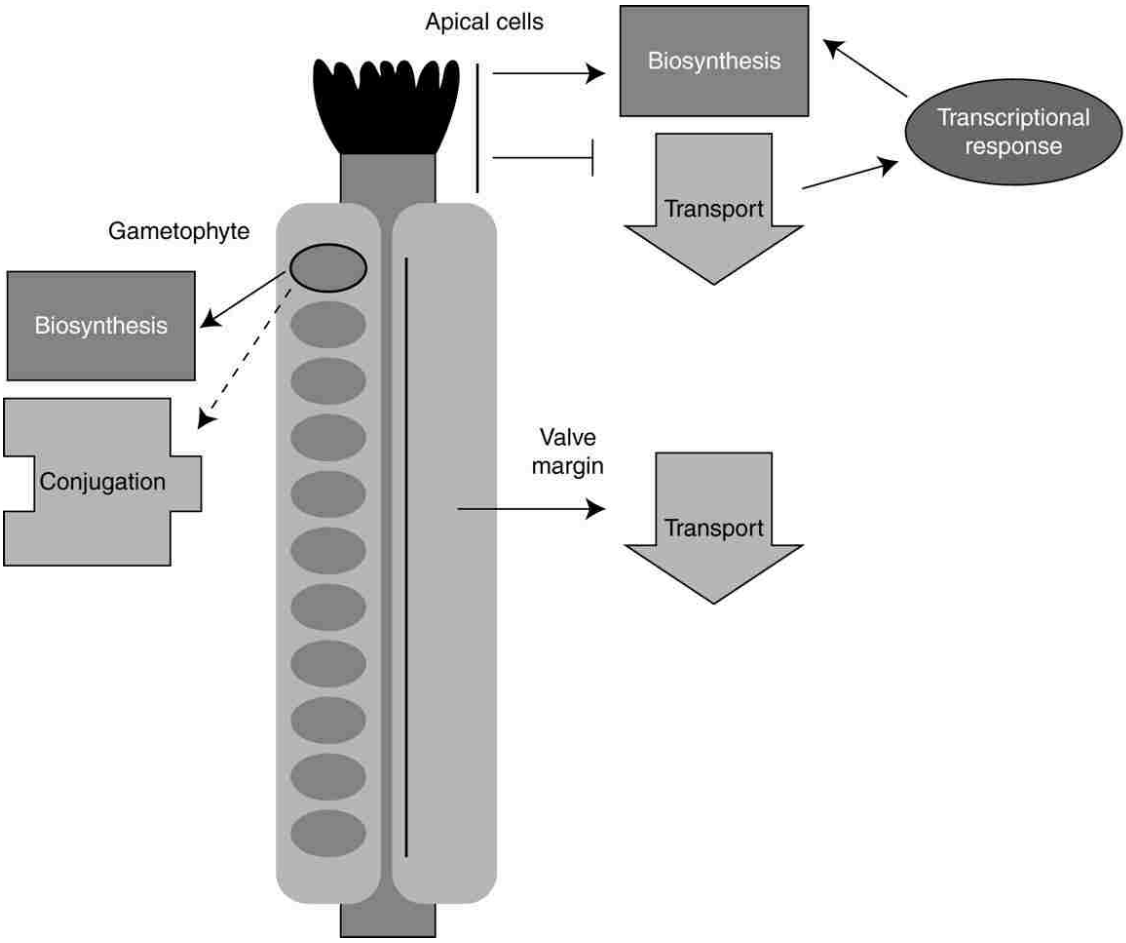
Apical cells
Biosynthesis
Transcriptional response
Transport
Gametophyte
Biosynthesis
Conjugation
Valve margin
Transport

Figure 2

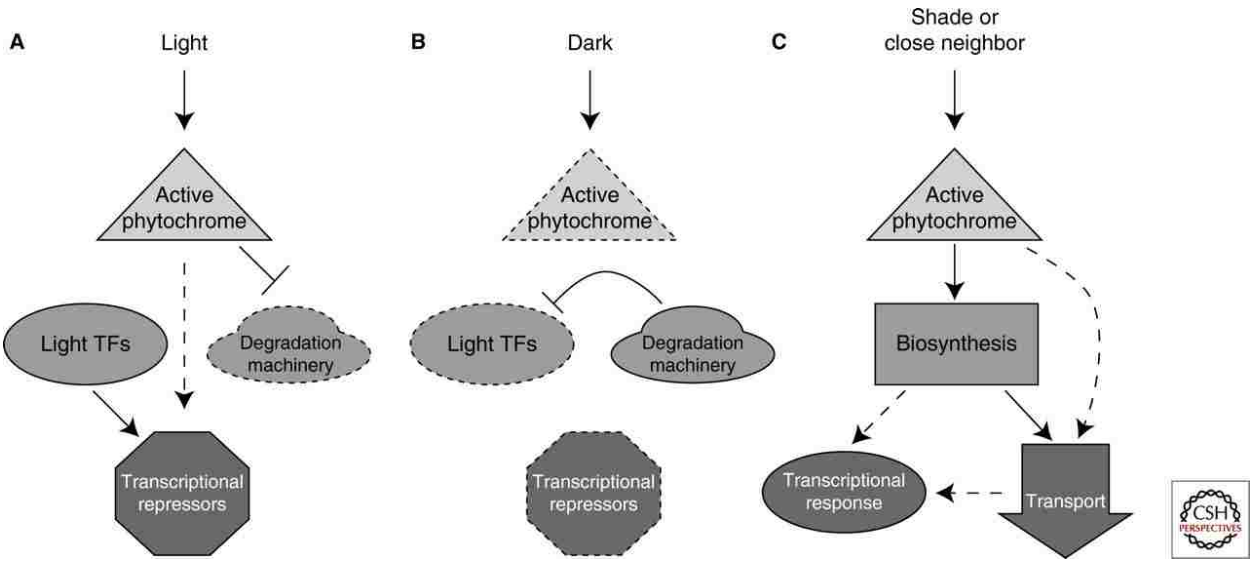
A
Light
Active phytochrome
Light TFs
Degradation machinery
Transcriptional repressors
B
Dark
Active phytochrome
Light TFs
Degradation machinery
Transcriptional repressors
C
Shade or close neighbor
Active phytochrome
Biosynthesis
Transcriptional response
Transport
CSH PERSPECTIVES

Figure 3

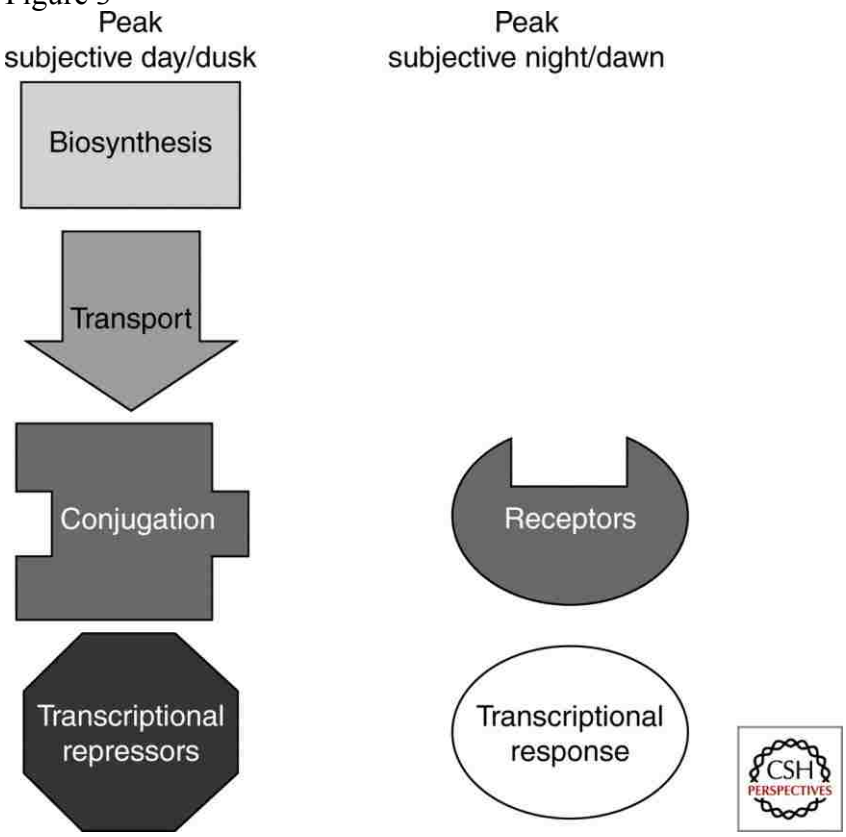
Peak
subjective day/dusk
Peak
subjective night/dawn
Biosynthesis
Transport
Conjugation
Receptors
Transcriptional
repressors
Transcriptional
response
CSH
PERSPECTIVES

Figure 4

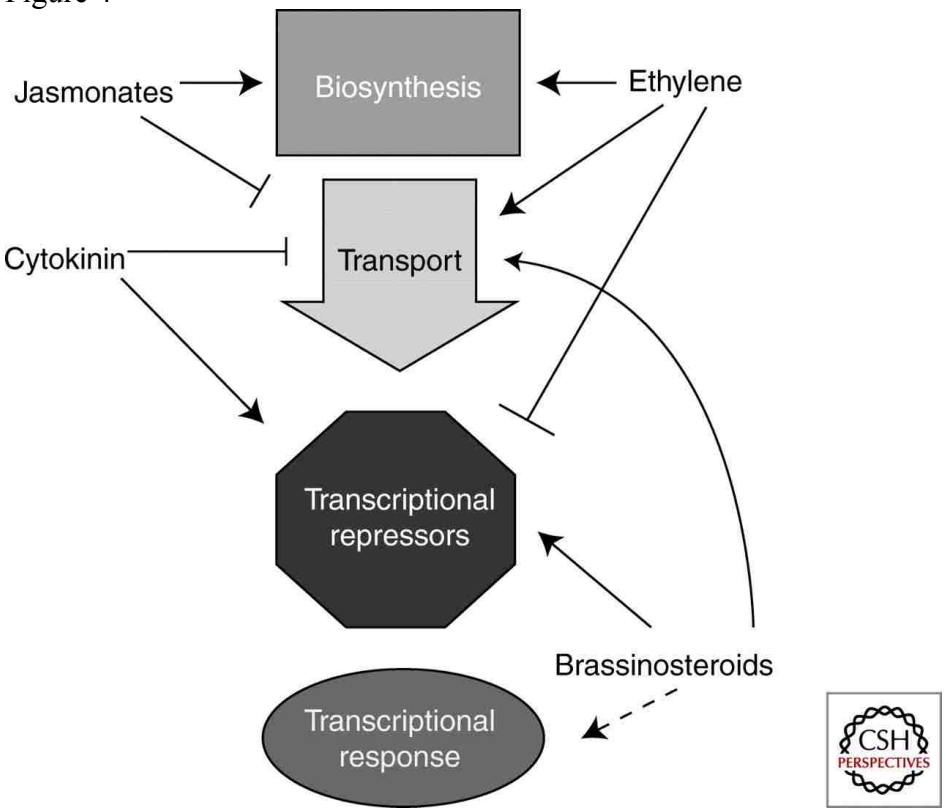
Jasmonates
Biosynthesis
Ethylene
Cytokinin
Transport
Transcriptional repressors
Brassinosteroids
Transcriptional response
CSH PERSPECTIVES

Figure 5

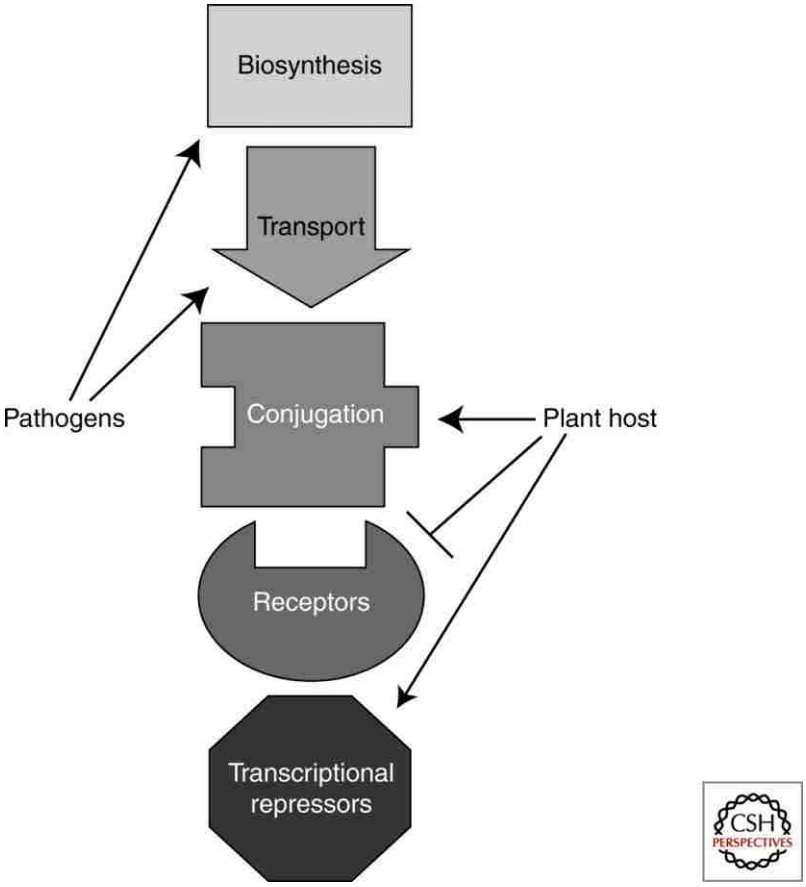
Biosynthesis
Transport
Pathogens
Conjugation
Plant host
Receptors
Transcriptional repressors

Chapter 2

PIF genes mediate the effect of sucrose on seedling growth dynamics

Stewart JL, Maloof JN, Nemhauser JL (2011) *PIF* genes mediate the effect of sucrose on seedling growth dynamics. PLoS One 6(5): p. e19894.

ABSTRACT

As photoautotrophs, plants can use both the form and amount of fixed carbon as a measure of the light environment. In this study, we used a variety of approaches to elucidate the role of exogenous sucrose in modifying seedling growth dynamics. In addition to its known effects on germination, high-resolution temporal analysis revealed that sucrose could extend the number of days plants exhibited rapid hypocotyl elongation, leading to dramatic increases in ultimate seedling height. In addition, sucrose changed the timing of daily growth maxima, demonstrating that diel growth dynamics are more plastic than previously suspected. Sucrose-dependent growth promotion required function of multiple phytochrome-interacting factors (PIFs), and overexpression of *PIF5* led to growth dynamics similar to plants exposed to sucrose. Consistent with this result, sucrose was found to increase levels of PIF5 protein. PIFs have well-established roles as integrators of response to light levels, time of day and phytohormone signaling. Our findings strongly suggest that carbon availability can modify the known photomorphogenetic signaling network.

INTRODUCTION

As a plant emerges from the seed, it must make an accurate and nuanced assessment of the light environment. Light-directed development, or photomorphogenesis, is marked by establishment of photosynthetically-competent embryonic leaves (cotyledons) optimally positioned towards a light source by the embryonic stem (hypocotyl) [1]. Hypocotyl elongation contributes to the positioning of cotyledons largely through differential cell elongation–in *Arabidopsis*, hypocotyl epidermal cells can elongate up to 100 times their embryonic size [2]. Levels of photosynthate reflect the seedling environment, and transportation of fixed carbon from source to sink cells is essential for this growth. Over the course of every day, the form and abundance of carbon is adjusted to meet the plant's metabolic needs [3]. During the day, fixed carbon is primarily stored as starch in the chloroplasts of photosynthetically-active cells. At

night, starch is converted into sucrose which travels from the leaves into the rest of the plant. Expression of starch degrading enzymes is circadian regulated [4,5], allowing plants to anticipate future carbon demands. The degradation of starch is highly correlated with growth and is tightly regulated to prevent the plant from exhausting its resources [6]. Indeed, plants have been shown to rapidly adjust their starch accumulation strategy to take best advantage of changing light conditions [7].

In addition to stimulating production of photosynthate, light inhibits hypocotyl elongation through activation of photoreceptors, primarily the red-light absorbing phytochromes (phys) and blue-light absorbing cryptochromes (crys) [8]. Over the past 30 years, genetic screens have implicated more than two dozen factors downstream of photoreceptor function [9]. A number of recent studies have focused attention on one group of these proteins, a family of light labile basic helix-loop-helix (bHLH) transcription factors called phytochrome interacting factors (PIFs). Several of the PIFs have been shown to directly interact with light-activated phytochromes and subsequently be targeted for degradation [10]. The PIFs have varying dimerization and phytochrome-binding characteristics and have been shown to regulate separate aspects of photomorphogenesis [11]. For example, *PIF1*, *PIF3*, *PIF4*, and *PIF5* contribute to hypocotyl elongation, while *PIF1* and *PIF6* regulate seed germination [12,13,14]. Plants lacking *PIF1*, *PIF3*, *PIF4*, and *PIF5* function, called *pifq* mutants, phenocopy morphological and transcriptional responses of light-grown plants even when grown in complete darkness [15,16]. PIF proteins act in part through regulating phytohormone pathways, including auxin and gibberellins [17,18,19,20,21,22,23].

How the very large number of factors influencing seedling growth are integrated is a complex problem that remains to be solved. Time-lapse imaging studies suggest that growth can be partitioned into discrete regulatory modules. For example, blue light inhibition of hypocotyl elongation can be separated into short-term growth slowing and longer-term maintenance phases, each under the control of different blue light receptors [24,25,26]. Genetically distinct phases of growth cessation and maintenance have also been reported for ethylene responses [27]. To understand the molecular mechanisms of these regulatory modules, periods of sensitivity must be defined for each factor that regulates photomorphogenesis.

In this study, we found that sucrose could alter many seedling growth parameters, including: germination, growth duration, and maximal growth rate. In addition, the presence of

sucrose could dramatically shift daily growth rhythms of hypocotyl elongation. Sucrose promotion of growth required the function of several members of the PIF family of transcription factors. Surprisingly, growth dynamics of plants exposed to sucrose could be partially mimicked by overexpression of *PIF5*. While sucrose did not dramatically alter expression of any of the *PIF* genes, sucrose treatment did result in higher levels of PIF5 protein. Together, our results place the sensing of carbon availability in the same PIF-mediated growth network as photoreceptors, the circadian clock and phytohormones.

RESULTS AND DISCUSSION

Sucrose promotes seedling growth by extending the number of days of hypocotyl elongation

The addition of 88 mM (3%) sucrose to plant media nearly doubled the height of six day old seedlings (Figure 1A), while causing a delay in germination (Figure 1C,D), consistent with previous reports [28,29,30],[31]. Addition of comparable levels of mannitol caused a strong reduction in overall hypocotyl elongation (Figure S1A), and had no effect on timing of germination (Figure S1B,C), suggesting that sucrose effects were not the result of changes in osmotic potential. Given these observations, we hypothesized that sucrose must alter growth rate and/or duration of growth to cause dramatically increased final hypocotyl lengths despite a shorter growth period.

To test this hypothesis, we assessed seedling growth rate using time-lapse imaging. Our measurements were synchronized to begin when seedlings had a visible apical hook (shortly after stage 0.5 as described in [32]). Hypocotyls were then measured at 30 minute intervals for three subsequent days. For plants grown in standard media without sucrose, distinct hypocotyl elongation dynamics were observed for each of the developmental stages highlighted in Figure 1B. After the apical hook became visible, hypocotyls exhibited low but consistent levels of elongation during the day and first half of the night followed by a gradual rise in growth rate towards dawn (Figure S2). As the cotyledons became distinct from one another, growth rate spiked at dawn (Figure 2A). By the time the cotyledons were fully open, growth rates were at the lowest levels overall with small, waning growth peaks at day/night transitions (Figure 2A).

Sucrose addition caused the most dramatic change in growth dynamics in seedlings with fully opened cotyledons, a time when seedlings grown without sucrose had largely stopped

growing. In contrast, plants grown with exogenous sucrose showed sustained strong rhythmic growth patterns (Fig 2B), reminiscent of patterns observed in previous studies [33]. This growth extension phenotype was further exaggerated in plants over-expressing *CIRCADIAN CLOCK ASSOCIATED 1* (*CCA1*ox) (Figure 2C,D), where reduced circadian clock function causes rapid growth throughout the entire night period [33]. Extra growth phases were not a result of osmotic effects of sucrose, as mannitol did not alter seedling growth dynamics (Figure S1D). Thus, sucrose addition leads to taller seedlings by prolonging the duration of growth in combination with a modest increase in growth rate. This extended growth period allows sucrose treated seedlings to overcome their early developmental delay.

Sucrose and other environmental factors can change timing of maximal daily growth

The external coincidence model for rhythmic growth proposed by Nozue et al. relies on two independent effects on the key growth regulators PIF4 and PIF5: the circadian system regulates gene expression and light alters protein stability [33]. In our experiments, plants grown in all conditions showed an initial burst of rapid dawn elongation once cotyledons were distinct (Figure 2). On media without sucrose (Figure 3A), subsequent periods of rapid elongation occurred at both dawn and dusk with decreasing amplitude. This is in contrast to the sustained and predominant dawn growth peaks previously reported for seedlings grown on sucrose [33].

Addition of sucrose increased growth rates, particularly at dawn (Figure 3C, black arrow, dashed versus solid line). This pattern began to resemble the previously published growth pattern by Nozue and colleagues, although a small growth peak at dusk could still be detected in our conditions (Figure 3C, grey arrow). When light intensity was increased from 30 μmol m^{-2} sec^{-1} to 60 μmol m^{-2} sec^{-1} (the conditions used in Nozue et al., 2007), total hypocotyl elongation was reduced. The greatest decrease in growth rate was observed at dusk (Figure 3B, grey arrow, dashed vs. solid lines). These results demonstrate that both light levels and sucrose addition can act independently to change the distribution of growth throughout the day. When both conditions are used, their combined effects are essentially additive (Figure 3D, dashed vs. solid lines). This highlights the critical importance of assessing growth rates in each new condition, as additional factors may also shape ultimate growth patterns. Interestingly, addition of mannitol could partially reproduce the effects of sucrose on daily growth peaks, although with substantially lower maximum growth rates (Figure 3E,F). This suggests that unlike early developmental

delays, sucrose effects on diel growth rhythms were at least partially through altered osmotic potential. Previous studies have shown that *PIF4* and *PIF5* transcripts can be high at both dusk and dawn [33,34,35], creating symmetrical potential growth windows. These two windows for PIF activity are further supported by the strong dusk growth peaks observed in continuous light conditions [36]. Our results suggest that the timing of rhythmic hypocotyl elongation is plastic and can be altered with subtle changes in growth conditions, including light intensity and media formulation. While our plants were all grown in artificial laboratory conditions, it is likely that variations in natural environments resulting in altered photosynthetic or developmental rates could lead to similar changes in growth patterns.

Growth promoting effects of sucrose require PIF function

It is well-established that sucrose can interfere with light responses [37,38,39]. PIF transcription factors contribute to hypocotyl elongation [16,40], chlorophyll biogenesis [41], and seed germination [12,13,14,41]—all of which are also affected by exogenous sucrose. To test whether sucrose was acting through the *PIF* family, we grew a number of single and multiple *PIF* mutants with and without sucrose.

In conditions without added sucrose, hypocotyl phenotypes of *pif* mutants matched previous reports (Figure 1A) [11]. When sucrose was added to the media, the growth promotion responses of *pif3*, *pif4* and *pif5* were significantly diminished compared to wild type (Figure 1A). As *PIF4* and *PIF5* have been shown to act partially redundantly in rhythmic hypocotyl growth [33], we also examined *pif4 pif5* double mutants. Loss of both *pif4* and *pif5* caused a further reduction in sucrose response, and additional loss of *PIF1* and *PIF3* function in the *pifq* mutant nearly eliminated sucrose promotion of growth (Figure 1A). Hypocotyls of *pifq* mutants grew more slowly than those of wild-type plants and for fewer days (Figure 2E). While sucrose could still cause modest growth of older *pifq* seedlings, average growth rates remained substantially lower than wild-type plants (Figure 2F).

If sucrose was acting through PIF proteins, we reasoned that higher levels of PIF activity might phenocopy sucrose effects. To test this, we focused on *PIF5*, as loss of *PIF5* function is known to have the most dramatic effect on rhythmic hypocotyl elongation of single loss-of-function *pif* mutants [33]. *PIF5*ox seedlings were taller than wild-type seedling grown on sucrose and showed a statistically enhanced response (Figure 1A). Moreover, even in the absence of

exogenous sucrose, *PIF5*ox seedlings showed substantial late growth (Figure 2G). This late growth rate was higher than that observed in *CCA1*ox seedlings (Figure 2C,D vs. 2G,H), suggesting that the phenotype of *PIF5*ox plants was not solely the result of defects in clock function.

Sucrose increases levels of PIF5 protein

PIF family members are under transcriptional and post-translational control [42]. To test sucrose effect on *PIF* expression, we extracted mRNA from *CCA1*ox seedlings grown with or without exogenous sucrose (Figure 4A,B). The *CCA1*ox background was used to attenuate potentially confounding effects of the circadian clock on *PIF* gene expression. Sucrose had no effect on expression of *PIF1* or *PIF7*, caused a modest increase in expression of *PIF3* and *PIF6*, and led to a slight decrease in expression of *PIF4* and *PIF5* (Figure 4B). The small effects on *PIF3*, *PIF4*, and *PIF5*—the genes with the largest loss-of-function effects on sucrose promotion of growth—suggest that sucrose is unlikely to alter growth dynamics through transcriptional control of *PIF* genes.

To test for sucrose effects on PIF protein, we grew HA-tagged *PIF5*ox seedlings [33] with or without sucrose (Figure 4C). These lines had similar growth dynamics and sucrose sensitivity as the untagged *PIF5*ox lines (Figure 4D), including a strong developmental delay (Figure S3) making it impossible to match developmental stages. We found that when comparing seedlings of the same age, sucrose dramatically increased PIF5 abundance in both light and dark periods (Figure 4C), although the effect was strongest in the light. One possible mechanism for this increase in PIF5 levels is through reduced function of phyB, which is known to destabilize PIF5 protein [43]. Surprisingly, *phyB* null mutants showed a wild-type response to sucrose (Figure 1A, Figure 2I,J), suggesting that sucrose effect on PIF activity is phyB-independent. It is possible that other factors, such as closely related phytochrome family members, may take over phyB's role in its absence.

The morphological transformations of photomorphogenesis are happening concurrently with major shifts in metabolism. Given that sucrose is synthesized and transported throughout the plant, it is possible that exogenous sucrose may conflict with the seedling's own photosynthesis-derived signals. Our results suggest a model where light-directed degradation of PIF protein is antagonized by high carbon availability. Previous work [44], in combination with

the results presented here, suggest that adding sucrose to the media may have a similarly dramatic effect on photomorphogenesis as phytohormone treatments. Sucrose dependency on PIF function provides direct molecular integration of photoreceptor and phytohormone signal transduction pathways with a yet-to-be-determined carbon-sensing mechanism.

MATERIALS AND METHODS

Plant materials and growth conditions. Wild type is *Arabidopsis thaliana* ecotype Col-0. *CCA1*ox (also known as *CCA1-34*) [45], *pif4* (*pif4-101)* [46], *pif5* (*pil6-1*) [47], *pif4 pif5* [46], *PIF5*ox (PIF5-OXL2) [47], HA-tagged *PIF5*ox [46], and *phyB-9* (also known as *hy3-EMS142*) [48] are as previously described. *pif1* (also known as *pil5-1*) [12] and *pif6-2* [13] were provided by G. Choi (Korea Advanced Institute of Science and Technology) and K. Halliday (Edinburgh University), respectively. *pif3-3* [49] and *pifq* [40] were provided by P. Quail (University of California, Berkeley). Seeds were sterilized for 20 min in 70% ethanol, 0.01% Triton X-100, followed by a rinse in 95% ethanol. After sterilization, seeds were suspended in 0.1% agar (BP1423, Fisher Scientific) and spotted on plates containing 0.5X Linsmaier and Skoog (LS) (LSP03, Caisson Laboratories, Inc.) with 0.8% agar. Sucrose (S2, Fisher Scientific) and D-mannitol (69-65-8, Acros Organics) treatments were performed by mixing 88mM of either additive into the media before sterilization. Seeds were then stratified in the dark at 4°C for 3 days. Plates were placed vertically in a Percival E-30B growth chamber set at 20°C in 30 or 60 $\mu mol\ m^{-2}sec^{-1}$ white light. All plants were grown in short-day conditions (8 hours light, 16 hours dark) and placed in the growth chamber at dawn.

Microscopy and time-lapse photography. Time-lapse photography is essentially as described in Nozue et al. (2007), Images were captured every 30 minutes by a charge-coupled device camera (PL-B781F, PixeLINK) equipped with a lens (NMV-25M1, Navitar) and IR longpass filter (LP830-35.5, Midwest Optical Systems, Inc.). Image capture was accompanied by a 0.5 second flash of infrared light by a custom built LED infrared illuminator (512-QED234, Mouser Electronics). A custom LabVIEW (National Instruments) program controlled image capture and illumination. Color seedling images were collected at 10X magnification using a Leica dissecting scope (S8APO, Leica Microsystems) and camera (DFC290, Leica Microsystems).

Hypocotyl measurements. For end-point analysis**,** hypocotyl lengths were measured from 12-25, 6-day old seedlings per treatment by scanning vertical plates using ImageJ software (http:/rsb.info.nih.gov/ij/). For growth rate analysis, hypocotyl lengths from at least 12 individuals were measured using ImageJ software for each time-lapse image (2208 X 3000 pixels). Growth rates were calculated from hypocotyl lengths using a custom script in MATLAB (MathWorks), available on request.

RNA extraction and qRT-PCR analysis. Seedlings were grown vertically in three rows on 0.5X LS plates with 2% agar. *PIF* expression analysis was performed on *CCA1*ox seedlings collected 8 hours from lights off (midnight) on day 5 for plates without sucrose and on day 6 for plates with sucrose to match developmental stage. Roots were manually removed at the time of collection. Samples were collected using a light equipped with a green filter (LS139, Acey Decy Equipment Co., Inc.). All samples were immediately frozen in liquid nitrogen and stored at -80°C until processing. Total RNA was extracted from tissue of approximately 1000 seedlings using the Spectrum Plant Total RNA Kit (Sigma), total RNA was treated with DNaseI on columns (Qiagen) and 1µg of eluted RNA was used for complementary DNA (cDNA) synthesis using iScript (Biorad). Samples were analyzed using SYBR Green Supermix (Biorad) reactions run in a Chromo4 Real-Time PCR system (MJ Research). Expression for each gene was calculated using the formula $(E_{target})^{-\Delta CPtarget(control-sample)}/(E_{ref})^{-\Delta CPref(control-sample)}$ [50] and normalized to a reference gene (At1g13320).

Western blot analysis. PIF5-HA abundance was detected in extracts of whole *PIF5HA*ox and wild-type seedlings collected 4 hours from lights on (midday) or 8 hours from lights off (midnight) on day 5. Total protein was extracted from approximately 100mg of tissue using the method described in [51], except that anti-HA-peroxidase (Roche) was used at a 1:1000 dilution. Samples were loaded at two concentrations (1X and 0.5X) to better estimate relative abundance. Anti-ACTIN antibodies (A0480, Sigma) were used at a 1:2000 dilution and detected with anti-Mouse (172-1011, Biorad) used at a 1:20,000 dilution. SuperSignal West Femto Maximum Sensitivity Substrate (Pierce) was used to detect signals.

Acknowledgments

We are indebted to Robert Cleland, Takato Imaizumi, Benjamin Kerr, Cristina Walcher, Matthew Offenbacher and Travis Lilley for careful reading of this manuscript. We would also like to thank Robert Cleland and Elizabeth Van Volkenburgh for insightful discussions; Takato Imaizumi for invaluable help with experimental design; Christopher Gee, Andrew Chen, Alex Leone, Young Hun Song, Shogo Ito, Armin Hinterwirth, Dave Hurley and Sylvia Yang for excellent technical assistance; and Giltsu Choi, Karen Halliday and Peter Quail for generous sharing of seed stocks.

LITERATURE CITED

1. Parks BM, Folta KM, Spalding EP (2001) Photocontrol of stem growth. Curr Opin Plant Biol 4: 436-440.
2. Gendreau E, Traas J, Desnos T, Grandjean O, Caboche M, et al. (1997) Cellular basis of hypocotyl growth in Arabidopsis thaliana. Plant Physiol 114: 295-305.
3. Stitt M, Lunn J, Usadel B (2010) Arabidopsis and primary photosynthetic metabolism - more than the icing on the cake. Plant J 61: 1067-1091.
4. Smith SM, Fulton DC, Chia T, Thorneycroft D, Chapple A, et al. (2004) Diurnal changes in the transcriptome encoding enzymes of starch metabolism provide evidence for both transcriptional and posttranscriptional regulation of starch metabolism in Arabidopsis leaves. Plant Physiol 136: 2687-2699.
5. Graf A, Schlereth A, Stitt M, Smith AM (2010) Circadian control of carbohydrate availability for growth in Arabidopsis plants at night. Proc Natl Acad Sci U S A 107: 9458-9463.
6. Smith AM, Stitt M (2007) Coordination of carbon supply and plant growth. Plant Cell Environ 30: 1126-1149.
7. Gibon Y, Pyl ET, Sulpice R, Lunn JE, Hohne M, et al. (2009) Adjustment of growth, starch turnover, protein content and central metabolism to a decrease of the carbon supply when Arabidopsis is grown in very short photoperiods. Plant Cell Environ 32: 859-874.
8. Vandenbussche F, Verbelen JP, Van Der Straeten D (2005) Of light and length: regulation of hypocotyl growth in Arabidopsis. Bioessays 27: 275-284.
9. Chory J (2010) Light signal transduction: an infinite spectrum of possibilities. Plant J 61: 982-991.
10. Monte E, Al-Sady B, Leivar P, Quail PH (2007) Out of the dark: how the PIFs are unmasking a dual temporal mechanism of phytochrome signalling. J Exp Bot 58: 3125-3133.
11. Castillon A, Shen H, Huq E (2007) Phytochrome Interacting Factors: central players in phytochrome-mediated light signaling networks. Trends Plant Sci 12: 514-521.
12. Oh E, Kim J, Park E, Kim JI, Kang C, et al. (2004) PIL5, a phytochrome-interacting basic helix-loop-helix protein, is a key negative regulator of seed germination in Arabidopsis thaliana. Plant Cell 16: 3045-3058.
13. Penfield S, Josse EM, Halliday KJ (2009) A role for an alternative splice variant of PIF6 in the control of Arabidopsis primary seed dormancy. Plant Mol Biol 73: 89-95.

14. Piskurewicz U, Tureckova V, Lacombe E, Lopez-Molina L (2009) Far-red light inhibits germination through DELLA-dependent stimulation of ABA synthesis and ABI3 activity. EMBO J 28: 2259-2271.
15. Leivar P, Tepperman JM, Monte E, Calderon RH, Liu TL, et al. (2009) Definition of early transcriptional circuitry involved in light-induced reversal of PIF-imposed repression of photomorphogenesis in young Arabidopsis seedlings. Plant Cell 21: 3535-3553.
16. Shin J, Kim K, Kang H, Zulfugarov IS, Bae G, et al. (2009) Phytochromes promote seedling light responses by inhibiting four negatively-acting phytochrome-interacting factors. Proc Natl Acad Sci U S A 106: 7660-7665.
17. Koini MA, Alvey L, Allen T, Tilley CA, Harberd NP, et al. (2009) High temperature-mediated adaptations in plant architecture require the bHLH transcription factor PIF4. Curr Biol 19: 408-413.
18. Oh E, Yamaguchi S, Kamiya Y, Bae G, Chung WI, et al. (2006) Light activates the degradation of PIL5 protein to promote seed germination through gibberellin in Arabidopsis. Plant J 47: 124-139.
19. Oh E, Yamaguchi S, Hu J, Yusuke J, Jung B, et al. (2007) PIL5, a phytochrome-interacting bHLH protein, regulates gibberellin responsiveness by binding directly to the GAI and RGA promoters in Arabidopsis seeds. Plant Cell 19: 1192-1208.
20. de Lucas M, Daviere JM, Rodriguez-Falcon M, Pontin M, Iglesias-Pedraz JM, et al. (2008) A molecular framework for light and gibberellin control of cell elongation. Nature 451: 480-484.
21. Feng S, Martinez C, Gusmaroli G, Wang Y, Zhou J, et al. (2008) Coordinated regulation of Arabidopsis thaliana development by light and gibberellins. Nature 451: 475-479.
22. Alabadi D, Gallego-Bartolome J, Orlando L, Garcia-Carcel L, Rubio V, et al. (2008) Gibberellins modulate light signaling pathways to prevent Arabidopsis seedling de-etiolation in darkness. Plant J 53: 324-335.
23. Stavang JA, Gallego-Bartolome J, Gomez MD, Yoshida S, Asami T, et al. (2009) Hormonal regulation of temperature-induced growth in Arabidopsis. Plant J.
24. Parks BM, Cho MH, Spalding EP (1998) Two genetically separable phases of growth inhibition induced by blue light in Arabidopsis seedlings. Plant Physiol 118: 609-615.
25. Folta KM, Spalding EP (2001) Unexpected roles for cryptochrome 2 and phototropin revealed by high-resolution analysis of blue light-mediated hypocotyl growth inhibition. Plant J 26: 471-478.
26. Folta KM, Pontin MA, Karlin-Neumann G, Bottini R, Spalding EP (2003) Genomic and physiological studies of early cryptochrome 1 action demonstrate roles for auxin and gibberellin in the control of hypocotyl growth by blue light. Plant J 36: 203-214.
27. Binder BM, O'Malley R C, Wang W, Moore JM, Parks BM, et al. (2004) Arabidopsis seedling growth response and recovery to ethylene. A kinetic analysis. Plant Physiol 136: 2913-2920.
28. Kazama H, Katsumi M (1973) Auxin-gibberellin relationships in their effects on hypocotyl elongation of light-grown cucumber seedlings. Responses of sections to auxin, gibberellin and sucrose. Plant and Cell Physiology 14: 449-458.
29. Zhang Y, Liu Z, Wang L, Zheng S, Xie J, et al. (2010) Sucrose-induced hypocotyl elongation of Arabidopsis seedlings in darkness depends on the presence of gibberellins. J Plant Physiol 167: 1130-1136.

30. Kurata T, Yamamoto KT (1998) petit1, a conditional growth mutant of Arabidopsis defective in sucrose-dependent elongation growth. Plant Physiol 118: 793-801.
31. Dekkers BJ, Schuurmans JA, Smeekens SC (2004) Glucose delays seed germination in Arabidopsis thaliana. Planta 218: 579-588.
32. Boyes DC, Zayed AM, Ascenzi R, McCaskill AJ, Hoffman NE, et al. (2001) Growth stage-based phenotypic analysis of Arabidopsis: a model for high throughput functional genomics in plants. Plant Cell 13: 1499-1510.
33. Nozue K, Covington MF, Duek PD, Lorrain S, Fankhauser C, et al. (2007) Rhythmic growth explained by coincidence between internal and external cues. Nature 448: 358-361.
34. Yamashino T, Matsushika A, Fujimori T, Sato S, Kato T, et al. (2003) A Link between circadian-controlled bHLH factors and the APRR1/TOC1 quintet in Arabidopsis thaliana. Plant Cell Physiol 44: 619-629.
35. Niwa Y, Yamashino T, Mizuno T (2009) Circadian Clock Regulates Photoperiodic Response of Hypocotyl Elongation through a Coincidence Mechanism in Arabidopsis thaliana. Plant Cell Physiol 50: 838-854.
36. Dowson-Day MJ, Millar AJ (1999) Circadian dysfunction causes aberrant hypocotyl elongation patterns in Arabidopsis. Plant J 17: 63-71.
37. Dijkwel PP, Huijser C, Weisbeek PJ, Chua NH, Smeekens SC (1997) Sucrose control of phytochrome A signaling in Arabidopsis. Plant Cell 9: 583-595.
38. Dijkwel PP, Kock P, Bezemer R, Weisbeek PJ, Smeekens S (1996) Sucrose Represses the Developmentally Controlled Transient Activation of the Plastocyanin Gene in Arabidopsis thaliana Seedlings. Plant Physiol 110: 455-463.
39. Cheng CL, Acedo GN, Cristinsin M, Conkling MA (1992) Sucrose mimics the light induction of Arabidopsis nitrate reductase gene transcription. Proc Natl Acad Sci U S A 89: 1861-1864.
40. Leivar P, Monte E, Oka Y, Liu T, Carle C, et al. (2008) Multiple phytochrome-interacting bHLH transcription factors repress premature seedling photomorphogenesis in darkness. Curr Biol 18: 1815-1823.
41. Huq E, Al-Sady B, Hudson M, Kim C, Apel K, et al. (2004) Phytochrome-interacting factor 1 is a critical bHLH regulator of chlorophyll biosynthesis. Science 305: 1937-1941.
42. Leivar P, Quail PH (2011) PIFs: pivotal components in a cellular signaling hub. Trends Plant Sci 16: 19-28.
43. Shen Y, Khanna R, Carle CM, Quail PH (2007) Phytochrome induces rapid PIF5 phosphorylation and degradation in response to red-light activation. Plant Physiol 145: 1043-1051.
44. Rolland F, Baena-Gonzalez E, Sheen J (2006) Sugar sensing and signaling in plants: conserved and novel mechanisms. Annu Rev Plant Biol 57: 675-709.
45. Wang ZY, Tobin EM (1998) Constitutive expression of the CIRCADIAN CLOCK ASSOCIATED 1 (CCA1) gene disrupts circadian rhythms and suppresses its own expression. Cell 93: 1207-1217.
46. Lorrain S, Allen T, Duek PD, Whitelam GC, Fankhauser C (2008) Phytochrome-mediated inhibition of shade avoidance involves degradation of growth-promoting bHLH transcription factors. Plant J 53: 312-323.
47. Fujimori T, Yamashino T, Kato T, Mizuno T (2004) Circadian-controlled basic/helix-loop-helix factor, PIL6, implicated in light-signal transduction in Arabidopsis thaliana. Plant Cell Physiol 45: 1078-1086.

48. Reed JW, Nagpal P, Poole DS, Furuya M, Chory J (1993) Mutations in the gene for the red/far-red light receptor phytochrome B alter cell elongation and physiological responses throughout Arabidopsis development. Plant Cell 5: 147-157.
49. Monte E, Tepperman JM, Al-Sady B, Kaczorowski KA, Alonso JM, et al. (2004) The phytochrome-interacting transcription factor, PIF3, acts early, selectively, and positively in light-induced chloroplast development. Proc Natl Acad Sci U S A 101: 16091-16098.
50. Pfaffl MW (2001) A new mathematical model for relative quantification in real-time RT-PCR. Nucleic Acids Res 29: e45.
51. Duek PD, Elmer MV, van Oosten VR, Fankhauser C (2004) The degradation of HFR1, a putative bHLH class transcription factor involved in light signaling, is regulated by phosphorylation and requires COP1. Curr Biol 14: 2296-2301.

FIGURE LEGENDS

Figure 1. Sucrose promotion of hypocotyl elongation requires activity of *PIF* genes.

(A) By six days, wild-type (WT) seedlings grown on 88 mM (3%) sucrose (light bars) were taller than seedlings grown without sucrose (dark bars). *pif3*, *pif4*, and *pif5* seedlings showed significantly reduced response to sucrose with further reductions observed in *pif4 pif5* mutants. Sucrose response was almost completely eliminated in *pifq* mutants lacking *pif1 pif3 pif4* and *pif5* function. Overexpression of *PIF5* (*PIF5*ox) resulted in elongated hypocotyls in the absence of exogenous sucrose and significantly enhanced growth promotion with added sucrose. *phyB* mutants where PIF5 levels are known to be increased resemble *PIF5*ox seedlings without sucrose, but show a wild-type response to sucrose. Error bars represent standard error for at least two independent experiments with 15-20 seedlings of each genotype in each experiment. Asterisks indicate significantly different responses between tested genotype and wild type (* = $p<0.05$, ** = $p<0.01$, *** = $p<0.001$) using a linear regression. Note the broken y-axis.

(B) After emergence, the radicle extended, tightly-hooked cotyledons became visible, and collet hairs at the hypocotyl/root junction appeared. Cotyledons then became distinct from one another, opening until the maximum angle between the cotyledons was reached.

(C-D) Three representative seedlings are shown at the dawn of day 3, 4, 5 and 6 in each panel.

(C) Wild-type seedlings entered the labeled stages shown in (B) by the dawn of day 3, 4 and 5, respectively.

(D) Addition of sucrose to the growth media resulted in the hook becoming visible approximately one day later (day 4). Sucrose also caused a modest delay in cotyledon opening. Seedlings were grown in short-day conditions in 30 μmol $m^{-2}sec^{-1}$ white light.

Figure 2. Sucrose requires *PIF* function to extend the number of days of seedling growth.

(A) Wild-type hypocotyl elongation rates diminished after the cotyledons opened.

(B) Addition of sucrose caused sustained high growth rates.

(C, D) In *CCA1*ox, sucrose caused a similar increase in duration of high hypocotyl elongations rates.

(E) *pifq* hypocotyls had lower average growth rates but similar dynamics to wild type.

(F) In *pifq* mutants, sucrose had substantially reduced effects on later stage hypocotyl elongation rates.

(G, H) Hypocotyls of *PIF5*ox seedlings had elevated early and late elongation rates without exogenous sucrose (G) but showed enhanced sensitivity to exogenous sucrose (H).
(I, J) *phyB* mutants showed similar growth rates to *PIF5*ox mutants with (I) and without (J) sucrose.
Each independent experiment is shown in grey and growth rates represent an average of 15-20 seedlings. Smoothed average growth rates are shown in black. A dashed black line representing wild-type growth rates without sucrose is shown for reference. Light and dark phases are indicated in the bars below the graphs. Schematic representations of seedling stages shown below the graphs are accurate for all seedlings, except *PIF5*ox (G,H). *PIF5*ox seedlings show an enhanced developmental delay phenotype, further exaggerated by addition of sucrose (Figure S3). Scale bar equals 0.05 mm/hr.

Figure 3. Diel patterns of rapid hypocotyl elongation phases are highly plastic.
(A) Hypocotyl elongation occurred at dusk (grey arrow) and dawn (black arrow) in our standard light conditions (30µmol m^{-2} sec^{-1}).
(B) Growth rates were lowered by increased light intensity (60µmol m^{-2} sec^{-1}), most notably at dusk.
(C) Seedlings grown on sucrose showed higher rates of hypocotyl elongation. This was particularly evident at dawn.
(D) When sucrose and higher light intensity (60µmol m^{-2} sec^{-1}) were combined, both the reduced growth rate at dusk and the increased growth rate at dawn were observed.
(E) Addition of mannitol caused increased hypocotyl elongation at dawn, similar to the effects of sucrose albeit with lower magnitude.
(F) Higher light intensity (60µmol m^{-2} sec^{-1}) reduced growth rates in mannitol, as was observed in other conditions.
Each independent experiment is shown in grey and growth rates represent an average of 15-20 seedlings. Smoothed average growth rates are shown in black. A dashed black line representing wild-type growth rates without additives is shown for reference. Light and dark phases are indicated in the bars below the graphs. Schematic representations of seedling stage are shown below the graphs. Scale bar equals 0.05 mm/hr.

Figure 4. Sucrose effects on seedling growth dynamics are likely mediated by stabilized PIF proteins.

(A) Expression of *PIF* genes at midnight on day 5 is shown for the no sucrose condition in *CCA*ox seedlings. Expression values are shown relative to a control gene. Error bars represent the standard error from three biological replicates.

(B) Relative values are shown for *PIF* gene expression in plants grown on sucrose normalized to expression in the no sucrose condition (shown in A). Sucrose had only modest effects on *PIF* gene expression. *PIF3* and *PIF6* were induced by sucrose, while *PIF4* and *PIF5* were slightly repressed. Seedlings were collected 8 hours after lights off (midnight) on day 5 (no sucrose) or day 6 (with sucrose) to match developmental stage. Error bars represent the standard error from three biological replicates.

(C) Sucrose increased PIF5-HA levels in both light and darkness. Wild-type or 35S::PIF5-HA seedlings [46] were collected 4 hours after lights on (Light) or 8 hours after lights off (Dark) on day 5. Anti-HA antibodies were used to detect PIF5-HA proteins (upper panel) and anti-ACTIN antibodies were used as a loading control (lower panel). Two concentrations (approximately 1X and 0.5X) are shown for each PIF5-HA sample. "N" and "S" indicate the no sucrose and sucrose treatments, respectively. Note that overall levels of protein are higher in light samples, as indicted by increased signal in the loading control. The blots shown here are representative of at least two experiments with independent biological replicates.

(D) High growth rates continue into day 5 for 35S::PIF5-HA seedlings supplied with exogenous sucrose. Each independent experiment is shown in grey and growth rates represent an average of 15-20 seedlings. Smoothed average growth rates are shown in black. Light and dark phases are indicated in the bars below the graphs. Asterisks indicate collection times for protein abundance assays. Note that *PIF5*ox seedlings have developmental defects, making it impossible to align collections by developmental stage (Figure S3). Scale bar equals 0.05 mm/hr.

Figure S1. Mannitol does not increase growth or delay early seedling development

(A) By day 6, seedlings grown on mannitol were significantly shorter than those grown on standard media. Error bars show standard error for three experiments with 12-25 six day old seedlings in each experiment. Asterisk indicates significance (Student's t-test: $p<0.05$).

(B, C) Addition of mannitol did not alter seedling progression through development (B). Wild-type seedlings grown on standard media are the same as those shown in Fig 1C. Three representative seedlings are shown at the dawn of day 3, 4, 5 and 6.
(D) Duration of rapid hypocotyl elongation was not sensitive to mannitol. Each independent experiment is shown in grey and growth rates represent an average of 15-20 seedlings. Smoothed average growth rates are shown in black. A dashed black line representing wild-type growth rates without mannitol is shown for reference. Light and dark phases are indicated in the bars below the graphs. Schematic representations of growth stages are shown below the graph. Scale bar equals 0.05 mm/hr.

Figure S2. In their earliest phase, hypocotyls showed low but consistent rates of elongation
Each independent experiment is shown in grey and growth rates represent an average of 15-20 seedlings. Smoothed average growth rates are shown in black. Light and dark phases are indicated in the bars below the graphs. Dawn of day 3 is shown. Schematic representation of growth stage is shown below the graph. Scale bar equals 0.05 mm/hr.

Figure S3. *PIF5*ox seedlings were developmentally delayed with and without sucrose
(A, B) Wild-type seedlings are the same as those shown in Fig 1C.
(C) *PIF5*ox seedlings were delayed in cotyledon opening.
(D) The *PIF5*ox developmental delay phenotype was exaggerated in the presence of sucrose. Three representative seedlings are shown at the dawn of day 3, 4, 5 and 6.

Figure 1

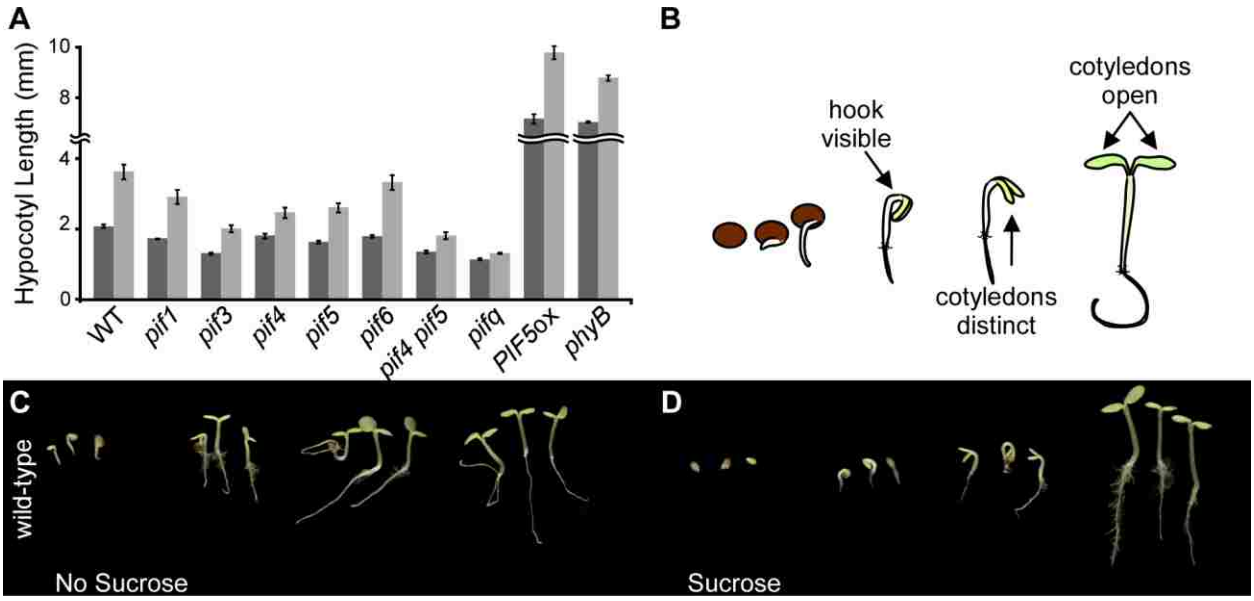
A
Hypocotyl Length (mm)
10
8
4
2
0
WT
pif1
pif3
pif4
pif5
pif6
pif4 pif5
pifq
PIF5ox
phyB
B
hook visible
cotyledons open
cotyledons distinct
C
wild-type
No Sucrose
D
Sucrose

Figure 2

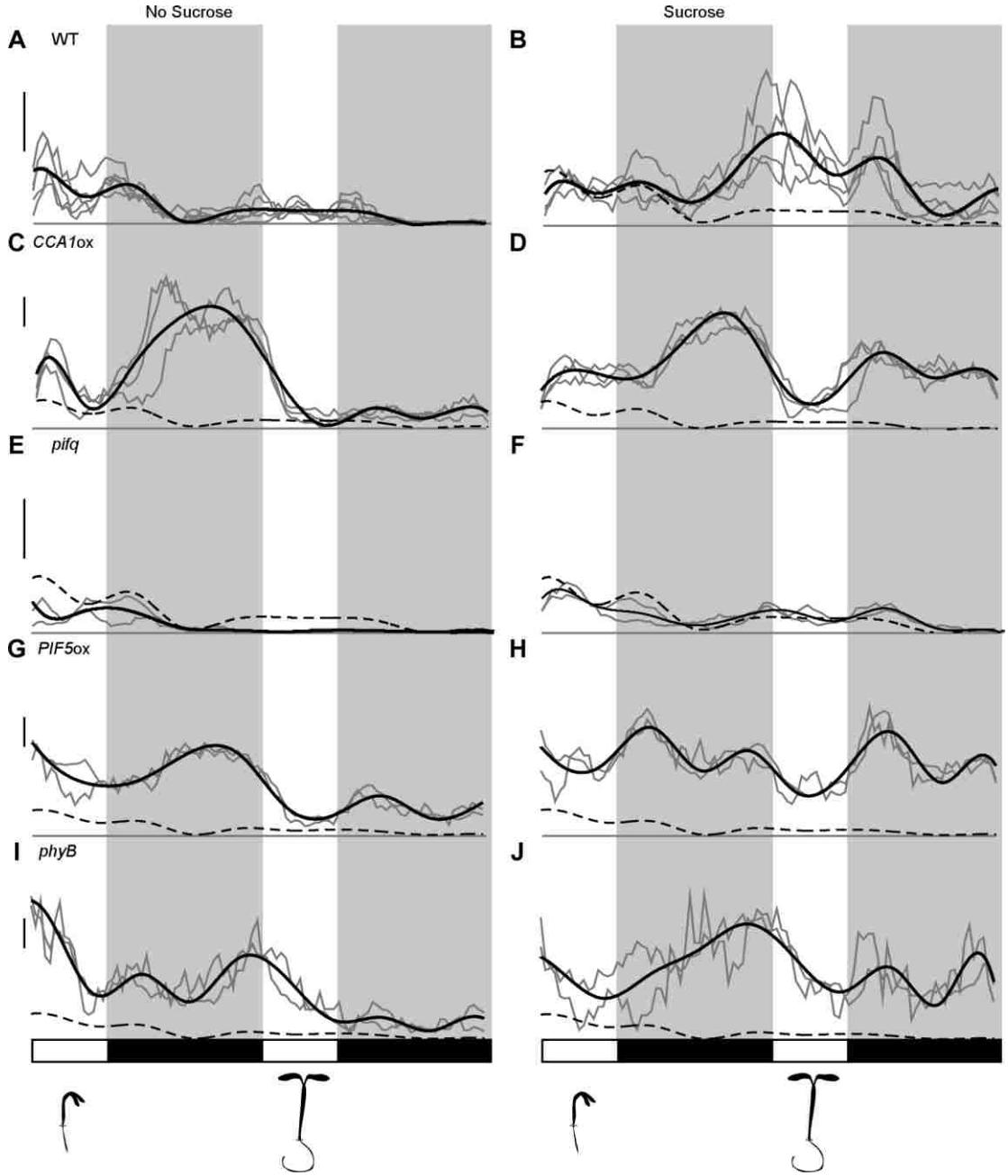

Figure 3

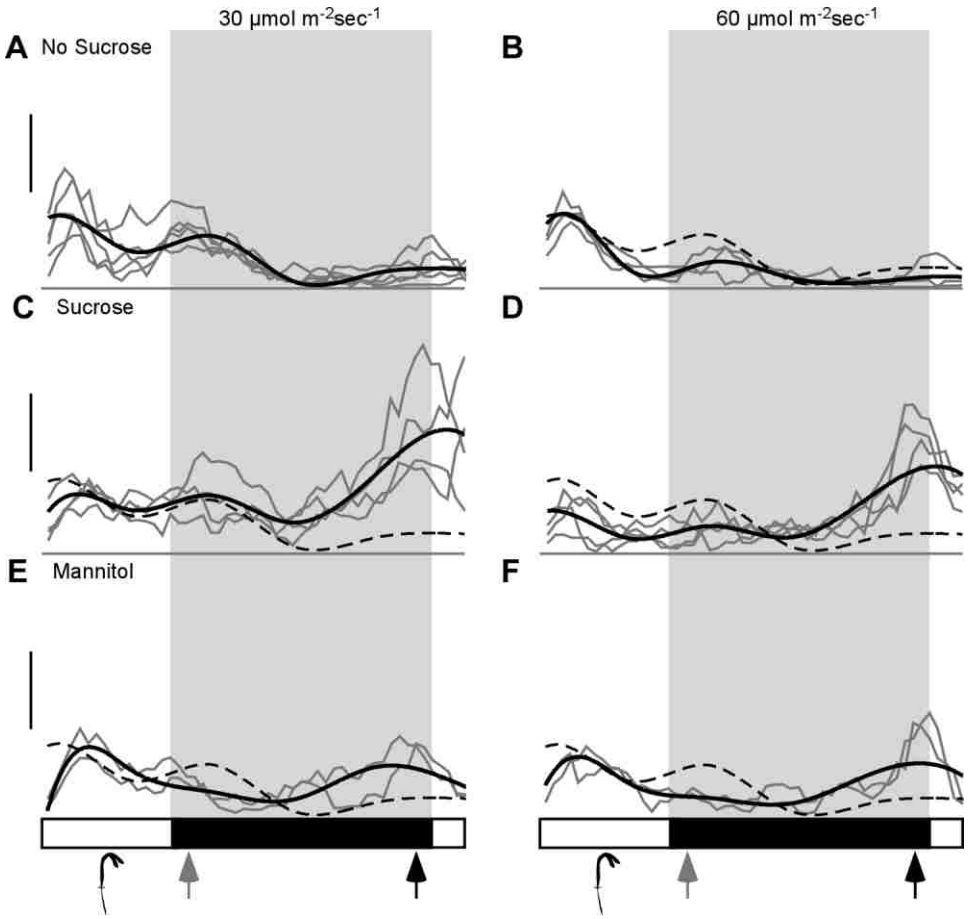
30 µmol m-2sec-1
60 µmol m-2sec-1
A No Sucrose
B
C Sucrose
D
E Mannitol
F

Figure 4

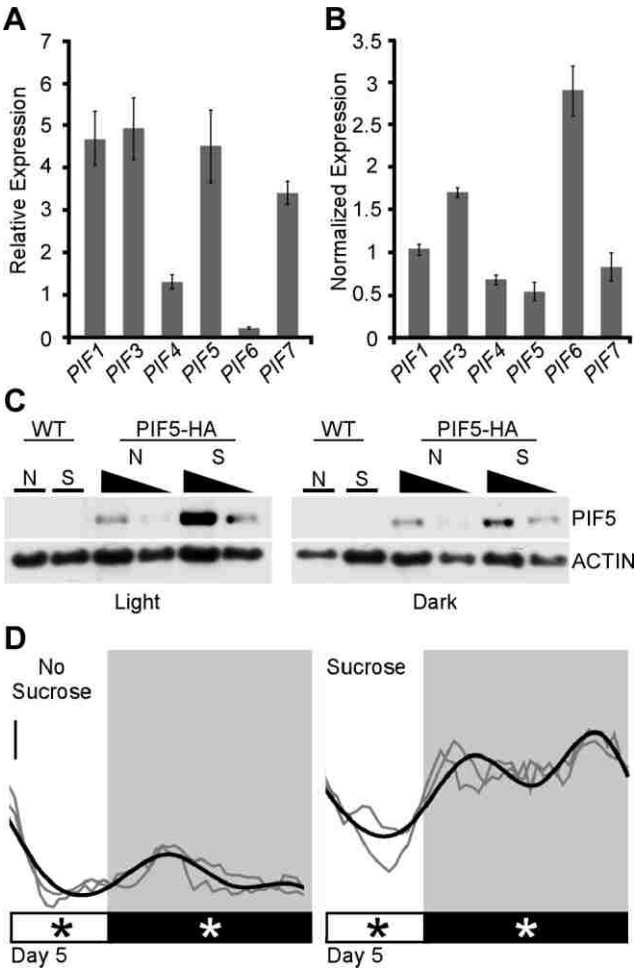
A
Relative Expression
0
1
2
3
4
5
6
7
PIF1
PIF3
PIF4
PIF5
PIF6
PIF7
B
Normalized Expression
0
0.5
1
1.5
2
2.5
3
3.5
PIF1
PIF3
PIF4
PIF5
PIF6
PIF7
C
WT
PIF5-HA
N
S
N
S
WT
PIF5-HA
N
S
N
S
PIF5
ACTIN
Light
Dark
D
No Sucrose
Sucrose
Day 5
Day 5

Figure S1

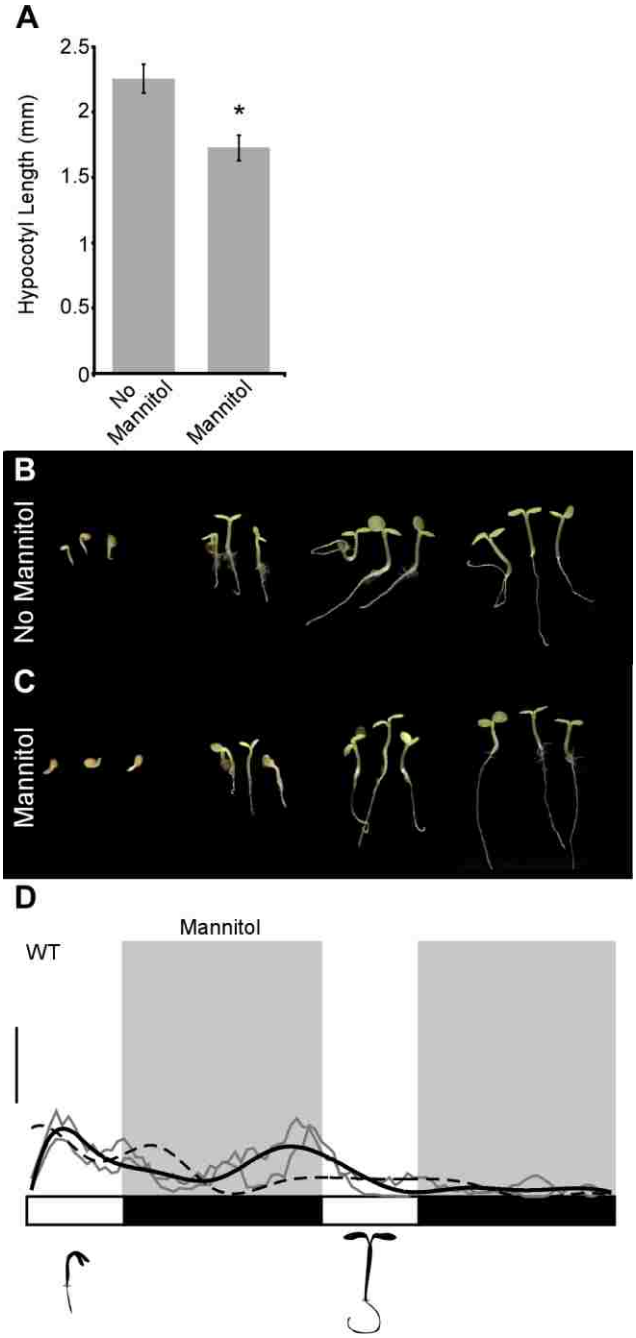
A
Hypocotyl Length (mm)
2.5
2
1.5
1
0.5
0
*
No Mannitol
Mannitol
B
No Mannitol
C
Mannitol
D
Mannitol
WT

Figure S2

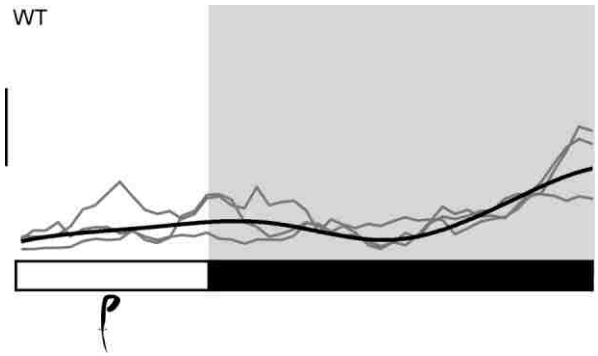

Figure S3

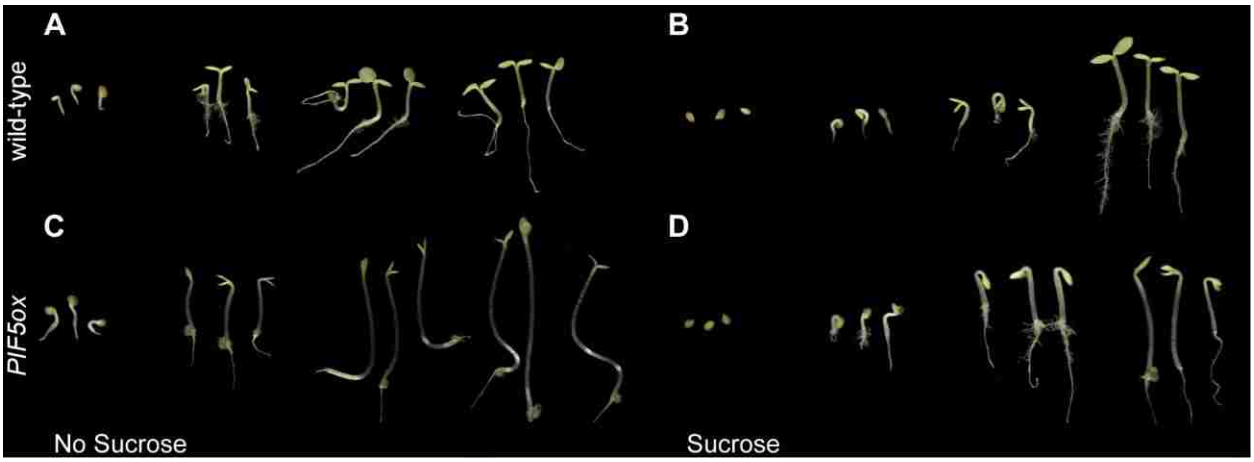

Chapter 3

An endogenous carbon-sensing pathway triggers increased auxin flux and hypocotyl elongation

Lilley JLS, Gee CW, Sairanen I, Ljung K, Nemhauser J. (2012) An endogenous carbon-sensing pathway triggers increased auxin flux and hypocotyl elongation. Plant Physiol 160(2): 2261-70.

ABSTRACT

The local environment has a substantial impact on early seedling development. Applying excess carbon in the form of sucrose is known to alter both timing and duration of seedling growth. Here, we show that sucrose changes growth patterns by increasing auxin levels and rootward auxin transport. Sucrose likely interacts with an endogenous carbon-sensing pathway via the PHYTOCHROME INTERACTING FACTOR (PIF) family of transcription factors, as plants grown in elevated CO_2 showed the same *PIF*-dependent growth promotion. Overexpression of *PIF5* was sufficient to suppress photosynthetic rate, enhance response to elevated CO_2, and prolong seedling survival in nitrogen limiting conditions. Thus, PIF transcription factors integrate growth with metabolic demands, and thereby facilitate functional equilibrium during photomorphogenesis.

INTRODUCTION

Nutrient and energy availability are key factors controlling growth in all organisms. This is particularly true of sessile plants, which use growth patterns to optimally exploit their local environment. 'Functional equilibrium' describes the balancing act whereby plants modify the allocation of biomass to match resource availability and utilization across diverse environments (Poorter et al., 2012). Even in suboptimal light conditions, seedlings will undergo photomorphogenesis—unfurling their embryonic leaves (cotyledons) and decelerating growth in the embryonic stem (hypocotyl)—to develop their photosynthetic capacity before seed reserves are exhausted. Seed reserves also contain nutrients required to support photomorphogenesis, but the developing root must quickly take over the task of nutrient acquisition. Photosynthetic rates in above-ground tissues shape the extent and pattern of growth in below-ground organs, although how this growth is coordinated is largely unknown. The hypocotyl is a likely path for such

signals as it acts as a physical bridge between the carbon-fixing leaves and nutrient-acquiring roots, and the extent of hypocotyl elongation has long been used as a proxy for the strength of the light cue.

In addition to external environmental cues like light, hypocotyl growth is regulated by an endogenous timing mechanism (Nozue and Maloof, 2006). Circadian bursts of hypocotyl elongation occur even when plants are exposed to constant light, although light intensity can strongly influence growth rate within these windows. A model has recently been proposed to explain how dual control by light and the circadian clock produces peaks and troughs in hypocotyl growth rates. Both cues converge on the PHYTOCHROME INTERACTING FACTOR (PIF) family of transcription factors, with clock regulation of *PIF* transcription and light regulation of PIF protein stability (Nozue et al., 2007). The result is a crepuscular pattern where seedling growth can occur at dawn and/or dusk. The relative proportion of growth at each twilight depends on the intensity of light, whether there are light/dark cycles, and the presence of supplemental sucrose in the media (Dowson-Day and Millar, 1999; Nozue et al., 2007; Stewart et al., 2011). The effect of sucrose on hypocotyl growth patterns, as with light, is through modulation of PIF protein abundance. While light promotes PIF protein turn-over, sucrose increases PIF abundance (Stewart et al., 2011).

Originally identified by their ability to directly bind with phytochrome photoreceptors, PIF transcription factors are now known to act as key growth regulators in response to a variety of environmental conditions (Leivar et al., 2009; Kumar et al., 2012; Li et al., 2012). Several recent studies have connected PIF-mediated growth control to the hormone auxin (Nozue et al., 2011; Franklin et al., 2011; Li et al., 2012; Sun et al., 2012). *YUCCA8* and *TRYPTOPHAN AMINOTRANSFERASE OF ARABIDOPSIS 1 (TAA1)*, encoding auxin biosynthetic enzymes, have been shown to be direct targets of PIF4 (Sun et al., 2012; Franklin et al., 2011). PIF7 has also been shown to directly bind to *YUCCA8* to increase stem growth in response to shade (Sun et al., 2012). Loss of function in PIF family members reduces auxin responsiveness (Nozue et al., 2011), and this relationship might partially explain circadian fluctuations in seedling sensitivity to exogenous auxin (Covington and Harmer, 2007).

In this study, we show that supplemental sucrose stimulates an endogenous carbon-sensing pathway that regulates hypocotyl elongation through altered auxin levels and distribution. Previously, we have shown that sucrose is required for sustained and rhythmic

hypocotyl elongation (Stewart et al., 2011). Here, we found that exogenous auxin could mimic the spatial and temporal growth effects of sucrose. Seedlings grown with supplemental sucrose had higher levels of free auxin and increased rootward auxin transport. As sucrose-driven changes in both auxin levels and seedling growth were *PIF*-dependent, we propose that PIF proteins integrate information about fixed carbon availability with other photormorphogenetic cues to shape seedling morphology. In support of this model, exposure to elevated levels of carbon dioxide (CO_2) stimulated hypocotyl growth in a *PIF*-dependent manner. Sucrose was also found to suppress seedling photosynthetic rates and increase nitrogen demand—physiological responses predicted for high fixed-carbon conditions. Consistent with the *PIF* family acting as a relay point in carbon sensing, overexpression of *PIF5* sensitized plants to elevated CO_2, strongly reduced photosynthetic rates and promoted prolonged seedling survival in nitrogen starvation conditions.

RESULTS

Sucrose increases auxin levels

The hypocotyl elongates until the cotyledons are fully opened, a period lasting approximately four days post germination (dpg) in short-day conditions (Stewart et al., 2011). Brassinosteroids, auxin, and gibberellins are well-studied promoters of seedling growth (Nozue and Maloof, 2006). Treatment with any of these hormones increased hypocotyl growth rates prior to day four (Fig. 1A). In contrast, only seedlings grown in the presence of the synthetic auxin picloram (pic) or the natural auxin indole-3-acetic acid (IAA) showed substantial growth into day 5 (Fig. 1, A-C). These auxin-induced effects on growth dynamics were strikingly similar to those caused by supplementation with sucrose (Stewart et al., 2011). In addition, auxin and sucrose treatments had a similar effect on a reporter marking the hypocotyl elongation zone [*PHYTOCHROME KINASE SUBSTRATE 4* (*PKS4*::GUS); (Schepens et al., 2008)]. While reporter expression was greatly reduced after 4 dpg in untreated seedlings, treatment with either sucrose or auxin led to strong staining through the fifth day (Fig. 1C), consistent with continued growth.

The similar pattern of growth between the two treatments led to the hypothesis that sucrose might be directly acting on the auxin pathway. Sucrose supplementation reduced the threshold for maximum auxin-induced growth by 5-fold (Fig. 1D). In addition, sucrose caused a

sharp reduction in the levels of the DII-VENUS reporter (Fig. 1E), which is rapidly turned over in the presence of auxin (Brunoud et al., 2012). Both of these results are consistent with sucrose leading to higher endogenous levels of auxin. Expression of a number of early auxin response genes, including *INDOLE-3-ACETIC ACID 17 (IAA17)*, *IAA19*, *IAA29* and *SMALL AUXIN UPREGULATED 15 (SAUR15)*, was modestly up-regulated in the presence of sucrose, especially in isolated shoots (Fig. 1F). A non-metabolizable sucrose analogue was previously shown to induce auxin-responsive genes (Gonzali et al., 2005), suggesting that sucrose may be acting as a direct signaling molecule.

Sucrose was found to significantly increase the amount of IAA per mg fresh weight in whole seedlings (Fig. 1G). Sucrose promotion of IAA levels was most clearly observed in dissected hypocotyls or roots (Fig. 1G). This finding is consistent with recent feeding experiments with heavy labeled auxin precursors that indicate that sugars can induce auxin biosynthesis in both shoot and root tissue (IS and KL, personal communication). The effect of sucrose on auxin levels may be through altered expression of auxin biosynthetic genes. Expression of *YUCCA8* was induced by sucrose in the shoot (Fig. 1F), but expression of *TAA1* was unchanged with sucrose treatment (Fig. 1F).

Sucrose promotes rootward auxin transport

Sucrose was able to promote primary root elongation (Fig. 2A), as might be expected given the higher levels of auxin in such conditions (Fig. 1G). Increasing endogenous auxin production in the *yucca-D* mutant could partially phenocopy this response and caused a reduced sensitivity to sucrose (Fig. 2A). As auxin is synthesized at a high rate in the shoot apex and in young, developing leaves (Ljung et al., 2001), we hypothesized that sucrose promotion of IAA levels in hypocotyls and roots might reflect an increase in rootward auxin transport. Inhibiting auxin transport with 1-N-Naphthylphthalamic acid (NPA) completely blocked sucrose-induced growth (Fig. 2B). *max2* mutants, which have a constitutively increased rate of auxin transport (Bennett et al., 2006), were taller than wild-type seedlings and had a 70% reduction in sucrose response (Fig. 2C). Moreover, wild-type seedlings grown on sucrose showed a nearly identical hypersensitivity to NPA treatments as untreated *max2* mutants (Fig. 2D). We analyzed expression of three genes encoding PIN-FORMED (PIN) auxin transporters strongly associated with auxin delivery to the root tip (Blilou et al., 2005). Of these, sucrose induced expression of

PIN7 (Fig. 2E). Expression of *IAA3*, encoding a negative regulator of *PIN7* (Dello Ioio et al., 2008), was repressed by sucrose in shoots but not in roots (Fig. 1F). Since the effect of sucrose on *PIN* expression is modest, sucrose may affect post-translational regulation of PIN activity (Grunewald and Friml, 2010).

To more directly test for a sucrose effect on auxin movement, we assayed the response dynamics of auxin reporters to local auxin application. We applied IAA microdrops to a single cotyledon of plants expressing the synthetic auxin response reporter DR5::GUS (Fig. 2F). In seedlings grown without sucrose, the reporter was induced throughout the treated cotyledon within a few hours. In the same time-frame, sucrose-grown seedlings showed a dramatic extension of reporter expression down the entire length of the hypocotyl (Fig. 2D). Results were similar with a natural auxin-responsive reporter (pS15-5E::GUS; Walcher and Nemhauser, 2012) (Supplemental Fig. S1). Exposing seedlings to double the intensity of light produced a hybrid phenotype (Fig. 2F). Light likely increases endogenous sucrose production through increased photosynthesis (Poorter et al., 2012), yet it also inhibits stem growth through degradation of *PIF* proteins (Leivar and Quail, 2011). Similar to sucrose treatment, seedlings grown in higher light showed an apparent increase in rootward auxin transport; yet, unlike sucrose treatment, they exhibited reduced hypocotyl elongation (Fig. 2F). This complex phenotype highlights potential organ-specific differences in composition and function of photomorphogenetic pathways.

Sucrose effects on the auxin pathway are both *PIF*-dependent and independent

As sucrose promotion of sustained seedling growth requires *PIF* genes (Stewart et al., 2011), we wondered whether the same would be true for auxin. We found that auxin increased late phase seedling growth rates by approximately 4-fold, and that this growth promotion was substantially reduced in *pifQ* mutants lacking functional *PIF1*, *PIF3*, *PIF4*, and *PIF5* (Fig. 3A). A reduced auxin sensitivity of *pifQ* mutants has been observed in previous studies (Nozue et al., 2011). This phenotype places the *PIF* genes downstream from the auxin signal; however, quantification of IAA levels in *pifQ* mutants found a substantial reduction in the effect of sucrose (Fig. 3B). To further complicate the genetic model, *pifQ* mutants showed modestly higher concentrations of IAA than wild-type plants. The same trend is observed in the primary root; *pifQ* roots are longer than WT without supplementary sucrose and show a reduced sucrose response (Supplemental Fig. S2). Auxin-induced gene expression is similarly complex in *pifQ*

mutants supplemented with sucrose. In shoots of wild-type plants, sucrose induced expression of *IAA17*, *IAA19* and *IAA29* by 2.3-, 5- and 2.6-fold, respectively (Fig. 1F). In *pifQ* mutants, sucrose response of these same genes was reduced to only 1.4-, 2- and 2.1-fold, while the approximate 3-fold induction of *SAUR15* was similar to the wild-type response (Fig. 3C). Sucrose induced expression of *YUCCA8* by 2.7-fold in wild-type shoots and by 5.4-fold in *pifQ* shoots (Fig. 1F; Fig. 3C). One possible explanation for these results is feedback regulation whereby *PIF* genes effectively act both up- and downstream of auxin, with differential response in particular tissues or on particular promoters. In this way, the *PIF*-auxin pathway may resemble the non-linear relationship between *PIF*s and the phytochrome photoreceptors (Leivar and Quail, 2011).

To further clarify the relationship between auxin and *PIF* genes, we tested the effects of auxin on *PIF* gene expression and levels of PIF5 protein. In these assays, we used the synthetic auxin picloram (pic), as IAA inhibits seed germination and interferes with early seedling development. Recent transcriptome studies on isolated hypocotyls found that pic and IAA effects were largely indistinguishable (Chapman et al., 2012). Similar to sucrose, auxin produced only modest changes in *PIF* gene expression (Supplemental Fig. S3). We have previously shown that sucrose dramatically increases the abundance of PIF5 in the dark and light (Stewart et al., 2011). However, unlike sucrose, we could not detect any effect of auxin on PIF5 abundance (Fig. 3D). This suggests that the effect of sucrose on PIF abundance is upstream of auxin biosynthesis and transport.

Sucrose triggers an endogenous carbon-sensing pathway

For a seedling germinating in natural settings, sucrose would be supplied largely through photosynthesis. *PIF* genes have an established role in repressing photomorphogenesis and development of the photosynthetic apparatus in the dark (Moon et al., 2008; Toledo-Ortiz et al., 2010). To assess the effects of sucrose on photosynthesis, we measured rates of carbon uptake in wild-type seedlings under a range of light conditions with and without supplemental sucrose. Addition of sucrose reduced rates of carbon uptake in our standard light conditions (60 μmol m^{-2} sec^{-1}), resulting in a net negative rate of CO_2 assimilation (Fig. 4A, inset). Sucrose may act on photosynthesis through sugar-mediated feedback (Paul and Foyer, 2001), by a shift in biomass allocation that increases respiration rates, or by a combination of these and yet to be determined

factors. *pifQ* mutants behaved essentially the same as wild-type plants in these experiments, suggesting that there is compensation for any increased expression of photosynthesis-related genes (Moon et al., 2008; Toledo-Ortiz et al., 2010). In contrast, plants overexpressing *PIF5* had dramatic reductions in assimilation rate at all light levels and a much-reduced light-saturated assimilation rate (Fig. 4A). This reduction in photosynthetic capacity likely reflects the limited expansion of the cotyledons in *PIF5ox* seedlings (Supplemental Fig. S4, A-C), as well as the antagonism between *PIF*s and the photomorphogenesis program. We also analyzed stomatal density as a possible cause of altered photosynthetic rates, but found that *PIF5ox* plants actually showed an increased number of stomata per cotyledon area when compared with wild type or pifQ mutants (Fig. S4D).

Another effect of supplemental sucrose is an increase in the seedling's carbon-to-nitrogen ratio, a driving force in models of functional equilibrium. To test whether sucrose was intersecting with an endogenous carbon-sensing pathway, we grew plants in approximately twice the concentration of atmospheric CO_2. Elevated CO_2 recapitulated the effects of sucrose on seedling growth: seedlings grown in higher CO_2 were significantly taller than controls, and this effect required *PIF* genes (Fig. 4B). *pifQ* mutants were unable to respond to elevated CO_2, while *PIF5ox* seedlings showed a stronger response than wild type (Fig. 4B). As an additional control, we measured the effects of elevated CO_2 on *max2* mutants, which are nearly as tall as *PIF5ox* seedlings in ambient CO_2. In contrast to *PIF5ox*, *max2* mutants showed a reduced response to elevated CO_2, indicating that increased rates of auxin transport alone are not sufficient to confer CO_2 hypersensitivity (Fig. 4B).

Excess carbon would be predicted to induce nitrogen assimilation pathways to balance carbon-to-nitrogen ratios. Sucrose addition caused a severe bleaching phenotype in plants germinated on nitrogen-deficient media, suggesting that sucrose led to a more rapid depletion of nutrients in seed reserves (Fig. 4C). *pifQ* mutants behaved similarly to wild-type plants, but *PIF5ox* plants were resistant to nitrogen limitation. This pattern may reflect the differential photosynthetic rates observed in these genotypes (Fig. 4A) and resulting differences in nitrogen demands. In relatively nitrogen-rich standard media, sucrose treatments increased expression of *NITRATE TRANSPORTER 1.1 (NRT1.1)*, encoding a transporter of both nitrate and auxin (Krouk et al., 2010) (Fig. 4D). Expression of this gene is associated with acquisition of nitrogen (Forde, 2002). The root nitrogen assimilation response does not require *PIF* genes, as *pifQ*

mutants showed similar patterns of gene expression as wild-type seedlings (Fig. 4D). Another consequence of adding sucrose is increased osmotic stress; however, treatment with equimolar mannitol did not recapitulate sucrose effects (Supplemental Fig. S5; Stewart et al., 2011).

DISCUSSION

In this study, we provide mechanistic links between several well-studied regulators of photomorphogenesis. First, we found that supplemental sucrose promoted hypocotyl elongation through altered auxin levels and distribution (Fig. 1; Fig. 2). Second, we found that sucrose likely activated an endogenous *PIF*-dependent carbon-sensing pathway (Fig. 3; Fig. 4). Overexpression of *PIF5* was sufficient to alter whole plant metabolism—decreasing both the rate of carbon assimilation and nitrogen demand (Fig. 4). It is already well-established that PIF transcription factors are key regulators of growth and development in response to a variety of environmental conditions (Leivar et al., 2009; Kumar et al., 2012; Li et al., 2012). Our results suggest an expanded model where PIF proteins act as points of integration for metabolic cues during photomorphogenesis and daily growth cycles (Fig. 5).

Our previous work demonstrated that rhythmic seedling growth requires supplementation with excess carbon in the form of sucrose, and that sucrose effects on growth are *PIF*-dependent (Stewart et al., 2011). The current study showed that auxin mimicked sucrose supplementation, and auxin-stimulated hypocotyl elongation required *PIF* genes. Our findings add weight to those of several recent studies proposing a strong link between auxin and the *PIF* family (Nozue et al., 2011; Franklin et al., 2011; Li et al., 2012; Sun et al., 2012). However, our data also show that the relationship between *PIF* genes and auxin is complex. While *pifQ* mutants were largely insensitive to the growth-promoting effects of exogenous auxin (Fig. 3A) and did not show significant changes in endogenous IAA levels following sucrose treatment (Fig. 3B), *pifQ* mutants did show overall higher levels of IAA (Fig. 3B). This result, in combination with differential effects of loss of *PIF* function on sucrose-induction of auxin-stimulated genes (Fig. 3C), suggests that there may be *PIF*-dependent and *PIF*-independent branches within the auxin biosynthetic and response pathways. In addition, PIFs have recently been shown to act as negative regulators of sugar-induced IAA biosynthesis in seedlings grown in liquid culture (IS and KL, personal communication). This suggests that even in the *PIF*-dependent branches of sucrose-induced auxin response, the PIFs may be playing both positive and negative roles.

Rhythmic hypocotyl elongation observed with supplemental sucrose may represent an amplified read-out of the endogenous daily rhythms of inter-organ communication. In support of this, IAA biosynthetic rates are nearly twice the level at dusk than at dawn without sugar supplementation (IS and KL, personal communication). This is precisely the period when hypocotyl elongation rates are the fastest in the absence of sucrose (Stewart et al., 2011). Information regarding carbon availability in the leaves must be conveyed to the roots, and the hypocotyl is the physical connection between these organs. Rhythmic hypocotyl elongation may reflect the coordination of growth with the availability of raw materials and energy tied to daily fluctuations in photosynthesis. The lack of sucrose response in the *pifQ* mutants (Fig. 3, A and B) and the altered metabolism of *PIF5ox* plants (Fig. 4, A-C) support a model where the *PIF* family is at the center of this coordination (Fig. 5). By refining the timing and magnitude of hypocotyl elongation through modulating levels of PIF proteins, carbon availability can be easily incorporated into an expanded coincidence model of rhythmic growth (Nozue et al., 2007). Here we have shown that sucrose increases both auxin content and transport to the root (Fig. 1G; Fig. 2F). While blocking auxin transport prevents sucrose-induced hypocotyl elongation (Fig. 2B), it is unclear if increased biosynthesis is also required for growth or if transport alone is sufficient. As levels of auxin strongly influence auxin transport rates (and perhaps vice versa), it is difficult to experimentally isolate effects on auxin biosynthesis from those on transport (Grunewald and Friml, 2010).

Our results suggest that, in addition to regulating hypocotyl elongation, auxin acts a shoot-to-root signal for nitrogen demand. Cytokinins have been identified as a systemic root-to-shoot signal of nitrogen supply (Ruffel et al., 2011; Kiba et al., 2011), but definitive identification of a complementary shoot-to-root signal has remained elusive. Auxin has been proposed as a candidate nitrogen demand signal, as it is transported from the shoots to the roots and positively regulates lateral root development (Forde, 2002; Walch-Liu et al., 2006; Macgregor et al., 2008; Kiba et al., 2011; Ruffel et al., 2011). In addition, plants show increased root auxin levels in response to a drop in nitrogen availability (Walch-Liu et al., 2006). Here, we show that auxin levels increased in response to higher carbon levels, and that this response was most striking in roots (Fig. 1G). Sucrose induction of the gene encoding the nitrate-sensitive auxin transporter NRT1.1 (Fig. 4D) strengthens the link between high carbon, increased auxin

accumulation in the roots, and, ultimately, increased nitrogen uptake (Krouk et al., 2010; Kircher and Schopfer, 2012).

Functional equilibrium during photomorphogenesis relies on differential biomass allocation between three organ systems: cotyledons, hypocotyls and roots. While the relative growth rate of cotyledons versus the hypocotyl is a key measure of light response, less attention has been paid to how root area affects metabolic homeostasis during the transition to photoautotrophy. A recent study reported that photosynthate from cotyledons is needed for substantial root growth, independent of the phytochrome and cryptochrome photoreceptors (Kircher and Schopfer, 2012). Previous studies have shown that application of sucrose to shoots alone is sufficient for promotion of lateral root outgrowth (Macgregor et al., 2008). The enhanced root growth and reduced sensitivity to sucrose seen in the *yucca-D* mutants (Fig. 2F) suggest a model for combinatorial regulation of root patterning by both photosynthate and auxin. This is further supported by the correlation of high auxin levels, elongated primary root, and low sucrose response observed in *pifQ* mutants (Fig. 3B; Supplemental Fig. S2).

Nutrient limitation is thought to partially explain why many plant species fail to sustain high growth rates in elevated CO_2 (Stitt and Krapp, 1999). The challenge of coordinating local metabolic conditions with growth across a multicellular organism is not unique to plants. In animals, the TOR pathway integrates nutrient and energy sensing with growth control (Hietakangas and Cohen, 2009). Intriguingly, recent transcriptional data suggest that sugar, auxin and cytokinin all converge on the plant TOR pathway (Dobrenel et al., 2011). While many of the specific members of the animal TOR pathway do not have readily identifiable plant homologs, further studies will be needed to judge the extent of functional conservation between animal and plant pathways. A mechanistic understanding of how metabolism shapes plant biomass allocation will be critical to predict and manage productivity across diverse environments, particularly in response to rising CO_2 levels.

MATERIALS AND METHODS

Plant materials and growth conditions. Wild type is *Arabidopsis thaliana* ecotype Col-0. *pifQ* (Leivar et al., 2009), HA-tagged *PIF5*ox (Lorrain et al., 2008), *PIF5*ox (PIF5-OXL2) (Fujimori et al., 2004), *max2-1* (Stirnberg et al., 2002), *yucca-D* (Zhao et al., 2001), *DR5::GUS* (Ulmasov et al., 1997), *pS15-5E::GUS* (Walcher and Nemhauser, 2012), and *DII-VENUS* (Brunoud et al.,

2012) are as previously described. True-breeding lines expressing *PKS4::GUS* (Schepens et al., 2008) were generated from seeds of primary transformants (T1 seeds) provided by Christian Fankhauser (University of Lausanne). Seeds were sterilized (20 min in 70% ethanol, 0.01% Triton X-100, followed by a rinse in 95% ethanol), suspended in 0.1% agar (BP1423, Fisher Scientific), spotted on plates containing 0.5X Linsmaier and Skoog (LS) (LSP03, Caisson Laboratories, Inc.) with 0.8% phytoagar (40100072-1, Plant Media: bioWORLD), and stratified in the dark at 4°C for 3 days. For nitrogen deprivation experiments, media was prepared from 0.5X Murashige and Skoog without nitrogenous compounds (MSP07, Caisson Laboratories, Inc.) and supplemented with either 0.5mM KNO_3 or 0.5mM KCl. Plates were placed vertically at dawn in a Percival E-30B growth chamber set at 20°C in 60 μmol m^{-2} sec^{-1} white light (unless otherwise specified) with short-day conditions (8 hours light, 16 hours dark). Controlled CO_2 chambers were as previously described (Kinmonth-Schultz, 2011). Briefly, chambers with either ambient CO_2 (~400 ppm) or elevated CO_2 (~800 ppm) were housed in the Douglas Research Conservatory (Center for Urban Horticulture, University of Washington). Seedlings were grown in two sets of paired chambers under natural light supplemented by 12 hours of artificial light (high-pressure sodium 400W single phase bulbs, Phillips Electronics North America Corp., Andover, MA, USA). Light intensity was variable across the day with an average intensity during the light period of approximately 75 μmol m^{-2} sec^{-1} and a maximum of 300 μmol m^{-2} sec^{-1}. Temperature was approximately 19°C at night and 24°C during the day.

Chemical treatments. Sucrose (S2, Fisher Scientific) and D-mannitol (69-65-8, Acros Organics) treatments were performed at a final concentration of 88 mM (equal to 3% w/v sucrose). NPA (N-1-naphthylphthalamic acid, 33371, Sigma-Aldrich) was suspended in DMSO. Picloram (4-Amino-3,5,6-trichloro-2-pyridinecarboxylic acid, P5575, Sigma-Aldrich) and IAA (indole-3-acetic acid, 705490, Plant Media) were suspended in 80% ethanol. NPA and Picloram were diluted directly into plate media. 1 mL of 125 μM IAA (in 0.5X LS) was sprayed onto seedlings on days 3 and 4. For application of microdrops, IAA was mixed with hydrous lanolin (NCD 0168-0051-31, Fougera Pharmaceuticals Inc.) to a final concentration of 1.5 mM. A control lanolin mixture was made with an equivalent volume of solvent. These mixtures were

thinned by warming to 50°C and applied to the distal portion of one cotyledon with a small wire loop. Treated seedlings were returned to growth chambers for 4.5 hours before GUS staining.

Seedling measurements and microscopy. Time-lapse photography is as previously described (Stewart et al., 2011). Briefly, images were captured every 30 minutes by a charge-coupled device camera (PL-B781F, PixeLINK) equipped with a lens (NMV-25M1, Navitar) and IR longpass filter (LP830-35.5, Midwest Optical Systems, Inc.). Image capture was accompanied by a 0.5 second flash of infrared light by a custom built LED infrared illuminator (512-QED234, Mouser Electronics). A custom LabVIEW (National Instruments) program controlled image capture and illumination. For growth rate analysis from time-lapse photography, hypocotyl lengths from at least 12 individuals were measured using ImageJ software for each time-lapse image (2208 X 3000 pixels). Growth rates were calculated from hypocotyl lengths using a custom script in MATLAB (MathWorks), available on request. Hypocotyl or primary root lengths of 12-25 seedlings per condition were measured from scans of vertical plates using ImageJ software (http:/rsb.info.nih.gov/ij/) in at least two independent experiments. Plates were scanned on day 5 for plates without sucrose and on day 6 for plates with sucrose to match developmental stage (Stewart et al., 2011). Scans for the growth rate analysis were performed on the days indicated in Fig.1A&B. Color seedling images were collected at 10X magnification using a Leica dissecting scope (S8APO, Leica Microsystems) and camera (DFC290, Leica Microsystems). Fluorescent images of root tips were captured directly from seedlings on plates using a Leica DMI 3000B microscope fitted with a Leica long-working 10X HCX PL FLUORTAR objective and illuminated with a Lumencor SOLA light source. Images were captured using Leica LAS AF version 2.6.0 software and a Leica DFC 345FX camera. Fluorescence quantification was done using ImageJ software (http:/rsb.info.nih.gov/ij/). Mean values for 25 primary root tips per treatment were estimated using an elliptical ROI centered on the root tip with values from root tips of untransformed plants used to subtract background fluorescence. Three biological replicates were performed with similar results.

GUS staining. Seedlings were collected on day 5 for plates without sucrose and day 6 for those with sucrose and immersed in 90% acetone (v/v with DI water) for 20 minutes, washed twice with 50 mM Na_2PO_4 pH 7.2 before a 16-17 hour incubation at 37°C in the dark with GUS

reaction buffer [50 mm $NaPO_4$, 0.1% Triton X-100, 1 mm $K_4Fe(CN_6)$-$3H_2O$, 1 mm $K_3Fe(CN_6)$, and 0.5 mg/ml 5-bromo-4-chloro-3-indolyl-β-d-GlcA (X-gluc; Rose Scientific, LTD.)]. Stained seedlings were fixed in FAA (50% ethanol, 3.7% formaldehyde, 5% acetic acid) and chlorophyll removed with an ethanol series. Seedlings were rehydrated and mounted on glass slides in 40% glycerol.

Quantification of photosynthetic rate. 15 mg of seeds were sterilized and sown on: no sucrose, sucrose, and mannitol media as described above. Seedling gas exchange measurements were quantified on day 6 with an open gas exchange system (LI-6400; Li-Cor, Inc., Lincoln, NE, USA) fitted with a specialized chamber (6400-17; Whole Plant Arabidopsis Chamber; Li-Cor, Inc.) and controllable light source (6400-18; RGB Light Source; Li-Cor, Inc.). Data for light response curves were collected directly from seedlings on plates with measurements taken at photosynthetically active radiation (PAR) levels of 750, 500, 250, 120, 60, 30, and 0 μmol m^{-2} s^{-1}. Chamber air temperature was maintained at 25 °C and CO_2 reference concentration was maintained at 380 μmol CO_2 mol^{-1}. Seedling tissue was weighed at the completion of the experiment. CO_2 assimilation rates were calculated with manufacturer equations modified to normalize to fresh weight.

Cotyledon area and stomatal density quantification. Seedlings were grown without sucrose. On day 6, seedlings were cleared with an ethanol series, fixed in FAA (50% ethanol, 3.7% formaldehyde, 5% acetic acid), stained with 0.5% toluidine blue O (TBO) (CAS number: 92-31-9) for 4 minutes , and then rehydrated and mounted in 25% glycerol. Stomata were manually counted in a 0.1mm^2 square area on the adaxial side of 10 cotyledons per genotype with the ImageJ Cell Counter plugin (http://rsbweb.nih.gov/ij/plugins/cell-counter.html).

IAA quantification. Seedlings were grown vertically on 0.5X LS plates with 2% phytoagar. Tissue was harvested from approximately 250-1000 seedlings and purified as described previously with minor modifications (Andersen et al., 2008). Hypocotyls or roots were manually dissected at the time of collection. All samples were immediately frozen in liquid nitrogen and stored at -80°C or on dry ice until processing. Before extraction and purification, 1000 or 500 pg $^{13}C_6$-IAA internal standard was added to each shoot and root sample, respectively. After

derivatization, the samples were analyzed by gas chromatography–selected reaction monitoring–mass spectrometry (Edlund et al., 1995). Four replicates were analyzed for each sample and normalized to fresh weight of source tissue (mg FW).

RNA extraction and qRT-PCR analysis. Seedlings were grown vertically on 0.5X LS plates with 2% phytoagar. Expression analysis was performed on seedlings collected at dawn on day 5 for plates without sucrose and on day 6 for plates with sucrose to match developmental stage. Shoots, cotyledon and hypocotyl tissue, and roots were manually dissected at the time of collection. All samples were immediately frozen in liquid nitrogen and stored at -80°C until processing. Total RNA was extracted from tissue of approximately 1000 seedlings using the Spectrum Plant Total RNA Kit (Sigma), total RNA was treated with DNaseI on columns (Qiagen) and 2 µg of eluted RNA was used for complementary DNA (cDNA) synthesis using iScript (Biorad). Samples were analyzed using SYBR Green Supermix (Biorad) reactions run in a Chromo4 Real-Time PCR system (MJ Research). Expression for each gene was calculated using the formula (Pfaffl, 2001) $(E_{target})^{-\Delta CPtarget(control-sample)}/(E_{ref})^{-\Delta CPref(control-sample)}$ and normalized to a reference gene.

Western blot analysis. PIF5-HA abundance was detected in extracts of whole *PIF5HA*ox and wild-type seedlings collected at dawn on day 5. All samples were immediately frozen in liquid nitrogen and stored at -80°C until processing. Total protein was extracted from approximately 100 mg of tissue using a previously described method (Duek et al., 2004), except that anti-HA-peroxidase (Roche) was used at a 1:1000 dilution. Anti-ACTIN antibodies (A0480, Sigma) were used at a 1:2000 dilution and detected with anti-Mouse (172-1011, Biorad) used at a 1:20,000 dilution. SuperSignal West Femto Maximum Sensitivity Substrate (Pierce) was used to detect signals. Blots shown are representative of at least two experiments with independent biological replicates.

ACKNOWLEDGEMENTS

We are indebted to Takato Imaizumi, Soo-Hyung Kim, Janneke Hille Ris Lambers, Elizabeth Van Volkenburgh, Hannah Kimonth-Schultz, and Britney Moss for critique of this manuscript and expert advice. We are also grateful to Andrej Arsovski and Emily Palm for providing assistance with the carbon assimilation assays and Kylee Peterson for guidance in stomatal

density assays. We thank Soo-Hyung Kim for allowing us access to his controlled CO_2 growth chambers and Ottoline Leyser, Christian Fankhauser, and Teva Vernoux for sharing seed stocks.

LITERATURE CITED

Andersen SU, Buechel S, Zhao Z, Ljung K, Novak O, Busch W, Schuster C, Lohmann JU (2008) Requirement of B2-type cyclin-dependent kinases for meristem integrity in Arabidopsis thaliana. Plant Cell 20: 88–100

Bennett T, Sieberer T, Willett B, Booker J, Luschnig C, Leyser O (2006) The Arabidopsis MAX pathway controls shoot branching by regulating auxin transport. Curr Biol 16: 553–63

Blilou I, Xu J, Wildwater M, Willemsen V, Paponov I, Friml J, Heidstra R, Aida M, Palme K, Scheres B (2005) The PIN auxin efflux facilitator network controls growth and patterning in Arabidopsis roots. Nature 433: 39–44

Brunoud G, Wells DM, Oliva M, Larrieu A, Mirabet V, Burrow AH, Beeckman T, Kepinski S, Traas J, Bennett MJ, et al (2012) A novel sensor to map auxin response and distribution at high spatio-temporal resolution. Nature 482: 103–6

Chapman EJ, Greenham K, Castillejo C, Sartor R, Bialy A, Sun T, Estelle M (2012) Hypocotyl Transcriptome Reveals Auxin Regulation of Growth-Promoting Genes through GA-Dependent and -Independent Pathways. PLoS ONE 7: e36210

Covington MF, Harmer SL (2007) The circadian clock regulates auxin signaling and responses in Arabidopsis. PLoS Biol 5: e222

Dello Ioio R, Nakamura K, Moubayidin L, Perilli S, Taniguchi M, Morita MT, Aoyama T, Costantino P, Sabatini S (2008) A genetic framework for the control of cell division and differentiation in the root meristem. Science 322: 1380–4

Dobrenel T, Marchive C, Sormani R, Moreau M, Mozzo M, Montane MH, Menand B, Robaglia C, Meyer C (2011) Regulation of plant growth and metabolism by the TOR kinase. Biochem Soc Trans 39: 477–81

Dowson-Day MJ, Millar AJ (1999) Circadian dysfunction causes aberrant hypocotyl elongation patterns in Arabidopsis. Plant J 17: 63–71

Duek PD, Elmer MV, van Oosten VR, Fankhauser C (2004) The degradation of HFR1, a putative bHLH class transcription factor involved in light signaling, is regulated by phosphorylation and requires COP1. Curr Biol 14: 2296–301

Edlund A, Eklof S, Sundberg B, Moritz T, Sandberg G (1995) A Microscale Technique for Gas Chromatography-Mass Spectrometry Measurements of Picogram Amounts of Indole-3-Acetic Acid in Plant Tissues. Plant Physiol 108: 1043–1047

Forde BG (2002) Local and long-range signaling pathways regulating plant responses to nitrate. Annu Rev Plant Biol 53: 203–24

Franklin KA, Lee SH, Patel D, Kumar SV, Spartz AK, Gu C, Ye S, Yu P, Breen G, Cohen JD, et al (2011) Phytochrome-interacting factor 4 (PIF4) regulates auxin biosynthesis at high temperature. Proc Natl Acad Sci U S A 108: 20231–5

Fujimori T, Yamashino T, Kato T, Mizuno T (2004) Circadian-controlled basic/helix-loop-helix factor, PIL6, implicated in light-signal transduction in Arabidopsis thaliana. Plant Cell Physiol 45: 1078–86

Gonzali S, Novi G, Loreti E, Paolicchi F, Poggi A, Alpi A, Perata P (2005) A turanose-insensitive mutant suggests a role for WOX5 in auxin homeostasis in Arabidopsis thaliana. Plant J 44: 633–45

Grunewald W, Friml J (2010) The march of the PINs: developmental plasticity by dynamic polar targeting in plant cells. EMBO J 29: 2700–2714

Hietakangas V, Cohen SM (2009) Regulation of tissue growth through nutrient sensing. Annu Rev Genet 43: 389–410

Kiba T, Kudo T, Kojima M, Sakakibara H (2011) Hormonal control of nitrogen acquisition: roles of auxin, abscisic acid, and cytokinin. J Exp Bot 62: 1399–409

Kinmonth-Schultz H and K (2011) Carbon gain, allocation and storage in rhizomes in response to elevated atmospheric carbon dioxide and nutrient supply in a perennial C3 grass, Phalaris arundinacea. Functional Plant Biology 797–807

Kircher S, Schopfer P (2012) Photosynthetic sucrose acts as cotyledon-derived long-distance signal to control root growth during early seedling development in Arabidopsis. PNAS 109: 11217–11221

Krouk G, Lacombe B, Bielach A, Perrine-Walker F, Malinska K, Mounier E, Hoyerova K, Tillard P, Leon S, Ljung K, et al (2010) Nitrate-Regulated Auxin Transport by NRT1.1 Defines a Mechanism for Nutrient Sensing in Plants. Developmental Cell 18: 927–937

Kumar SV, Lucyshyn D, Jaeger KE, Alós E, Alvey E, Harberd NP, Wigge PA (2012) Transcription factor PIF4 controls the thermosensory activation of flowering. Nature 484: 242–245

Leivar P, Quail PH (2011) PIFs: pivotal components in a cellular signaling hub. Trends Plant Sci 16: 19–28

Leivar P, Tepperman JM, Monte E, Calderon RH, Liu TL, Quail PH (2009) Definition of early transcriptional circuitry involved in light-induced reversal of PIF-imposed repression of photomorphogenesis in young Arabidopsis seedlings. Plant Cell 21: 3535–53

Li L, Ljung K, Breton G, Schmitz RJ, Pruneda-Paz J, Cowing-Zitron C, Cole BJ, Ivans LJ, Pedmale UV, Jung H-S, et al (2012) Linking photoreceptor excitation to changes in plant architecture. Genes Dev 26: 785–790

Ljung K, Bhalerao RP, Sandberg G (2001) Sites and homeostatic control of auxin biosynthesis in Arabidopsis during vegetative growth. Plant J 28: 465–74

Lorrain S, Allen T, Duek PD, Whitelam GC, Fankhauser C (2008) Phytochrome-mediated inhibition of shade avoidance involves degradation of growth-promoting bHLH transcription factors. Plant J 53: 312–23

Macgregor DR, Deak KI, Ingram PA, Malamy JE (2008) Root system architecture in Arabidopsis grown in culture is regulated by sucrose uptake in the aerial tissues. Plant Cell 20: 2643–60

Moon J, Zhu L, Shen H, Huq E (2008) PIF1 directly and indirectly regulates chlorophyll biosynthesis to optimize the greening process in Arabidopsis. Proc Natl Acad Sci U S A 105: 9433–8

Nozue K, Covington MF, Duek PD, Lorrain S, Fankhauser C, Harmer SL, Maloof JN (2007) Rhythmic growth explained by coincidence between internal and external cues. Nature 448: 358–61

Nozue K, Harmer SL, Maloof JN (2011) Genomic analysis of circadian clock-, light-, and growth-correlated genes reveals PHYTOCHROME-INTERACTING FACTOR5 as a modulator of auxin signaling in Arabidopsis. Plant Physiol 156: 357–72

Nozue K, Maloof JN (2006) Diurnal regulation of plant growth. Plant Cell Environ 29: 396–408

Paul MJ, Foyer CH (2001) Sink regulation of photosynthesis. J Exp Bot 52: 1383–1400

Pfaffl MW (2001) A new mathematical model for relative quantification in real-time RT-PCR. Nucleic Acids Res 29: e45

Poorter H, Niklas KJ, Reich PB, Oleksyn J, Poot P, Mommer L (2012) Biomass allocation to leaves, stems and roots: meta-analyses of interspecific variation and environmental control. New Phytol 193: 30–50

Ruffel S, Krouk G, Ristova D, Shasha D, Birnbaum KD, Coruzzi GM (2011) Nitrogen economics of root foraging: transitive closure of the nitrate-cytokinin relay and distinct systemic signaling for N supply vs. demand. Proc Natl Acad Sci U S A 108: 18524–9

Schepens I, Boccalandro HE, Kami C, Casal JJ, Fankhauser C (2008) PHYTOCHROME KINASE SUBSTRATE4 modulates phytochrome-mediated control of hypocotyl growth orientation. Plant Physiol 147: 661–71

Stewart JL, Maloof JN, Nemhauser JL (2011) PIF Genes Mediate the Effect of Sucrose on Seedling Growth Dynamics. PLoS One 6: e19894

Stirnberg P, van De Sande K, Leyser HM (2002) MAX1 and MAX2 control shoot lateral branching in Arabidopsis. Development 129: 1131–41

Stitt M, Krapp A (1999) The interaction between elevated carbon dioxide and nitrogen nutrition: the physiological and molecular background. Plant, Cell & Environment 22: 583–621

Sun J, Qi L, Li Y, Chu J, Li C (2012) PIF4-Mediated Activation of YUCCA8 Expression Integrates Temperature into the Auxin Pathway in Regulating Arabidopsis Hypocotyl Growth. PLoS Genet 8: e1002594

Toledo-Ortiz G, Huq E, Rodriguez-Concepcion M (2010) Direct regulation of phytoene synthase gene expression and carotenoid biosynthesis by phytochrome-interacting factors. Proc Natl Acad Sci U S A 107: 11626–31

Ulmasov T, Murfett J, Hagen G, Guilfoyle TJ (1997) Aux/IAA proteins repress expression of reporter genes containing natural and highly active synthetic auxin response elements. Plant Cell 9: 1963–71

Walcher CL, Nemhauser JL (2012) Bipartite promoter element required for auxin response. Plant Physiol 158: 273–82

Walch-Liu P, Ivanov I, Filleur S, Gan Y, Remans T, Forde BG (2006) Nitrogen regulation of root branching. Ann Bot 97: 875–81

Zhao Y, Christensen SK, Fankhauser C, Cashman JR, Cohen JD, Weigel D, Chory J (2001) A role for flavin monooxygenase-like enzymes in auxin biosynthesis. Science 291: 306–9

FIGURE LEGENDS

Figure 1: Sucrose stimulates the auxin pathway

(A) Hypocotyl elongation rates of seedlings exposed to the growth-promoting hormones brassinosteroids (BR), auxin (Aux), gibberellins (GA). Smoothed average growth rates from three independent experiments (representing an average of 15-20 seedlings per experiment) are shown. A dashed black line indicates growth rates on media without hormone supplementation (mock). Light and dark phases are indicated in the bars below the graphs, beginning with midnight of the third day post germination. Scale bar equals 0.05 mm/hr. **(B)** Sucrose (black), natural auxin (IAA, blue) and synthetic auxin (Pic, purple) prolonged hypocotyl elongation when compared to seedlings grown without any treatments (grey). Error bars represent standard error. Some error bars are within the boundaries of the markers. **(C)** Seedlings carrying the PKS4::GUS reporter showed similar GUS expression in the elongating region of the hypocotyl for sucrose and auxin treated seedlings. Scale bar equals 1 mm. **(D)** Seedlings grown on sucrose showed an increased sensitivity to Pic. Error bars represent standard error. Some error bars are within the boundaries of the markers. **(E)** Root tips of plants grown on sucrose had a reduction in fluorescence of the auxin-degradable DII-VENUS reporter. Representative images are shown with fluorescence quantification values normalized to the no sucrose mean ± SEM for 25 seedlings. **(F)** Quantitative RT-PCR shows that sucrose increases expression of several auxin-induced genes. Sucrose effects on gene expression are much stronger in shoots (S) compared with roots (R). Error bars represent standard error. **(G)** Sucrose (black) increased endogenous auxin levels when compared to plants grown without added sucrose (grey). Error bars represent standard error. Asterisks indicate significant differences between sucrose and no sucrose treatments for both genotypes (* $p<0.05$, ** $p<0.01$) using t-tests and a Hommel multiple comparison correction.

Figure 2: Sucrose promotes rootward auxin transport

(A) Sucrose increased primary root length. Higher endogenous auxin levels in the *yucca-D* mutants led to longer primary roots and a reduced response to sucrose. Error bars represent standard error. **(B)** Blocking auxin transport with 50 μM NPA eliminated sucrose-induced hypocotyl elongation. Error bars represent standard error. **(C)** Mutants with increased auxin transport (*max2*) were less sensitive to sucrose. Ratios of hypocotyl length in sucrose vs. non-

sucrose conditions are indicated. Error bars represent standard error. **(D)** Sucrose addition to WT seedlings (square) increased sensitivity to the auxin transport inhibitor NPA, making them resemble *max2* mutants (triangle) grown without sucrose. Error bars represent standard error. Some error bars are within the boundaries of the markers. **(E)** Sucrose induces expression of the gene encoding auxin efflux carrier PIN7 but has no measurable effects on genes encoding PIN1 or PIN3. Error bars represent standard error. **(F)** Sucrose increases rootward auxin transport, as measured by increased distance of auxin reporter staining from the site of local auxin application (depicted in schematic). Exposing seedlings to increased light intensity was sufficient to increase staining distance. Scale bar equals 1 mm for no sucrose panel, 1.3 mm for all others.

Figure 3: Sucrose effects on auxin require *PIF* genes

(A) Growth promotion by auxin or sucrose in wild-type seedlings (WT) was greatly diminished in *pifQ* mutants. Growth rates from day 5 are shown. Error bars represent standard error. Asterisks indicate significantly different rates ($p<0.05$) between the tested treatment and the no sucrose treatment for wild type and *pifq* using t-tests and a Hommel multiple comparison correction. **(B)** *pifQ* mutants show no significant effect of sucrose on IAA levels. Error bars represent standard error. **(C)** Sucrose effects on some but not all auxin responsive-genes were diminished in *pifQ* mutants. Error bars represent standard error. **(D)** Sucrose caused a clear increase in PIF5 levels, while auxin (Pic) had little effect. Wild-type or 35S::PIF5-HA seedlings were collected at dawn on day 5. Anti-HA antibodies were used to detect PIF5-HA proteins (upper panel) and anti-ACTIN antibodies were used as a loading control (lower panel).

Figure 4: Sucrose stimulates an endogenous carbon-sensing pathway

(A) CO_2 assimilation rates of wild-type (WT), *pifQ* and *PIF5ox* seedlings were quantified over a range of light intensities (PAR). Over-expression of *PIF5* reduced net carbon uptake. CO_2 assimilation rates of wild type seedlings on media with and without sucrose at the standard growth conditions of this study (60 µmol m^{-2} s^{-1}, grey shading) are shown in the inset. A black arrow indicates the photosynthetic rate under the conditions for the high light experiment shown in Figure 2D. Error bars represent standard error. **(B)** WT seedlings grown in elevated CO_2 (~800 ppm, black) showed a small but significant increase in height compared with seedlings grown in ambient CO_2 (~400 ppm, grey). This response was completely abolished in *pifQ* mutants.

Overexpression of *PIF5* (*PIF5*ox) greatly enhanced the growth promotion effect of elevated CO_2. In *max2* mutants where auxin transport is constitutively increased, response to increased CO_2 was reduced. Error bars represent standard error for four independent experiments. Asterisks indicate significant differences between ambient and elevated CO_2 treatments for each genotype using an ANOVA with Tukey pair-wise comparisons (*** $p<0.001$). **(C)** Sucrose supplementation led to bleaching in low nitrogen conditions by 8 dpg. Seedlings were grown on low nitrogen media supplemented with either 0.5 mM KNO_3 or equimolar KCl. *PIF5ox* seedlings remained green in all media conditions. Scale bar equals 5 mm. **(D)** Sucrose strongly induces the gene encoding NRT1.1, a nitrate-sensitive auxin transporter. The induction of *NRT1.1* can be detected in whole seedlings (W), but appears stronger in dissected roots (R) when compared to dissected shoots (S). This effect of sucrose is not *PIF*-dependent, as it is still detectable in *pifQ* mutants. Error bars represent standard error.

Figure 5: A model of a *PIF*- and auxin-mediated carbon sensing pathway

Light (light arrow) and CO_2 (dark arrow) elevate endogenous sucrose and thus carbon ('C') levels ('Before'). Sucrose then stimulates both PIF-dependent and independent auxin responses ('Response'), promoteing hypocotyl and root elongation. These elongated roots acquire nitrogen ('N') from the soil and the carbon:nitrogen balance is restored ('After').

Figure S1: Sucrose increases rootward staining of a reporter for an auxin-induced gene

An IAA-infused lanolin droplet was applied to a single cotyledon of *pS15-5E::GUS* seedlings, as depicted in the schematic. Scale bar equals 1 mm for seedlings grown without sucrose and 1.7 mm for seedlings grown with sucrose.

Figure S2: Primary roots of pifQ mutant seedlings are longer than WT and show a reduced response to sucrose.

Average primary root length is shown ±SEM of two replicates, each with 15-20 seedlings. Letters indicate significant differences determined by ANOVA and Tukey post-hoc test ($p<0.05$).

Figure S3: Neither sucrose or picloram have large effects on *PIF* gene expression

PIF gene expression in wild-type seedlings was measured at the dawn of day 5. Seedlings were grown with no treatment (grey), with sucrose (88 mM, black) or with pic (5 μM, purple). Error bars represent standard error.

Figure S4: Over-expression of *PIF5* results in altered cotyledon development

(A) *PIF5ox* seedlings are generally paler when an equal amount of seeds were weighed out and sown on agar petri dishes for gas exchange experiments. Seedlings were imaged on day 6. **(B)** *PIF5ox* seedlings have reduced average cotyledon area. Error bars represent standard error, n=17-20. **(C)** Representative seedlings used in (B) fixed and then stained with toluidine blue O on day 6. Scale bar is equal to 1 mm. **(D)** *PIF5ox* seedlings have increased stomatal density compared to WT and *pifq*. Error bars are equal to standard error of the mean; n=10 per genotype.

Figure S5: Effects of sucrose cannot be attributed solely to osmotic stress

(A) Unlike sucrose (black), equimolar mannitol (orange) was not able to increase the length of 7 day old seedlings. Data from seedlings grown without either treatment are shown in grey. **(B)** Mannitol was able to partially increase seedling sensitivity to synthetic auxin (pic), but the effect was much less than what is observed for sucrose. Data are from 7-day-old seedlings exposed to no treatment (grey) or equimolar mannitol or sucrose. **(C)** Mannitol can partially reduce levels of the DII-VENUS reporter in primary root tips, but not to the same extent as sucrose treatment. Relative signal intensity is shown for seedlings grown on no treatment, equimolar mannitol or sucrose. Values represent the average and standard error of normalized fluorescence intensity for 25 seedlings per treatment. Similar data were obtained in three independent biological replicates. **(D)** Unlike sucrose, mannitol does not change the sensitivity of seedlings to inhibition of auxin transport by NPA. **(E)** Unlike sucrose, mannitol does not increase rootward auxin transport. An IAA-infused lanolin droplet was applied on day 5 on a single cotyledon of reporter seedlings grown on mannitol as depicted in the schematic. Scale bar equals 1.1 mm. **(F)** Mannitol did not reduce CO_2 assimilation rates to the same extent as sucrose treatment. Gas exchange measurements shown were taken at our standard light intensity of 60 μmol m^{-2} s^{-1}. **(G)** Mannitol treatment did not sensitize seedlings to nitrogen deprivation. Seedlings were grown on media

without nitrogen that was supplemented with either 0.5 mM KNO_3 or 0.5 mM KCl and imaged on 8 days post germination.

Scale bar equals 5 mm. Error bars represent standard error for at least two independent experiments. Many error bars are within the boundaries of the markers. Hypocotyl lengths were measured in at least two independent replicates, consisting of 15-20 seedlings of each genotype and treatment.

Figure 1

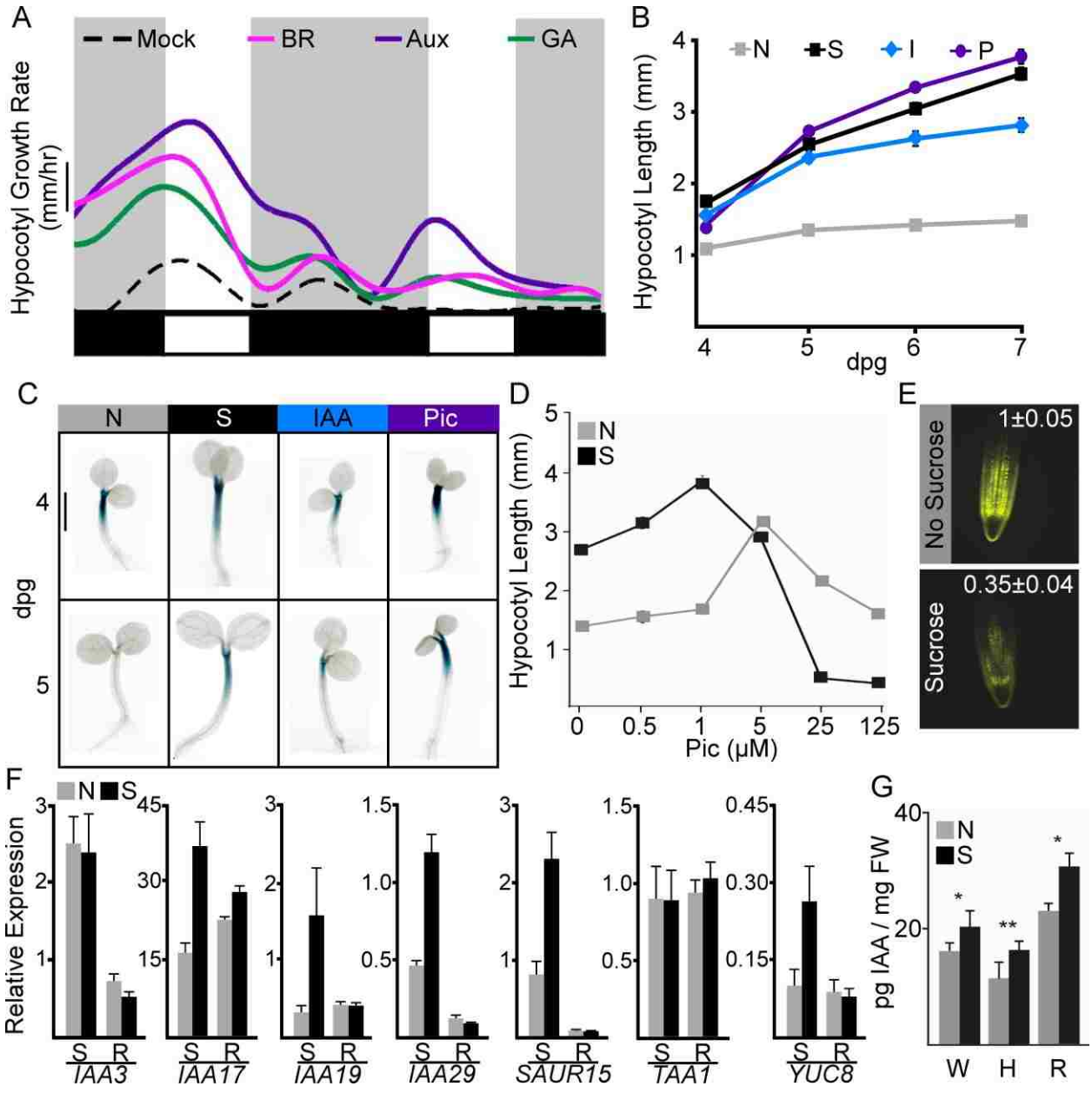
A
Mock
BR
Aux
GA
Hypocotyl Growth Rate (mm/hr)
B
N
S
I
P
Hypocotyl Length (mm)
dpg
C
N
S
IAA
Pic
dpg
D
N
S
Hypocotyl Length (mm)
Pic (μM)
E
No Sucrose
1±0.05
Sucrose
0.35±0.04
F
N
S
Relative Expression
IAA3
IAA17
IAA19
IAA29
SAUR15
TAA1
YUC8
G
N
S
pg IAA / mg FW
W
H
R

Figure 2

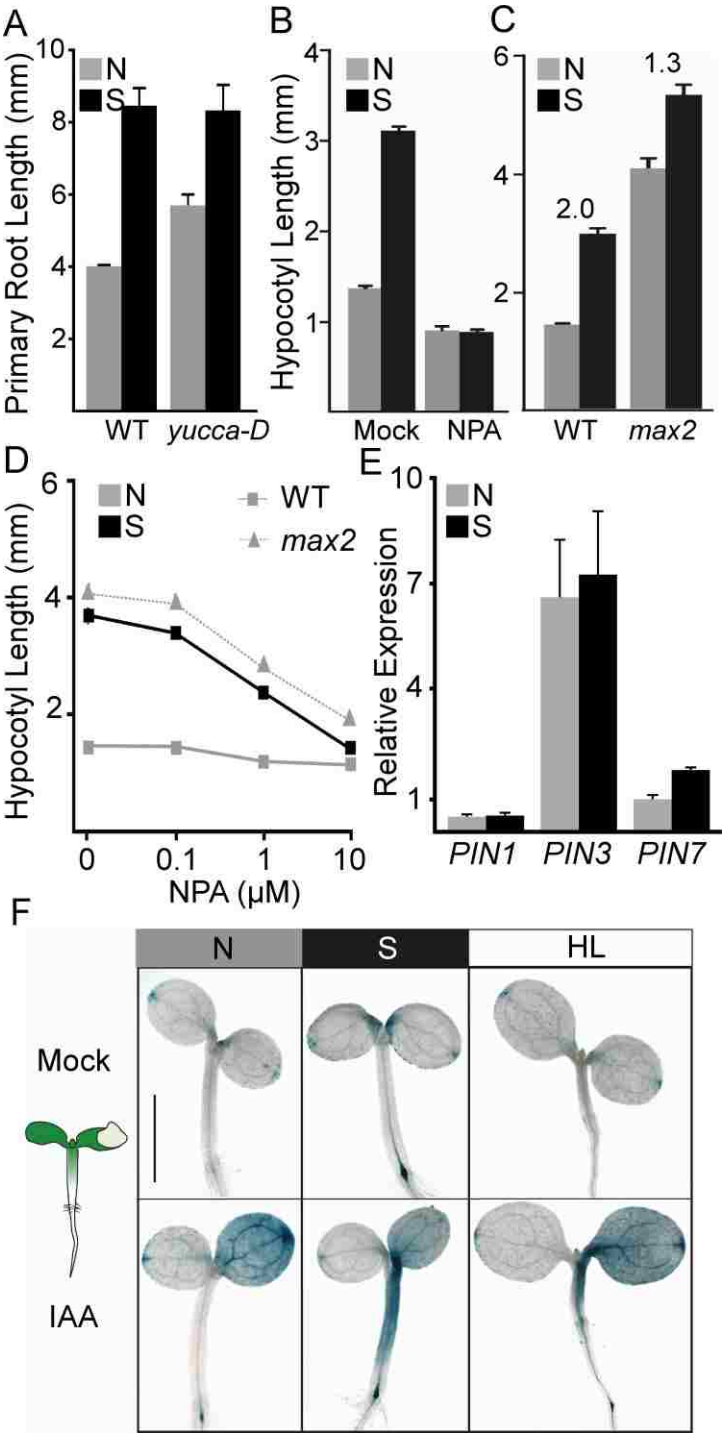
A
Primary Root Length (mm)
N
S
WT
yucca-D
B
Hypocotyl Length (mm)
Mock
NPA
C
2.0
1.3
WT
max2
D
Hypocotyl Length (mm)
WT
max2
NPA (μM)
E
Relative Expression
PIN1
PIN3
PIN7
F
N
S
HL
Mock
IAA

Figure 3

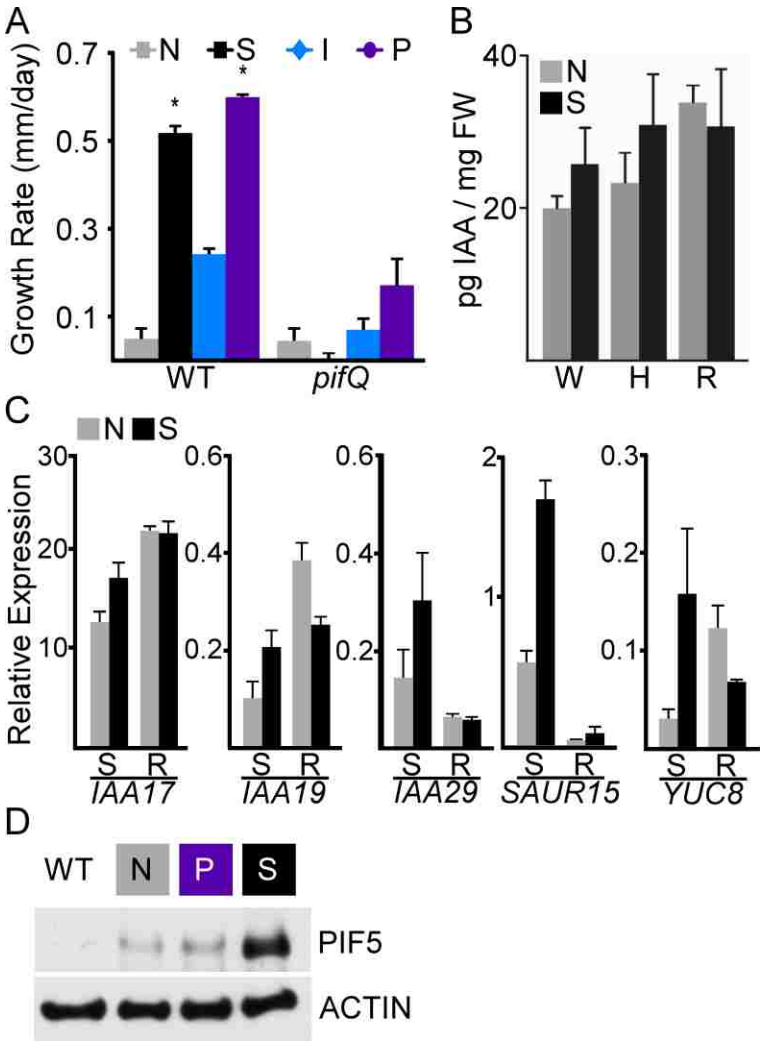
A
Growth Rate (mm/day)
0.7
0.5
0.3
0.1
N
S
I
P
*
*
WT
pifQ
B
pg IAA / mg FW
40
20
N
S
W
H
R
C
N S
Relative Expression
30
20
10
0.6
0.4
0.2
0.6
0.4
0.2
2
1
0.3
0.2
0.1
S R
IAA17
IAA19
IAA29
SAUR15
YUC8
D
WT
N
P
S
PIF5
ACTIN

Figure 4

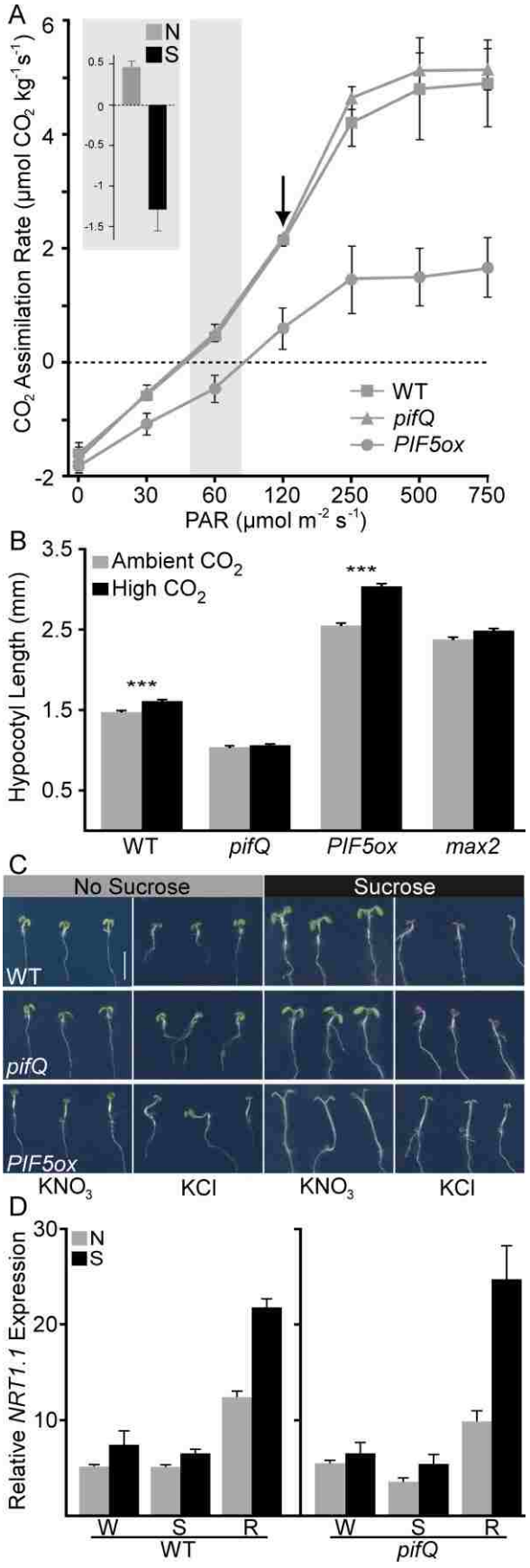
A
N
S
WT
pifQ
PIF5ox
CO2 Assimilation Rate (μmol CO2 kg-1 s-1)
PAR (μmol m-2 s-1)
B
Ambient CO2
High CO2
Hypocotyl Length (mm)
WT
pifQ
PIF5ox
max2
C
No Sucrose
Sucrose
KNO3
KCl
D
Relative NRT1.1 Expression
W
S
R

Figure 5

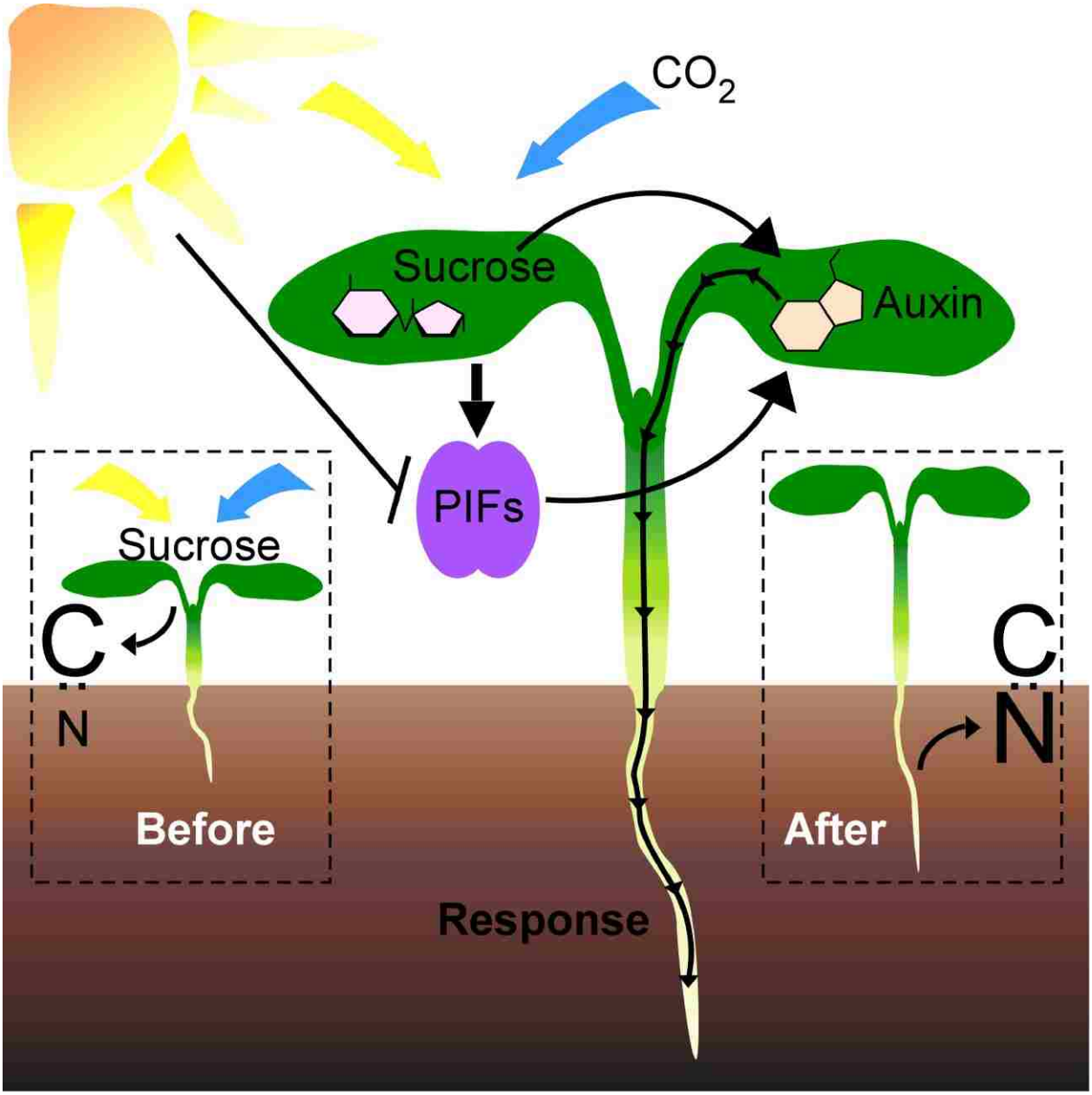

Figure S1

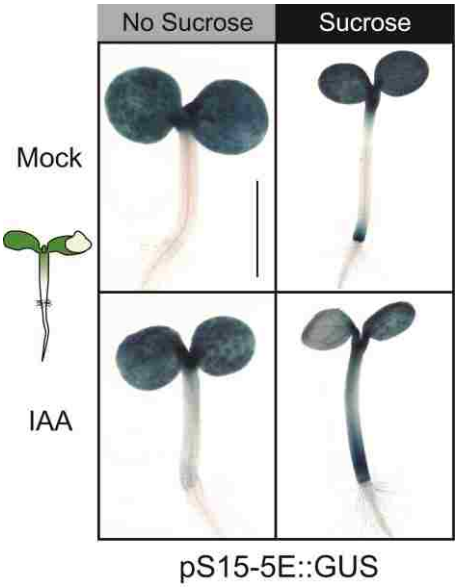

Figure S2

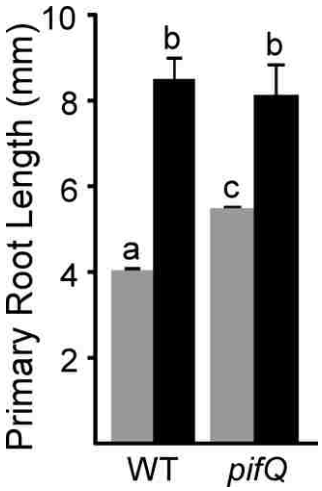

Figure S3

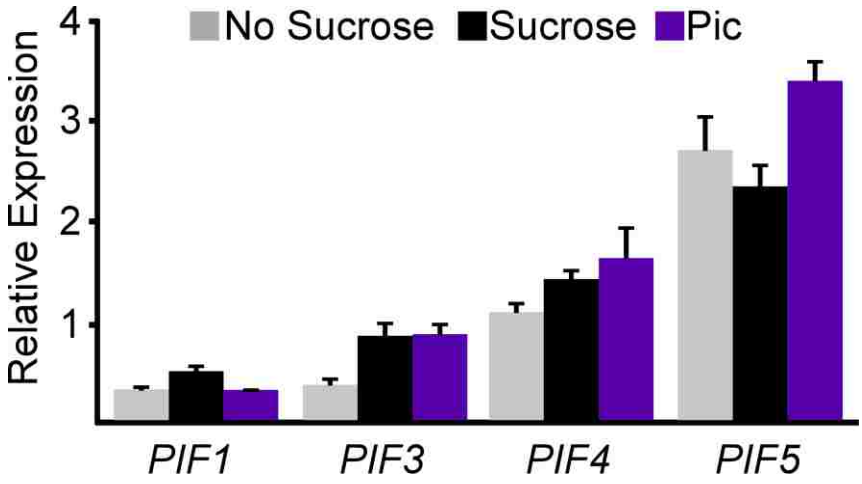
No Sucrose
Sucrose
Pic
Relative Expression
4
3
2
1
PIF1
PIF3
PIF4
PIF5

Figure S4

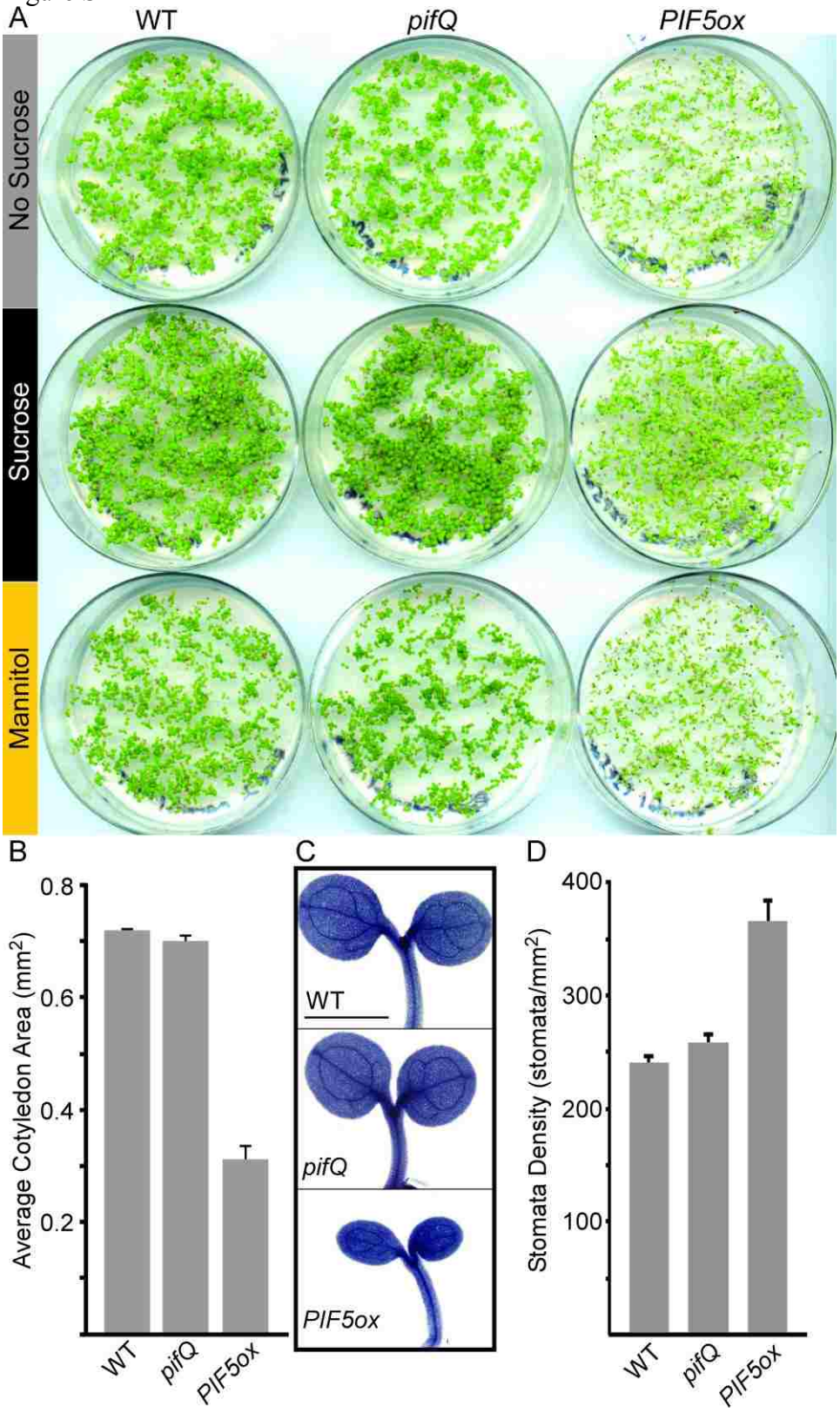
A
WT
pifQ
PIF5ox
No Sucrose
Sucrose
Mannitol
B
Average Cotyledon Area (mm2)
0.8
0.6
0.4
0.2
WT
pifQ
PIF5ox
C
WT
pifQ
PIF5ox
D
Stomata Density (stomata/mm2)
400
300
200
100
WT
pifQ
PIF5ox

Figure S5

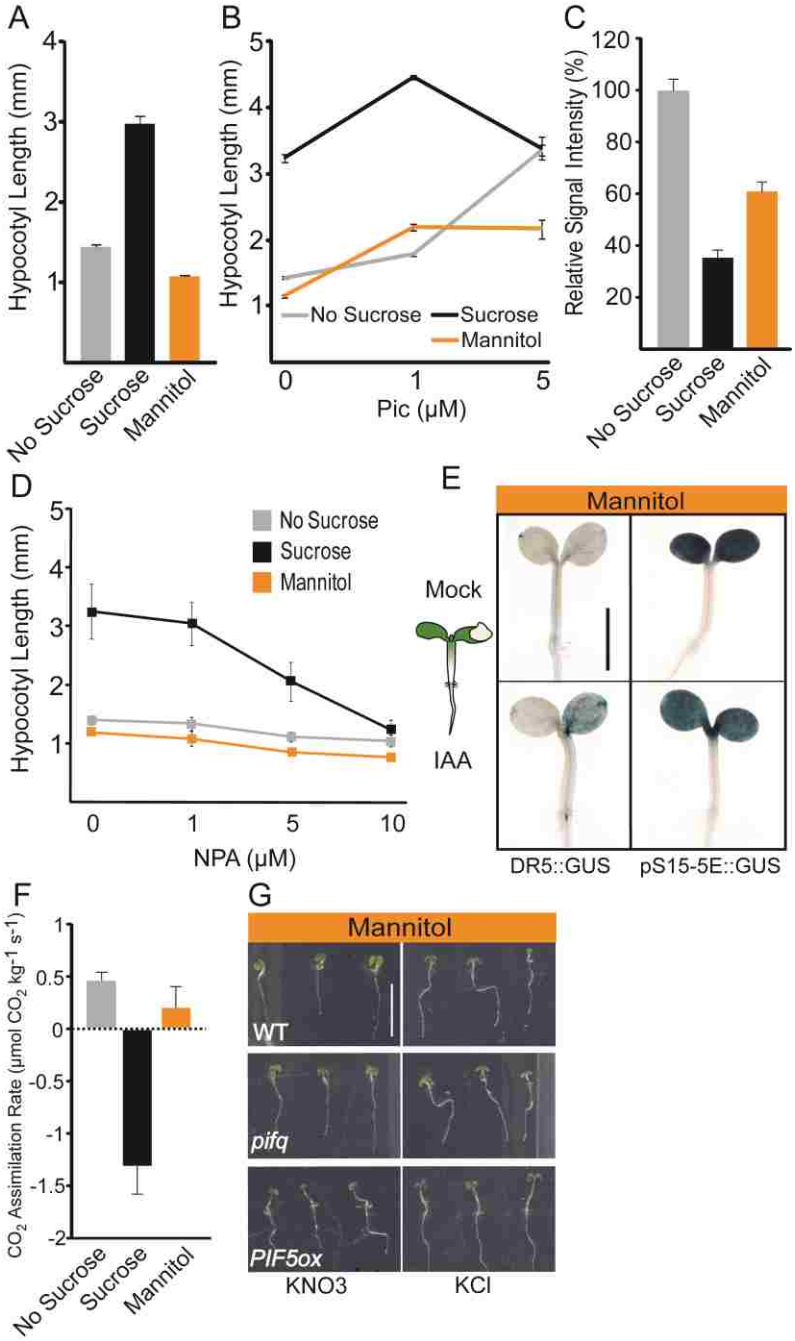
A
Hypocotyl Length (mm)
No Sucrose
Sucrose
Mannitol
B
Hypocotyl Length (mm)
No Sucrose
Sucrose
Mannitol
Pic (μM)
C
Relative Signal Intensity (%)
No Sucrose
Sucrose
Mannitol
D
Hypocotyl Length (mm)
No Sucrose
Sucrose
Mannitol
NPA (μM)
E
Mannitol
Mock
IAA
DR5::GUS
pS15-5E::GUS
F
CO2 Assimilation Rate (μmol CO2 kg-1 s-1)
No Sucrose
Sucrose
Mannitol
G
Mannitol
WT
pifq
PIF5ox
KNO3
KCl

Chapter 4

Growth control networks are re-wired during photomorphogenesis.

ABSTRACT

Photomorphogenesis has two stages. First, seedlings detect light and open their cotyledons. Second, seedlings optimize their light environment by regulated elongation of the hypocotyl. Several hormones, including brassinosteroids (BR) and gibberellins (GA), orchestrate the growth of the seedling stem. In this study, we used time-lapse imaging to investigate the relationship between BRs and GAs across photomorphogenesis. At a highly reproducible developmental window coincident with the transition between the two stages of photomorphogenesis, BR and GA effects switched from an additive to a synergistic promotion of growth. These BR responses, including the synergistic effects with GA, did not depend on the *PHYTOCHROME INTERACTING FACTOR* family. Members of the *DELLA* family, including *REPRESSOR of ga1-3 (RGA*) and *GA-INSENSITIVE (GAI)*, could either repress or enhance BR growth response, depending on developmental stage. At this transition in growth dynamics, the BR and GA pathways had opposite effects on *DELLA* protein levels. In contrast to GA-induced *DELLA* degradation, BR treatments increased the levels of RGA and mimicked the molecular effects of stabilizing *DELLA*s. In addition, *DELLA*s showed complex regulation of genes involved in BR biosynthesis, implicating them in BR homeostasis. These results point to a multi-level, dynamic relationship between the BR and GA pathways.

INTRODUCTION

During photomorphogenesis, seedlings begin to photosynthesize and then use growth to optimize their light environment. The proper positioning of the embryonic leaves (cotyledons) is critical for survival, thus the elongation of the embryonic stem (hypocotyl) is under tight regulation. A wealth of signaling pathways, including those involved in sensing light, hormones, time-of-day and metabolic state, have been implicated in regulating photomorphogenetic growth (1). To further complicate this network, there is extensive feedback within pathways, as well as significant cross-regulation (2).

Brassinosteroid (BR) and gibberellin (GA) pathways are key regulators of seedling growth. While the signaling pathway triggered by each hormone differs, responses to both hormones share a similar overall logic: activated receptors relieve repression on transcriptional

activators. BRs bind and activate the BRASSINOSTEROID-INSENSITIVE1 (BRI1)-associated receptor complex at the plasma membrane. A phospho-relay cascade culminates in dephosphorylated and nuclear-localized transcription factors, including BRI1-EMS-SUPPRESOR1 (BES1/BZR2) and BRASSINOZOLE-RESISTANT1 (BZR1) (3). GA binds the receptor GA-INSENSITIVE-DWARF1 (GID1) and forms an SCF complex with the F-box protein SLEEPY1 (SLY1). This complex forms a pocket that binds members of the DELLA family of repressors and targets them for ubiquitin-mediated degradation. In the absence of GA, the DELLAs bind and sequester transcriptional regulators, including *PHYTOCHROME INTERACTING FACTOR* (*PIF*) family members, thereby blocking GA response (4).

The transcription factor families downstream of the BR and GA pathways are highly inter-connected and integrate information across the growth network. The DELLAs regulate the function of a number of transcription factors, including BES1 and BZR1 (5,6,7). BES1 and BZR1 are able to dimerize with each other, as well as with PIFs, further linking downstream transcriptional responses. DELLAs also bind to *SPATULA (SPT),* a close relative to the *PIF* family. SPT lacks a phytochrome binding domain and is thought to have a DELLA-like effect by forming dimers with PIF proteins and blocking their function (8,9,10). The combinatorial possibilities of transcriptional complexes may explain the extensive plasticity of seedling growth responses.

In this study, we used time-lapse imaging to analyze the dynamic relationship of BRs and GAs across photomorphogenesis, particularly focusing on the understudied early stages of seedling growth. We found the relationship between BRs and GAs changed over developmental time, and known signaling components played unexpected roles. Synergistic growth promotion by BRs and GAs was only observed after cotyledons were open, and this strong growth effect was largely *PIF*-independent. *DELLAs* and *SPT,* proteins previously characterized as growth repressors, were critical for normal BR pathway function. Seedlings with either loss- or gain-of-function mutations in *DELLA* genes had increased BR response early in development. In the transitional period when cotyledons were opening, BR treatment increased RGA abundance in the hypocotyl and activated known *DELLA* outputs. Both *DELLA*s and *SPT* were required for the exaggerated growth phenotype of mutants overexpressing a BR-biosynthetic gene. These findings illustrate the dynamic and multi-level relationship of the BR, GA and phytochrome pathways during photomorphogenesis.

RESULTS

BRs and GAs induce stage-specific, *PIF*-independent synergistic growth

To determine the roles of BR and GA during photomorphogenesis, we measured hypocotyl growth in seedlings exposed to each hormone alone and in combination (Fig.1). We divided photomorphogenesis into five, 12-hour intervals, starting at 36 hours post germination (hpg) (Int.1-5, Fig.1a). As previously described, the majority of hypocotyl elongation occurred during Int. 1-2, before the cotyledons were fully open (Fig.1b,c) (11). BR treatment increased growth rates substantially in every interval. In contrast, GA treatment increased growth rates only during Int.1-3 (Fig.1b,c). The previously described synergistic growth response caused by combining BR and GA treatment (12) did not emerge until Int. 3 (Fig.1b,c). During Int. 1-2, treatment with both hormones resulted in less than or near additive effect on growth rates. Growth promotion by GAs required BRs. Seedlings with reduced BR biosynthesis [*de-etiolated2* (*det2*) or brassinozole (BRZ) treatment] or response (*bri1*) were dramatically less sensitive to GA treatment (Fig.1c).

The *PIF* family of transcription factors was required for growth promotion by GA, but they were not required for growth promotion by BR or by combined BR and GA treatments. Seedlings with loss of function of *PIF1*, *PIF3*, *PIF4*, *PIF5*, and *PIF6* (*pifP* mutants) had substantially reduced growth rates during Int. 3-5, but retained wild-type rates before Int.3 (Fig.1c vs. Fig.2a). *pifP* seedlings had very little response to GA treatment. This effect was most evident in Int. 3 where GA effects were most striking in wild-type seedlings (Fig.2a). *pifP* seedlings exhibited near wild-type growth responses to treatment with BR alone or in combination with GA (Fig.2a). Similar hormone response trends were observed with *pifP, piftQ* (*pif1 pif3 pif4 pif5*) and *pifT* (*pif3 pif4 pif5*) mutants, suggesting that *PIF3*, *PIF4* and *PIF5* are the primary *PIF* family members controlling hypocotyl growth during photomorphogenesis (Fig.2b). The bZIP transcription factor *ELONGATED HYPOCOTYL5 (HY5)* acts in opposition to the *PIF*s to inhibit hypocotyl growth and promote photomorphogenesis. Growth of *hy5* mutants was quite similar to wild-type seedlings treated with BR and GA, and this phenotype was largely insensitive to hormone treatments (Fig.2b).

***DELLAs* and *SPT* have interval-specific effects on BR growth promotion.**

As *DELLA*s have recently been identified as a point of cross-regulation between the BR and GA pathway (5,6,7), we next analyzed growth intervals for seedlings with reduced *DELLA* activity. We focused on *RGA* and *GAI*, as they are known to play the largest role in growth regulation in seedlings (4). Loss of *RGA* and *GAI* function resulted in increased growth primarily in Int. 2-3, consistent with the timing of strongest growth promotion by GA treatment (Fig.3a). Stabilization of GAI protein in the *gai-1* mutant reduced growth rates in all intervals with one exception (Fig.3a). Growth rates in Int. 3 were strikingly elevated in *gai-1* seedlings. As *SPATULA* (*SPT*) acts alongside *DELLA*s in many aspects of growth regulation, we examined growth rates in *spt* mutants. In contrast to *rga gai* mutants, *spt* mutants showed the greatest increase in growth rates in Int. 1, rather than Int. 2-3 (Fig3.a). When the function of all three repressors was lost (*rga gai spt*), growth rates phenotypes were largely additive (Fig3.a).

Loss of *DELLA* function generally increased sensitivity to BR treatment, confirming their role as growth repressors. This relationship was particularly obvious in Int.2, where BR treatment of *rga gai* seedlings had the most dramatic effect on growth (Fig. 3a). However, the role of *DELLAs* may be stage- and dose-dependent, as *gai-1* seedlings retained BR sensitivity in several intervals (Fig. 3a). During Int. 3, *gai-1* mutants were actually more sensitive than wild-type seedlings to BR treatment (Fig.3a). Seedlings without *SPT* function (*spt*) had a very similar response to BR treatment as wild-type seedlings, except in Int.3 where *spt* mutants treated with BRs grew faster than wild type. When all three repressors were lost (*rga gai spt*), no further BR-sensitivity was observed beyond that of *rga gai* seedlings (Fig.3a).

We next analyzed the function of *DELLA*s, and *SPT* in plants overproducing BRs endogenously. To do this, we first analyzed the growth dynamics of an activation tagged allele of the BR biosynthetic gene *DWF4* (*DWF4ox*). *DWF4ox* seedlings had increased growth rates in most intervals with Int. 3 being the most dramatically affected (Fig.3b). In *DWF4ox rga gai* triple mutants, all of the increased growth rates were strongly suppressed (Fig.3b). This result was unexpected, as all single mutants showed elevated growth. *DWF4ox spt* mutants showed similar, although more subtle, growth trends as those seen in *DWF4ox rga gai* (Fig.3b). In quadruple *DWF4ox rga gai spt* mutants, growth rates were further reduced. For example, growth rates of *DWF4ox rga gai spt* mutants in Int. 3 were less than half of those of *DWF4ox* seedlings

(Fig.3b). At the end of 5 days, the long hypocotyl phenotype observed in *DWF4ox* seedlings was completely suppressed in *DWF4ox rga gai spt* mutants (Fig.3c).

Suppression of the *DWF4ox* phenotype was caused by the loss of expression of *DWF4* (Fig.3d), suggesting a role for *DELLA*s in BR homeostasis. To test whether *DELLA*s normally affect genes encoding BR biosynthetic enzymes, we quantified expression levels of three targets of BR negative feedback regulation: *CPD*, *DWF4*, and *BR6ox1* in wild-type and *gai-1* mutants. BR treatment decreased expression of all three genes, as expected (Fig.3e). Surprisingly, *DWF4* expression was unchanged, *CPD* expression was up-regulated, and *BR6ox1* was down-regulated by greater than 50-fold (Fig.3e). While these results clearly implicate *DELLA*s in BR homeostasis, the complicated pattern of changes makes it difficult to predict the effect of GA treatment on BR levels.

Brassinosteroids regulate the abundance and activity of *RGA*.

Growth analysis of *rga gai* and *gai-1* seedlings revealed that, unlike their consistently negative role in the GA pathway, *DELLAs* could positively regulate BR growth responses at specific time points. To determine if DELLA abundance was regulated by BRs at any point during early seedling development, we measured the effect of BRs on RGA abundance at 48, 72 and 96 hpg (Fig. 4a). We first examined *RGA* levels in the elongation zone of the hypocotyl using transgenic plants carrying *RGA::GFP-RGA*. In agreement with previous reports, GA treatment reduced the GFP-RGA signal to background levels (Fig.4a). BRs were able to increase the GFP-RGA signal, particularly at 72 hpg. Combining BR and GA treatments could counteract the effects of BRs (Fig.4a). Western blot analysis on protein extracts from whole seedlings confirmed the effects observed with fluorescence microscopy (Fig.4b). Our result is consistent with the observed increase in the rice DELLA protein SLENDER-RICE1 in BR-treated seedlings (13).

To quantify the functional impact of BR-induced RGA accumulation, we analyzed the expression of genes induced by *DELLA*s (10). BR-treatment induced expression of *GID1a*, *GID1b*, *bHLH137* and *XERICO* to similar levels observed in *gai-1* (Fig.4c). BR effects are reduced in *rga gai* mutant seedlings, suggesting that BRs act through *DELLA*s to increase target gene expression. *DWF4ox* seedlings also showed a modest increase in *DELLA* target gene expression (Fig.4c), although there was no apparent increase in RGA levels in these mutants. We

also tested whether BRs reduced levels of SPT protein, as this is another molecular read-out of DELLA activity (10). Indeed, BR treatments led to a *DELLA*-dependent decrease in SPT abundance (Fig. 4d). BR-induced decreases in SPT levels were similar whether seedlings were exposed to BR alone or a combined BR and GA treatment (Fig.4 b vs. d). Combined with the DELLA-dependency of BR effects, this result suggests there may be differences in timing or strength of BR and GA effects in exogenously treated seedlings.

To investigate potential mechanisms for BR-induced DELLA accumulation, we analyzed the expression of the *DELLA*s themselves, *SPT*, as well as genes encoding GA biosynthetic enzymes. BR treatment had little effect on expression of *DELLA* family members [*RGA*, *GAI*, *RGA-LIKE1* (*RGL1)*, *RGL2*, or *RGL3*] or *SPT*. Expression of *GA20ox1*, *GA20ox2*, and *GA20ox5* is well correlated with GA levels and should therefore be anti-correlated with levels of DELLA proteins. We observed exactly the opposite trend. Expression of all three GA biosynthetic genes was up-regulated by BR treatment and overexpression of *DWF4* (Fig.4e). These results suggest that BRs likely act to stabilize DELLAs through post-translational modifications, such as facilitating formation of degradation-resistant complexes.

DISCUSSION

Cotyledon opening is coincident with a fundamental shift in hormone response and growth control, including a striking inhibition of hypocotyl elongation (11). Several lines of evidence suggest that the onset of photosynthesis may be the signal for re-wiring of the growth network (14,15). In this study, we found that BRs promoted hypocotyl growth throughout seedling development, while GA growth promotion was limited primarily to early time points before cotyledons were fully open. Both hormones applied together evoked strong growth acceleration in late-stage seedlings, a novel effect not seen with application of either hormone separately. The hubs in the growth control network remained somewhat elusive, especially for early time points. Hormone-stimulated growth promotion did not always require the *PIF*s, and the growth repressors *DELLAs* and *SPT* could increase or decrease growth in a stage-specific manner. The temporal analysis of growth presented here did reveal new regulatory connections between BR and GA biosynthesis and between BRs and *DELLA*s, highlighting the plasticity of the growth network.

Since the synergistic BR and GA growth response was first carefully characterized (12), the molecular mechanism linking the two pathways has remained elusive. Recent studies have found that BZR1and PIF4 are both required for GA-mediated growth promotion, bind to one another, and share many transcriptional targets (5,16). In addition, both RGA and GAI have been shown to negatively regulate BES1 and BZR1 function through direct binding (5,6,7). These observations have led to a model where GA-mediated release of DELLA repression, in combination with BR increase in BES1 and BZR1 function, allow for maximum PIF-mediated growth promotion (3). The synergistic BR and GA growth response described in this study is not explained by such a model, as it is neither consistently repressed by *DELLA*s nor *PIF*-dependent.

Growth promotion by the well-established growth repressors *RGA*, *GAI* and *SPT* was one of the most unexpected findings from the current study. Seedlings with stabilized GAI (*gai-1*) had faster growth and increased BR sensitivity during Int. 3 compared to wild-type seedlings (Fig.3a), and the *DWF4ox* mutant phenotype was dependent on intact repressor function (Fig.3b). Altered gene expression of *CPD* and *BR6ox1* in *gai-1* seedlings suggests the *DELLAs* may regulate BR biosynthesis (Fig.3e). While our study did not detect any significant change in *DWF4* expression in *gai-1* mutants, *GAI*-dependent increases in expression have been found in other studies (7). Nearly all BR biosynthetic genes are subject to negative feedback regulation, mediated by BES1 and BZR1 (17). As both RGA and GAI can bind to BES1 and BZR1, it is likely that *DELLAs* impact the strength of this feedback. Such a model could explain the increase in DELLA function we observed in BR treated seedlings (Fig.4). BRs may induce DELLA function as another feedback mechanism attenuating flux through the pathway. BR-induced DELLA accumulation could also modulate GA biosynthesis (Fig.4e). An increase in the DELLA SLR1 in response to BR-treatment was also recently found in rice (13).

While the synergistic BR and GA growth was *PIF*-independent, *hy5* mutants did resemble seedlings exposed to both hormones and were insensitive to hormone treatments (Fig.2b). These results connect the combined BR and GA growth response to skotomorphogenesis, potentially through similar changes in chromatin structure and gene expression. Several lines of evidence connect BR response to chromatin remodeling (18). The chromatin remodeling factor PICKLE (PKL) has long been linked to the GA pathway and is a positive regulator of GA responses (19,20). Recently, transcriptional activation by HY5 has been directly connected with its interaction with PKL, providing a link between chromatin de-

condensation to growth control (21). Our results would predict distinct phases of chromatin states over a photomorphogenetic time course, perhaps explaining different phases of hormone responses.

The photomorphogenetic network facilitates nuanced growth responses by relying on a variety of transcriptional complexes drawn from multiple families, such as *PIFs* and *DELLA*s. Repression of a given complex can be achieved through increased repressor production or through modulating the abundance and composition of other potential binding partners in the cellular population. For example, atypical HLHs PHYTOCHROME RAPIDLY REGULATED1 (PAR1) and LONG HYPOCOTYL IN FR1 (HFR1) suppress the shade avoidance syndrome by binding and inactivating PIF4 and PIF5 (22,23). PACLOBUTRAZOL-RESISTANT1 (PRE1), another HLH, promotes growth by binding the negative regulator of HOMOLOG OF BEE2 INTERACTING WITH IBH1 (HBI1) (24). A comprehensive understanding of plant growth regulation will require systematic elucidation of tissue-, developmental- and environmentally-specific transcription factor 'interactomes'.

MATERIALS AND METHODS

Plant materials and growth conditions. Wild type is *Arabidopsis thaliana* ecotype Col-0. *det2-1*, *DWF4ox*, *gai-1*, *hy5-215*, *pifQ*, *RGA::GFP-RGA*, *rga-28 gai-t6*, and *spt-12*, and are as previously described. *35S::SPT-HA* in the Col-0 background was constructed by the Ian Graham . True-breeding *pif3 pif4 pif5 (pifT)* and *pif1 pif3 pif4 pif5 pif6 (pifP)* lines were generated by crossing *pifq* to wild-type or *pif6* seedlings, respectively. True-breeding *DWFox rga gai*, *DWF4ox spt*, *DWF4ox GFP-RGA*, and *rga gai SPT-HA* were generated by crossing homozygous parents. Heterozygous *rga gai spt* and *DWF4ox rga gai spt* lines were generated and homozygous progeny were genotyped and analyzed for growth assays. Seeds were sterilized (20 min in 70% ethanol, 0.01% Triton X-100, followed by a rinse in 95% ethanol), suspended in 0.1% agar (BP1423, Fisher Scientific), spotted on plates containing 0.5X Linsmaier and Skoog (LS) (LSP03, Caisson Laboratories, Inc.) with 0.8% phytoagar (40100072-1, Plant Media: bioWORLD), and stratified in the dark at 4°C for 3 days. BR (brassinolide, 101, Chemiclones, Inc.) and GA (GA_3, 77-06-5, Phytotechnology Laboratories) were suspended in 80% ethanol and diluted directly into plate media. Plates were placed vertically at dawn in a Percival E-30B

growth chamber set at 20°C in 60 μmol m^{-2} sec^{-1} white light with short-day conditions (8 hours light, 16 hours dark).

Seedling measurements and microscopy. Time-lapse photography is as previously described (11). Briefly, images were captured every 12 hours by a charge-coupled device camera (PL-B781F, PixeLINK) equipped with a lens (NMV-25M1, Navitar) and IR longpass filter (LP830-35.5, Midwest Optical Systems, Inc.). Image capture was accompanied by a 0.5 second flash of infrared light by a custom built LED infrared illuminator (512-QED234, Mouser Electronics). A custom LabVIEW (National Instruments) program controlled image capture and illumination. For growth rate analysis from time-lapse photography, hypocotyl lengths from at least 12 individuals were measured using ImageJ software for each time-lapse image (2208 X 3000 pixels). Growth rates were calculated from hypocotyl lengths using a custom script in MATLAB (MathWorks), available on request. Fluorescent images of hypocotyl elongation zone were captured using a Leica DMI 3000B microscope fitted with a Leica long-working 10X HCX PL FLUORTAR objective and illuminated with a Lumencor SOLA light source. Images were captured using Leica LAS AF version 2.6.0 software and a Leica DFC 345FX camera.

RNA extraction and qRT-PCR analysis. Seedlings were grown vertically on 0.5X LS plates with 2% phytoagar. Expression analysis was performed on seedlings collected at dawn on day 4 (72 hpg). All samples were immediately frozen in liquid nitrogen and stored at -80°C until processing. Total RNA was extracted from 100 mgs of whole seedling tissue using the Spectrum Plant Total RNA Kit (Sigma), total RNA was treated with DNaseI on columns (Qiagen) and 2 μg of eluted RNA was used for complementary DNA (cDNA) synthesis using iScript (Biorad). Samples were analyzed using SYBR Green Supermix (Biorad) reactions run in a Chromo4 Real-Time PCR system (MJ Research). Expression for each gene was calculated using the formula (25) $(E_{target})^{-\Delta CPtarget(control-sample)}/(E_{ref})^{-\Delta CPref(control-sample)}$ and normalized to a reference gene. Primer sequences are listed in TableSX.

Western blot analysis. GFP-RGA and SPT-HA abundance was detected in extracts of whole seedlings collected at dawn on day 4. All samples were immediately frozen in liquid nitrogen and stored at -80°C until processing. Total protein was extracted from approximately 200 mg of

seedling tissue expressing *GFP-RGA* using a previously described method (26), except that anti-GFP-peroxidase (ab6663, Abcam - check) was used at a 1:10,000 dilution. Total protein was extracted from approximately 100 mg of seedling tissue expressing *SPT-HA* using a previously described method (26), except that anti-HA-peroxidase (11867423001, Roche) was used at a 1:1000 dilution. Anti-ACTIN antibodies (A0480, Sigma) were used at a 1:2000 dilution and detected with anti-Mouse (172-1011, Biorad) used at a 1:20,000 dilution. SuperSignal West Femto Maximum Sensitivity Substrate (Pierce) was used to detect signals. Blots shown are representative of at least two experiments with independent biological replicates.

LITERATURE CITED

1. Arsovski AA, Galstyan A, Guseman JM, Nemhauser JL (2012) Photomorphogenesis. *The Arabidopsis Book*:e0147.

2. Nozue K, Maloof JN (2006) Diurnal regulation of plant growth. *Plant Cell Environ* 29:396–408.

3. Wang Z-Y, Bai M-Y, Oh E, Zhu J-Y (2012) Brassinosteroid Signaling Network and Regulation of Photomorphogenesis. *Annual Review of Genetics* 46:701–724.

4. Davière J-M, de Lucas M, Prat S (2008) Transcriptional factor interaction: a central step in DELLA function. *Current Opinion in Genetics & Development* 18:295–303.

5. Bai M-Y et al. (2012) Brassinosteroid, gibberellin and phytochrome impinge on a common transcription module in Arabidopsis. *Nat Cell Biol* 14:810–817.

6. Gallego-Bartolomé J et al. (2012) Molecular mechanism for the interaction between gibberellin and brassinosteroid signaling pathways in Arabidopsis. *Proc Natl Acad Sci USA* 109:13446–13451.

7. Li Q-F et al. (2012) An interaction between BZR1 and DELLAs mediates direct signaling crosstalk between brassinosteroids and gibberellins in Arabidopsis. *Sci Signal* 5:ra72.

8. Khanna R et al. (2004) A novel molecular recognition motif necessary for targeting photoactivated phytochrome signaling to specific basic helix-loop-helix transcription factors. *Plant Cell* 16:3033–44.

9. Reymond MC et al. (2012) A Light-Regulated Genetic Module Was Recruited to Carpel Development in Arabidopsis following a Structural Change to SPATULA. *Plant Cell* 24:2812–2825.

10. Josse EM et al. (2011) A DELLA in disguise: SPATULA restrains the growth of the developing Arabidopsis seedling. *Plant Cell* 23:1337–51.

11. Stewart JL, Maloof JN, Nemhauser JL (2011) PIF Genes Mediate the Effect of Sucrose on Seedling Growth Dynamics. *PLoS One* 6:e19894.

12. Tanaka K et al. (2003) Physiological Roles of Brassinosteroids in Early Growth of Arabidopsis: Brassinosteroids Have a Synergistic Relationship with Gibberellin as well as Auxin in Light-Grown Hypocotyl Elongation. *J Plant Growth Regul* 22:259–271.

13. Vleesschauwer DD et al. (2012) Brassinosteroids Antagonize Gibberellin- and Salicylate-Mediated Root Immunity in Rice. *Plant Physiol* 158:1833–1846.

14. Lilley JLS, Gee CW, Sairanen I, Ljung K, Nemhauser JL (2012) An endogenous carbon-sensing pathway triggers increased auxin flux and hypocotyl elongation. *Plant Physiol* 160:2261–2270.

15. Sairanen I et al. (2012) Soluble Carbohydrates Regulate Auxin Biosynthesis via PIF Proteins in Arabidopsis. *Plant Cell* 24:4907–4916.

16. Oh E, Zhu J-Y, Wang Z-Y (2012) Interaction between BZR1 and PIF4 integrates brassinosteroid and environmental responses. *Nat Cell Biol* 14:802–809.

17. Zhao B, Li J (2012) Regulation of Brassinosteroid Biosynthesis and InactivationF. *Journal of Integrative Plant Biology* 54:746–759.

18. Li J (2010) Regulation of the nuclear activities of brassinosteroid signaling. *Curr Opin Plant Biol* 13:540–7.

19. Ogas J, Cheng J-C, Sung ZR, Somerville C (1997) Cellular Differentiation Regulated by Gibberellin in the Arabidopsis thaliana pickle Mutant. *Science* 277:91–94.

20. Henderson JT et al. (2004) PICKLE Acts throughout the Plant to Repress Expression of Embryonic Traits and May Play a Role in Gibberellin-Dependent Responses. *Plant Physiol* 134:995–1005.

21. Jing Y et al. (2013) Arabidopsis Chromatin Remodeling Factor PICKLE Interacts with Transcription Factor HY5 to Regulate Hypocotyl Cell Elongation. *Plant Cell* 25:242–256.

22. Hornitschek P, Lorrain S, Zoete V, Michielin O, Fankhauser C (2009) Inhibition of the shade avoidance response by formation of non-DNA binding bHLH heterodimers. *EMBO J* 28:3893–902.

23. Galstyan A, Cifuentes-Esquivel N, Bou-Torrent J, Martinez-Garcia JF (2011) The shade avoidance syndrome in Arabidopsis: a fundamental role for atypical basic helix-loop-helix proteins as transcriptional cofactors. *Plant J*. Available at: http://www.ncbi.nlm.nih.gov/entrez/query.fcgi?cmd=Retrieve&db=PubMed&dopt=Citation&list_uids=21205034.

24. Bai M-Y, Fan M, Oh E, Wang Z-Y (2012) A Triple Helix-Loop-Helix/Basic Helix-Loop-Helix Cascade Controls Cell Elongation Downstream of Multiple Hormonal and Environmental Signaling Pathways in Arabidopsis. *Plant Cell* 24:4917–4929.

25. Pfaffl MW (2001) A new mathematical model for relative quantification in real-time RT-PCR. *Nucleic Acids Res* 29:e45.

26. Duek PD, Elmer MV, van Oosten VR, Fankhauser C (2004) The degradation of HFR1, a putative bHLH class transcription factor involved in light signaling, is regulated by phosphorylation and requires COP1. *Curr Biol* 14:2296–301.

FIGURE LEGENDS

Figure 1: BR and GA show stage-specific growth promotion

(A) Hypocotyl elongation rates were measured in 12-hour intervals (Int.) spanning the 36 to 96 hours post germination (hpg) as follows: 36 to 48 (Int. 1, brown), 48 to 60 (Int. 2, orange), 60 to 72 (Int. 3, yellow), 72 to 84 (Int. 4, light green), and 84 to 96 (Int. 5, dark green). Images of representative seedlings are shown for the beginning of each interval to show developmental progression. **(B)** Average hypocotyl lengths (representing 12-20 seedlings per experiment) are shown for seedlings exposed to no hormone (Mock, black), brassinosteroids (BR, green), gibberellins (GA, blue) and both hormones (BR&GA, purple). Hypocotyl lengths predicted by an additive model are shown in grey. **(C)** Hormone treatment of wild-type seedlings differentially promoted growth across intervals. Scale bar equals 0.05 mm/hr. Bar graphs are shown to highlight the differences between Int. 2 and Int. 3. Int. 3 showed the largest growth promotion by GA (blue dots and blue bars), while BR (green dots and green bars) had strong effects in both windows. Mock (black) and combined BR and GA (purple) treatments are also shown. Rates predicted by an additive model are shown by grey lines in Int. 2 and Int. 3. Growth promotion by GA was eliminated in BR-deficient *det2* mutants. Error bars in (C) represent standard error and those shown are of similar magnitude with the error associated with all rate bars (sup). Some error bars in (B) are within the boundaries of the markers.

Figure 2: Synergistic growth in response to BR and GA is *PIF*-independent

(A) *pifP* (*pif1 pif3 pif4 pif5 pif6*) mutants had reduced GA responses (blue dot); however, *pifP* mutants retained sensitivity to BRs (green dot) and combined BR and GA treatments (BR&GA; purple dot). Growth rates from each interval are shown, centered to the border between Int. 2-3 with mock-treated seedlings in the first row (no dot). The scale bar equals 0.05 mm/hr. The bar graph shows wild-type (WT) and *pifP* growth rates for all treatments during Int. 3. **(B)** The hypocotyl hormone response for WT, *pifT* (*pif1 pif3 pif4*), *pifQ* (*pif1 pif3 pif4 pif5*), *pifP* and *hy5* after five days of growth is shown. Seedlings lacking *PIF* function had increased sensitivity to BR and BR&GA treatment compared to wild-type seedlings. *hy5* mutants were largely insensitive to hormone treatments. Hormone response is the ratio of the average hypocotyl lengths from each treatment to that of mock-treated seedlings. Error bars represent standard

error. Letters indicate significant differences ($p<0.05$) between hormone responses for genotypes within each treatment using an ANOVA with Tukey pair-wise comparisons.

Figure 3: *DELLA*s and *SPT* can increase or decrease BR promotion of growth
(A) Growth rates of seedlings with loss- or gain- of *DELLA* or *SPT* function were altered in a stage-specific manner. These effects could be seen in mock (no dot) or BR (green dot) treatments. Growth rate responses in Int. 2 and 3 are shown below the rate bars . Loss of repressor function (*rga gai spt*, light grey diamond) had a greater increase in growth rates over the wild type (WT, black square) during Int. 2 compared to Int. 3. In contrast, gain of *DELLA* function (*gai-1*, dark grey circle) suppressed growth rates during Int. 2 but increased growth rates during Int. 3. Growth rates in response to BR treatment during Int. 2 and 3 for WT and *gai-1* seedlings are shown in a separate bar graph. While growth rates in response to BR are similar between the two intervals for WT seedlings, *gai-1* seedlings showed increased sensitivity during Int. 3. **(B)** High growth rates of *DWF4ox* seedlings are suppressed by reduced *DELLA* (*DWF4ox rga gai*) or *SPT* (*DWF4ox spt*) function. Loss of all three repressors (*DWF4ox rga gai spt*) reduces growth rates by approximately 50%. Growth rates during Int. 3 are shown. Scale bar equals 0.05 mm/hr. Error bars represent standard error. **(C)** The long hypocotyl phenotype of 5-day old *DWF4ox* seedlings required functional *RGA*, *GAI* and *SPT*. **(D)** Quantitative RT-PCR shows that loss of *RGA* and *GAI* returns *DWF4* expression to wild-type levels in *DWF4ox* seedlings. **(E)** Increased *DELLA* function (*gai-1*, grey) had complex effects on expression of BR biosynthetic genes. While expression of *DWF4*, *CPD* and *BR6ox1* was decreased by BR treatment (green) as expected, expression was unchanged, slightly increased, and dramatically decreased for *DWF4*, *CPD*, and *BR6ox1*, respectively in *gai-1* seedlings. A simplified schematic of BR biosynthesis including the genes assayed here and relevant intermediates is shown. CR: campesterol; CS: castasterone; BL: brassinolide. Error bars represent standard error. Letters indicate significant differences in the relative expression for each gene ($p<0.05$) using an ANOVA with Tukey pair-wise comparisons.

Figure 4: BRs increase DELLA abundance and activity
(A) BR treatment strongly increased GFP-RGA signal at 72 hpg. When seedlings were grown on GA alone or BR and GA together (BR&GA), the signal was reduced to background levels at all

time points. An untransformed wild-type (WT) seedling is shown for comparison. **(B)** Western blots using proteins extracted from seedlings at 72 hpg showed a similar effect of BR and GA treatments on RGA levels as was observed with fluorescence. **(C)** Expression of *DELLA* target genes was increased with BR treatment, as well as in *DWF4ox* and *gai-1* mutants. **(D)** Seedlings grown on BR or BR&GA had decreased levels of SPT. BR effects were greatly reduced in *rga gai* mutants. **(E)** BRs increased the expression of GA biosynthetic genes. ACTIN was used as a loading control for western blots. Error bars represent standard error. Error bars represent standard error. Letters indicate significant differences in the relative expression for each gene ($p<0.05$) using an ANOVA with Tukey pair-wise comparisons.

Figure 1

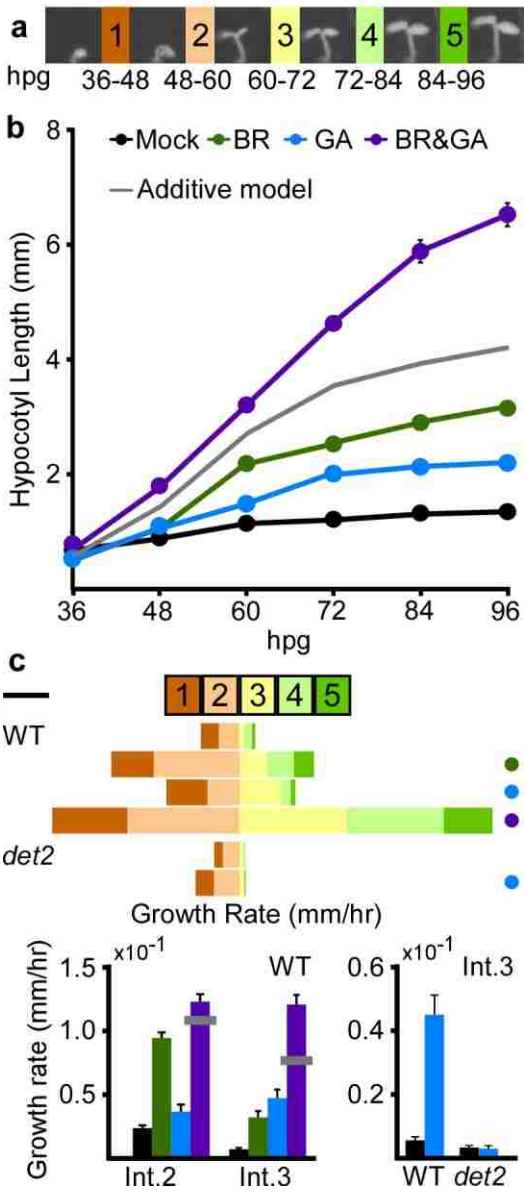
a
1
2
3
4
5
hpg
36-48
48-60
60-72
72-84
84-96
b
Mock
BR
GA
BR&GA
Additive model
Hypocotyl Length (mm)
hpg
c
WT
det2
Growth Rate (mm/hr)
Growth rate (mm/hr)
WT
Int.3
Int.2
Int.3
WT
det2

Figure 2

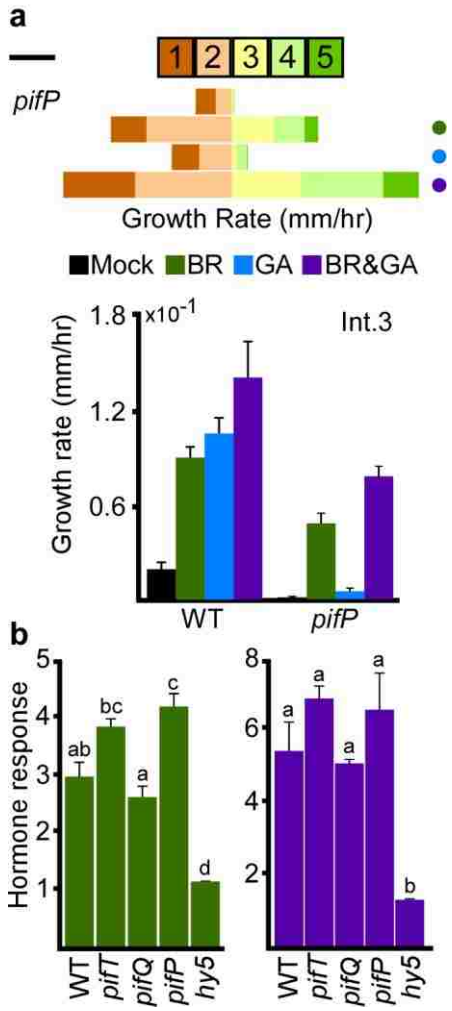
a
1 2 3 4 5
pifP
Growth Rate (mm/hr)
Mock BR GA BR&GA
Growth rate (mm/hr)
1.8 x10-1
1.2
0.6
Int.3
WT
pifP
b
Hormone response
5
4
3
2
1
ab
bc
a
c
d
8
6
4
2
a
a
a
a
b
WT
pifT
pifQ
pifP
hy5

Figure 3

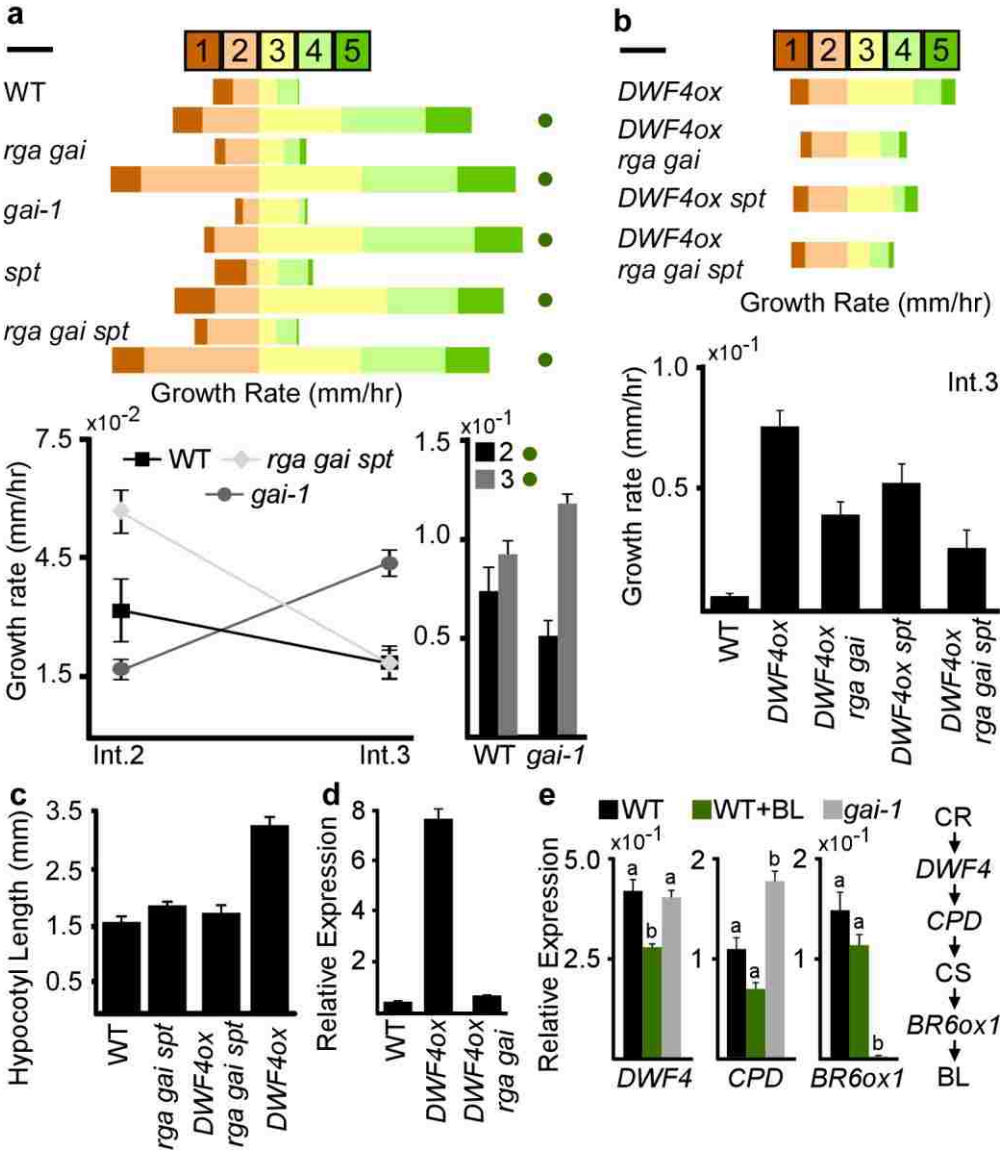
a
1 2 3 4 5
WT
rga gai
gai-1
spt
rga gai spt
Growth Rate (mm/hr)
x10-2
7.5
4.5
1.5
Growth rate (mm/hr)
WT
rga gai spt
gai-1
Int.2
Int.3
x10-1
1.5
1.0
0.5
2
3
WT
gai-1
b
1 2 3 4 5
DWF4ox
DWF4ox rga gai
DWF4ox spt
DWF4ox rga gai spt
Growth Rate (mm/hr)
x10-1
1.0
0.5
Growth rate (mm/hr)
Int.3
WT
DWF4ox
DWF4ox rga gai
DWF4ox spt
DWF4ox rga gai spt
c
Hypocotyl Length (mm)
3.5
2.5
1.5
0.5
WT
rga gai spt
DWF4ox rga gai spt
DWF4ox
d
Relative Expression
8
6
4
2
WT
DWF4ox
DWF4ox rga gai
e
WT
WT+BL
gai-1
Relative Expression
x10-1
5.0
2.5
a
b
a
DWF4
x10-1
2
1
a
a
b
CPD
x10-1
2
1
a
a
b
BR6ox1
CR
DWF4
CPD
CS
BR6ox1
BL

Figure 4

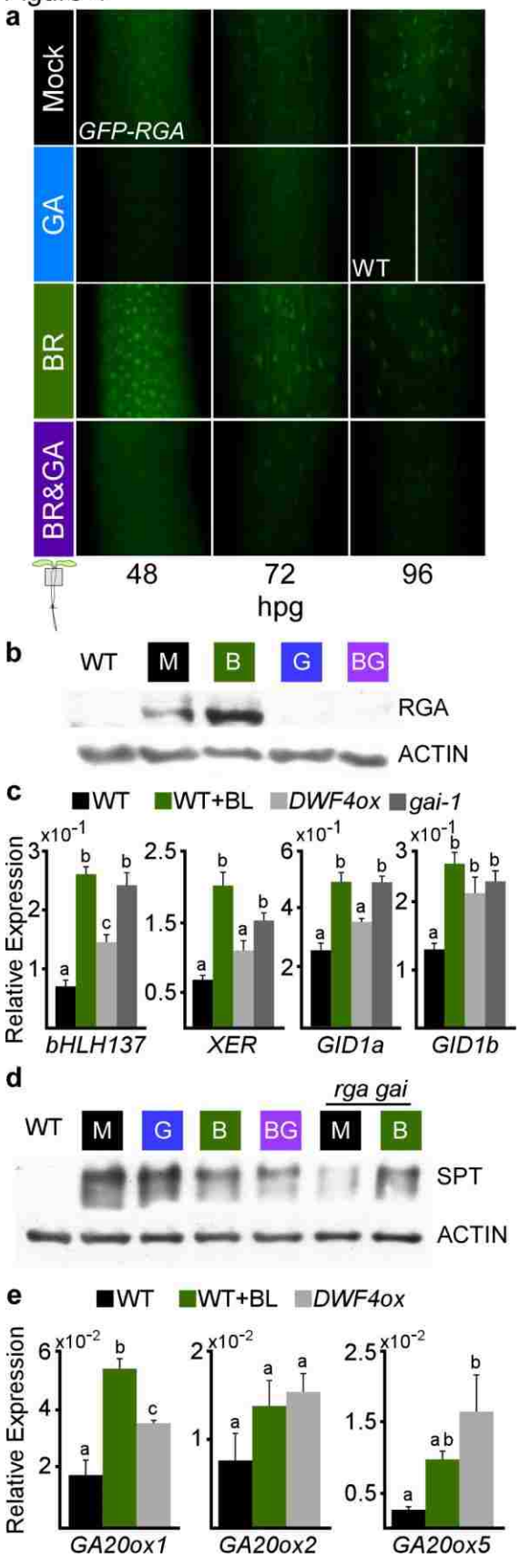
a
Mock
GFP-RGA
GA
WT
BR
BR&GA
48
72
96
hpg
b
WT
M
B
G
BG
RGA
ACTIN
c
WT
WT+BL
DWF4ox
gai-1
Relative Expression
x10-1
bHLH137
XER
GID1a
GID1b
d
rga gai
WT
M
G
B
BG
M
B
SPT
ACTIN
e
WT
WT+BL
DWF4ox
Relative Expression
x10-2
GA20ox1
GA20ox2
GA20ox5

Chapter 5

CONCLUSION: Complexities in genetic networks

Seedlings live in a complex world

Temperature, light quantity and quality, day-length, nutrient availability, and biotic interactions are among the conditions affecting plant growth. This environmental information is coupled by developmental cues and integrated through a network of pathways. Hormones, light receptors and the circadian system integrate signals and execute growth. To control and predict plant growth responses, we need a complete understanding of this network. The Arabidopsis embryonic stem (hypocotyl) has emerged as a key model system for dissecting growth regulation. The benefits of studying hypocotyl elongation include its simple organization and experimental tractability. The hypocotyl only has a few major functions. It functions as a conduit, moving nutrients and water between the leaves and roots. It functions as a moving pedestal, positioning the embryonic leaves (cotyledons) in optimum lighting. It also has a magnificent growth potential that occurs without significant cell division. It is easy to see why plant biologists were seduced by this little stem into thinking it was 'simple'. The switch to photo-autotrophy is crucial for seedlings like Arabidopsis. For these seedlings, more light means more food, more food means more seed, and more seed means more chances for the lineage to survive. In all conditions, the seedling must run its cost/benefit analysis and execute a balanced hypocotyl growth response.

The seedling growth network is complex

When I first encountered the network controlling hypocotyl elongation I was amazed to find a web of arrows and lines so interwoven a spider would be impressed. I was even more amazed when I realized how much we still did not know. How many more lines were out there waiting to be drawn? The resulting network was amazing but seemed impenetrable. I set out to see if this network could be simplified into hubs defined by developmental stage. In this way the larger network could be subdivided into regulatory units that are more or less important given the specific developmental and spatial context. Perhaps some of the complexity apparent in the network was due to collapsing all of seedling development into a single measurement. Thus we built a time-lapse system to sample growth throughout development in both dark and light periods. This method uncovered many surprising responses previously hidden during particular

windows of development. For example, seedlings could grow rapidly at more times during each day than we previously thought. We also found that seedlings were not uniformly sensitive to growth promoters including sucrose, auxin, brassinosteroids (BR) and gibberellins (GA) during all developmental stages. This suggested the importance of each member in the network changes. By grouping regulators with similar effects on growth rate dynamics we discovered novel molecular mechanisms behind pathway interactions.

While this work has added mechanistic insight to many growth responses, it has not reduced the apparent complexity in the growth network. As I step back, I have to ask myself the same question many audience members ask me after I give a talk on this work: "Is it hopeless? Is it possible to understand biological networks this interconnected?" I believe there is hope, but we have to embrace the challenge these networks present. We will have to continually reject the voices in the audience that say: "See, this is why I hate hormones…especially auxin, it does everything!"

Why complex networks are hard to deal with

There are many reasons why complicated interactions are frustrating. As geneticists at heart, we want to construct a model, predict what will happen when we break it, and then test those predictions with a cleverly designed experiment. Pathways with feedback rob us of that important process because we cannot make predictions. When we cannot make predictions and test them we are left never making the leap from correlation to causation. The best understood pathways are those that consist of 'switches', responses that either occur or not. Beautiful examples of this include the elegant relay of transcription factors that step by step guide the development of stomata in the leaf epidermis. Another example is the stereotypical divisions that lead to lateral root emergence in the root epidermis. In these linear pathways we can determine epistasis and hierarchy between regulatory genes in the process. But there are many important biological processes that are not binary but quantitative in nature. We need new ways of generating predictions in these processes if we really want to understand the molecular mechanisms behind them.

We can rise to the challenge of complex responses

Computer simulations offer a new way of extending our thought capabilities to include quantitative responses and mutli-variable systems. Mathematical modeling has been used with great success to expose the dynamics of complex systems over time. People use models to forecast what will happen with climate change, disease dynamics and predator-prey dynamics in natural communities. Computational models can be used to increase our understanding of genetic networks if we use them in a slightly different way. The forecast models, including the ones mentioned above, take the dynamics that you know occur in a certain situation and project them into an unknown situation, like the future. In these models how well the simulation 'fits' the real data is very important, thus the parameters you select are also really important. In a toy theoretical model, the trends in the outputs are more important than the exact values predicted by the model. Here the relationship between variables is really important and you are looking for sufficiency. Is there enough in your model to capture the basic dynamics? One of the most important results of the model is the effect the method has on your thinking. The model is an explicit form of all the assumptions you are making about your system. It forces you to do the thinking that you should be doing anyway, but often cut corners on.

"All models are wrong; some models are useful."
-- George Box

In brief, the method to the modeling madness is a series of steps. The first step is to figure out what you want to include in your model and what you want to get out of it. What variables are important and which ones can you leave out? You then need to know what each of the variables depends on. What determines the rate that variable X is produced or degraded? It is then helpful to draw graphs of how you think the rates of each variable change with changing concentrations of each variable it depends on. This will help you figure out what mathematical equation captures the dynamics of that relationship. Once you have all your equations, code them in some computational environment and simulate. Three rules to follow as you make your way through the method [adapted from Ellner and Guckenheimer (2006) Dynamic Models in Biology]:

(1) Lie

Your model will force you to simplify some biological detail to the point where you know it is not true anymore. That is OK, it helps you decide what you think is important in your system.

(2) Cheat

If your equation works well enough but you know it is not exactly legitimate, this is one of those times when that *IS* good enough.

(3) Steal

Do not reinvent the wheel. If someone has code or equations that worked for something else, see if they will work for you no matter how they were previously used.

The recipe for mechanistic insight into complex systems requires three main ingredients: precisely defined systems, computational methods, and a change in expectations. My graduate work shows that time is an important consideration when trying to understand the growth network. By looking at a very specific time in development, you can help reduce the number of variables you must pay attention to. We also need to incorporate tissue specificity into our understanding of the growth network. Different layers and regions of the hypocotyl likely process different information during growth. Models can then be constructed of sub-networks at particular times and places. We must then let go of dreams of producing a 'grand unified theory' of growth. No simple diagram is going to capture a generalized growth network as seedling growth reflects a complex and ever-changing set of conditions. I believe a complete understanding of growth responses will include a set of network sub-routines initiated by particular input combinations.

If you want things to be simple, first let them be complex.
-- inspired by the Tao Te Ching